THE EFFECT OF OXYGENATES ON THE OLIGOMERISATION OF PROPENE OVER ZEOLITE ZSM-5

by

STEVEN THOMAS LANGFORD
B.Sc. (Chem. Eng.) UCT

A thesis submitted to the University of Cape Town in fulfilment of the requirements for the degree of Master of Science (Engineering).

Department of Chemical Engineering
University of Cape Town
Rondebosch
Cape Town

April 1993

ACKNOWLEGEMENTS

The number of people to whom a big thank-you is owed is large and I apologise now for forgetting anyone. In particular I would like to extend my thanks to the following: Leslie, Pam, Rob, Tony, Bill and Granville who all helped to make my work easier.

Connie Wishart deserves a medal for her patience at doing graphs etc. and other work, always at short notice! Thanks very much.

Thanks to Klaus for his superb technical support.

Thanks to Dr. Jack Fletcher for his advice and guidance.

To Professor Cyril O'Connor. Thanks Prof. for everything, especially for the motivation in times of need.

To Sasol Limited for the sponsorship of the project.

To the rest of the postgrad. team - it was great!

Finally to James Vaughan. It's difficult to quantify my appreciation for all your help both as a work colleague and friend but thank you.

To my parents

Ken and Irene Langford

SYNOPSIS

The oligomerisation of alkenes such as propene and butene represents an important route to the production of enviromentally clean transportation fuels. When these olefins originate from Fischer-Tropsch product streams they are often contaminated with small amounts of oxygenates such as acetic acid, ethanol, butanol, methyl-ethyl-ketone (MEK), acetone and water[94]. Complex feeds can result in competitive reaction between the feed components and may result in observed selectivities that cannot be predicted from pure component data alone[95]. ZSM-5 has been shown to be an excellent catalyst for alkene oligomerisation[85,86,87] and is also active for the conversion of oxygenates[12,13,21,53,59].

When pure oxygenates are fed over ZSM-5 at oligomerisation temperatures, acetone and MEK cause the catalyst to deactivate and the conversions are low whereas ethanol and n-butanol are completely converted and no deactivation occurs. At 250°C acetic acid undergoes a low conversion (4%) and at higher temperatures a decrease in conversion is also observed with time. The decrease in conversion of acetone has been attributed to the formation of a surface cyclic ketonic species[50,51,53]. During acetic acid reaction dehydroxylation of the zeolite[13] has been proposed as the cause of decreasing activity with time but this work has shown that the catalyst is regenerable and the acidity of the catalyst, as determined by ammonia TPD, remains unchanged after reaction with acetic acid.

The propene oligomerisation and hexane cracking activity of ZSM-5 (Si/Al = 30) is reduced when the catalyst is exposed to oxygenates such as acetic acid, ethanol, n-butanol, MEK, acetone and water (mole fraction in feed < 0.01). In the case of all except acetic acid the activity is almost

completely restored when the oxygenate is removed. Acetic acid causes irreversible loss of activity for propene oligomerisation and hexane cracking at 250°C. For MEK and acetone the activity for propene oligomerisation is restored to a greater extent (90% for acetone and 50-60% for MEK) than acetic acid but not fully.

The decrease in activity for propene oligomerisation and hexane cracking at 250°C is proposed to be due to site poisoning by preferential strong adsorption of the oxygenates, especially acetic acid, onto the zeolite surface. An adsorption complex for acetic acid and the surface hydroxyls has been proposed in which the bond angles and lengths of the molecule are similar to those observed in the formation of the acetic acid dimer, consistent with the proposed strong adsorption.

PUBLICATION

A paper, based on this work, entitled:

The effect of oxygenates on the propene oligomerisation activity over ZSM-5.

by

C. T. O'Connor, S. T. Langford and J. C. Q. Fletcher

was presented at the 9th International Zeolite Conference, Montreal, 5-10 July, 1992 and will be published in Vol. 72 of Studies in Surface Science and Catalysis.

TABLE OF CONTENTS

LIST OF FIGURES

LIST OF TABLES

NOMENCLATURE

Symbol		Units
$Area_i$	area under peak for component i	
B	virial coefficient	
B^o, B^1	used in calculation of B, functions of temperature only.	
C_{oxy}	number of carbon atoms in an oxygenate molecule	
M_{oxy}	oxygenate mass rate	g/hr
PPM	parts per million	
P	pressure	Pa
P_c	critical pressure	Pa
P_r	reduced pressure	
RF_i	response factor for component i	
T	temperature	K
T_c	critical temperature	K
T_r	reduced temperature	
V_{oxy}	oxygenate flowrate	cm^3/hr
V_c	critical volume	
W	mass flowrate	g/hr
w	accentric factor	
y_i	mole fraction of component i	
Z	compressibility factor	
Z_c	critical compressibility factor	
ρ	oxygenate density	g/cm^3

NOMENCLATURE (cont.)

Subscripts

oxy	- oxygenate
CO	- carbon monoxide
CO_2	- carbon dioxide
N_2	- nitrogen
ij	- indicate the value is due to interaction between species i and j in a mixture.

Abbreviations

MEK	- methyl-ethyl-ketone
MO	- mesityl oxide
DAA	- diacetone alcohol
DEK	- diethyl-ketone
DMK	- acetone
R^+	- carbonium ion

1 INTRODUCTION

1.1 Zeolites

Zeolites are crystalline microporous solids containing cavities and channels occupied by large ions and water molecules, both of which have considerable freedom of movement. Although as recently as 1982 they were chemically restricted to aluminosilicates, developments now include elements such as Li, Be, B, Mg, Co, Mn, Zn, P, As and Ti. Zeolites dominate most areas of the petroleum field due to the molecular control of the many reactions.

1.1.1 The Structure of Zeolites

The primary building block (Figure 1.1) is a tetrahedron consisting of four oxygen atoms surrounding a central T-atom (Generally Si). These primary units are linked through the oxygen atoms to form secondary units. There are 16 Secondary Building Units (SBU)[2] as shown in Figure 1.2 where the open circles represent tetrahedral sites (usually silicon and aluminium) and the solid lines represent the bridging oxygens. These SBU's join resulting in polyhedra. The polyhedra are responsible for the frameworks of the various zeolite crystal structures whose ideal chemical formula is represented by:

$$M_pD_q[Al_{p+2q}Si_rO_{2p+4q+2r}].sH_2O \quad (Smith^1)$$

where M and D are mono- and di-valent cations respectively.

The diversity of the zeolite structure is not only determined by the different combinations of the secondary units but also through the substitution of the central

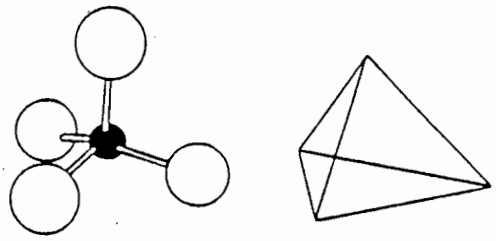

Figure 1.1 Schematic of $[SiO_4]^{4-}$ and $[AlO_4]^{5-}$ tetraheda

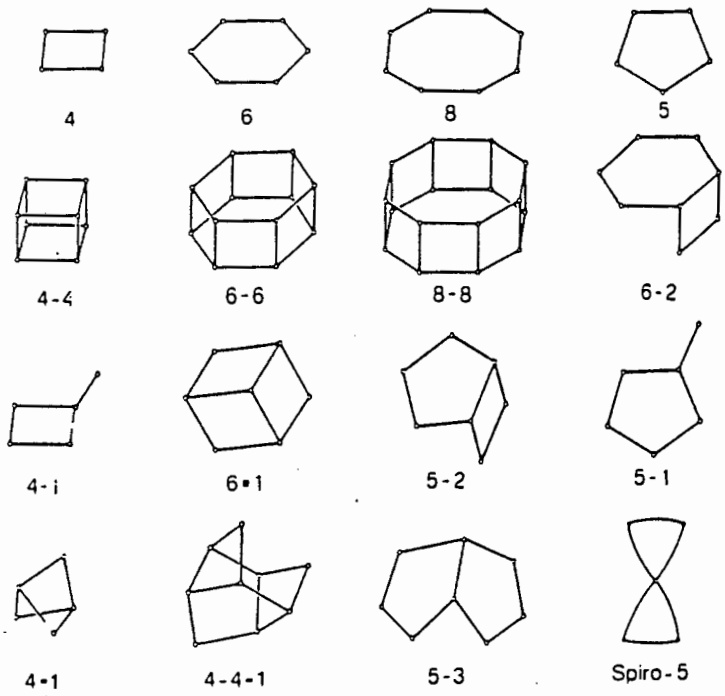

Figure 1.2 Secondary Building Units (Meier and Olson[2])

silicon atom by others (Al, Ga, Ge, P). The substitution of Al^{3+}, for example, for Si^{4+} results in a single negative charge which is neutralised by the non-framework cations (e.g. Na^{+}) located in the pores or cavities[3]. The mobility of this cation allows it to be exchanged for others, giving versatility to the properties of the catalyst. However not all the cations may be amenable to removal by conventional exchange processes.

Zeolites can be divided into 1-, 2- and 3-dimensional pore structures: pathways that are parallel and without cross-section (mordenite), interconnected channels in 2-dimensional (ZSM-5) and 3-dimensional (Zeolite A) patterns. The channel systems are further divided into 8-, 10- and 12-membered ring structures known as small (usually < 5Å), medium and large pore catalysts. ZSM-5 belongs in the pentasil medium pore size group with two sets of intersecting channels[10] (Figure 1.3), one sinusoidal and nearly circular (5.4 x 5.6Å) and the other straight but elliptical (5.1 x 5.5Å). There are no large supercages with smaller windows that cause bottlenecks and molecules larger than the pore dimensions do not form inside the channels.

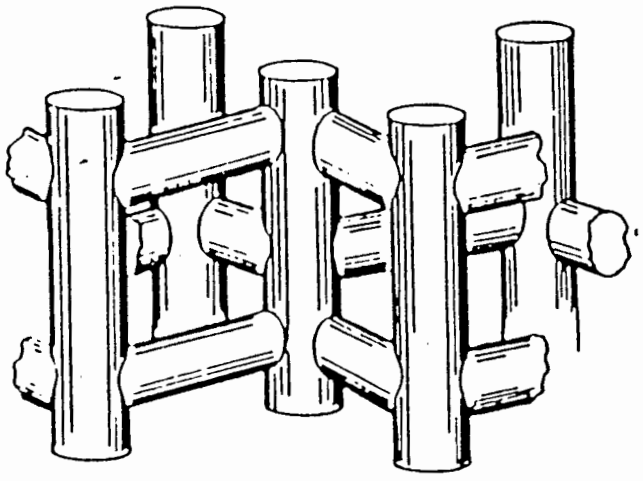

Figure 1.3 Schematic of ZSM-5 Channel System

1.1.2 Occurrence and Synthesis

Zeolites occur in nature in vugs and vesicles of basaltic lava, in specific kinds of rocks subjected to moderate temperatures and pressures and in reacted volcanic ash deposits. Only the last are economically viable in terms of extraction with large tonnages being mined from the surface. These deposits are typically formed when ash and lava from erupting volcanoes are washed into lakes and rivers where the aqueous environment results in reaction to clays and zeolites[3].

Most commercial catalysts are synthetic products manufactured from high purity chemicals at specific conditions of temperature, pressure, time and reaction enviroment. Temperatures between 100°C and 160°C are generally used. ZSM-5 is synthesised in both the Na- and the OH-form depending largely on the compound used to increase the pH of the mother liqour to about 10.5.

1.1.3 The Nature of Zeolite Acidity

As discussed earlier (Section 1.1.1) the substitution of aluminium for silicon in the zeolite framework results in a charge imbalance, a net negative charge for each aluminium present, that is neutralised by the presence of cations. The mobility of these ions allows them to be exchanged for others. Zeolites are commonly synthesised in the Na^+ form which can be easily exchanged for ammonium (NH_4^+) cations. Heat treatment produces ammonia resulting in an active protonic form as shown in Figure 1.4 and protons can be supplied (Brönsted acidity) through the equilibrium[6] represented in Figure 1.5.

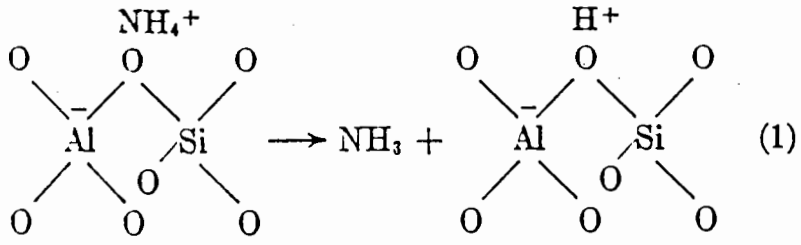

Figure 1.4 Zeolite Deammoniation - generation of protonic sites

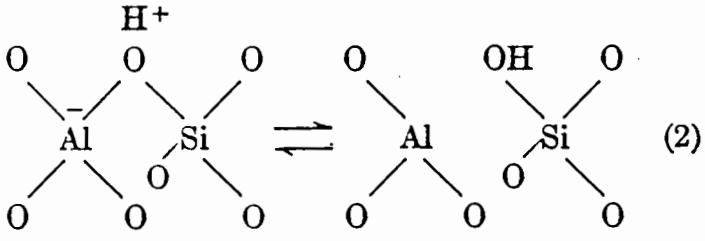

Figure 1.5 Zeolite acid site equilibria (Uytterhoeven et al[6])

Ward[4], in a study on the nature of acidity of Y Zeolite, found the presence of three structural hydroxyl groups at 3742, 3643 and 3540 cm^{-1}. The 3742 cm^{-1} band has been attributed to terminal Si-OH groups and the 3663 and 3540 cm^{-1} bands to hydroxyl groups at different crystallographic locations. The temperature at which the hydroxyl band intensity reached maximum intensity corresponded to the temperature at which ammonia ceased to be evolved. These bands reached maximum intensity at 350°C and remained constant until approximately 500°C after which they declined (Figure 1.6).

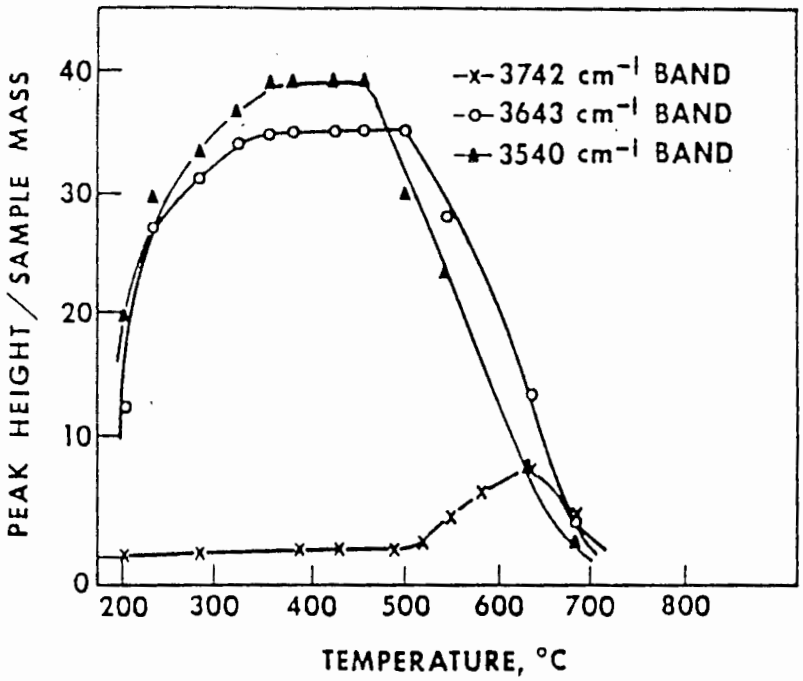

Figure 1.6 Intensity of hydroxyl bands on H-Y as a function of temperature.

The removal the hydroxyl groups, accompanied by an endothermic weight loss, results in a new site and can be pictured by:

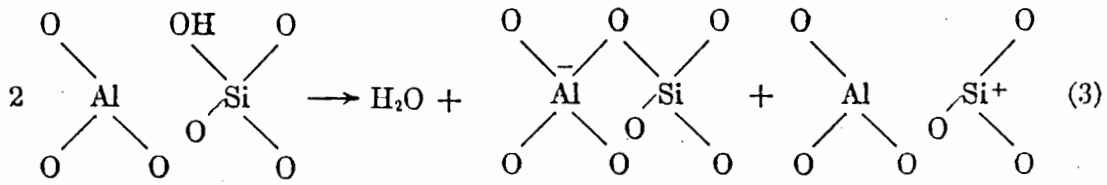

Figure 1.7 Dehydroxylation - generation of tri-coordinated framework aluminium

Using the adsorption of pyridine, Ward probed the acid character of zeolite-Y as the IR band at 1545 cm^{-1} indicates proton acidity and that at 1440-1455 cm^{-1} indicates aprotic

or Lewis acidity. Figure 1.8 shows his results. The quantity of pyridine bound to Brönsted sites increases with calcination temperature up to 375°C and remains constant until 500°C after which it decreases, in a manner parallel to the hydroxyl group represented by the 3663 cm^{-1} band. If the Brönsted acid sites are hydroxyl groups then a conversion to Lewis sites (Figure 1.7) will occur above 500°C as the surface becomes more dehydroxylated. Figure 1.8 shows no Lewis acidity until 475°C after which the concentration increases rapidly.

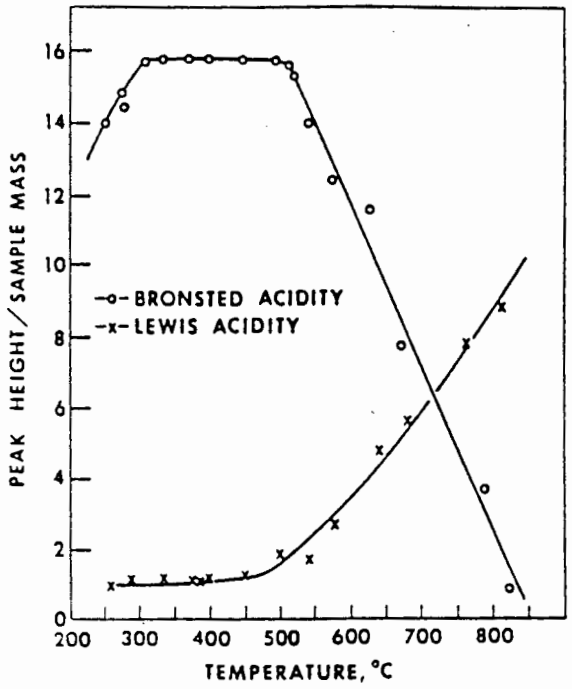

Figure 1.8 Acid site distribution, variation with calcination temperature

Ward concluded that Brönsted acidity was responsible for the catalytic activity however he later conceded[5] that other factors are involved. The representation of Lewis acidity by a $[SiO_3]^+$ (Figure 1.7) has been superceded recently since it has been shown (Karge[99] and Barthomeuf[100]) that tightly bound and extraframework $[Al_xO_y]^+$ species can account for significant amounts of Lewis acidity in zeolites.

1.1.4 Shape Selectivity

Selectivity is the ability to discriminate between different sizes and shapes of molecules and thus cause specific product spectrums from certain reactions over zeolites. Generally this is found in all zeolites and can be further subdivided into: reactant selectivity, product selectivity and transition state selectivity.

Reactant selectivity[9] (Figure 1.9 (a)) occurs when only a fraction of the reacting molecules has access to the active sites due to molecular sieving effects

Product selectivity[9] (Figure 1.9 (b)) occurs when only some products with the correct dimensions will diffuse out and those larger will remain in the pores until cracked to smaller molecules which can diffuse out.

Transition state selectivity[9] (Figure 1.9 (c)) results when certain reactions are prevented as the transition state required is too big and it is prevented from forming due to insufficient space in the pores.

Diffusivity, coulombic field interaction and the presence of windows or cages also help to influence the product spectrum of certain reactions.

In the case of ZSM-5 its 10-membered ring channnel system accepts by decreasing order of preference, normal paraffins, isoparaffins, other monomethyl substituted paraffins, monocyclic aromatic hydrocarbons and dimethyl-substituted paraffins. The absence of cages along the channels reduces the formation of carbonaceous residues, strong diffusion restrictions imposed on dimethyl-paraffins and o,m-xylenes and molecular traffic control where reactants and products use different channels to diffuse into and out of the

Figure 1.9 Schematics of Shape Selectivity

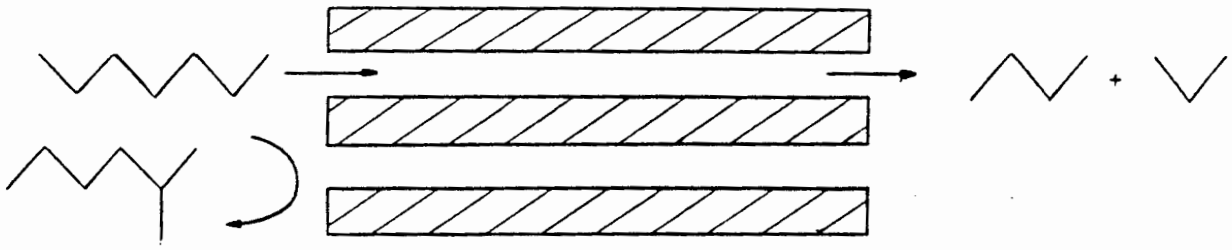

(a) Reactant Selectivity

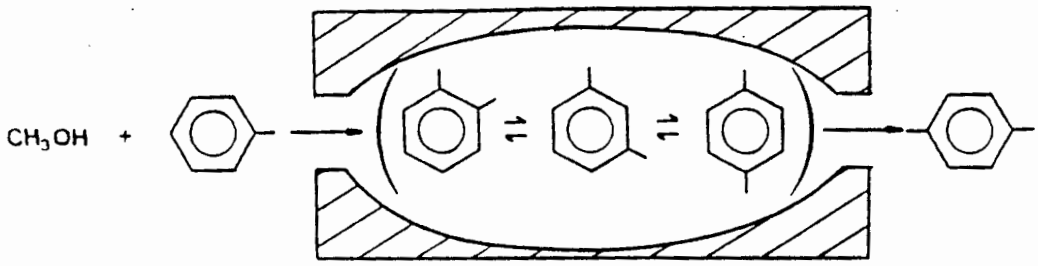

(b) Product Selectivity

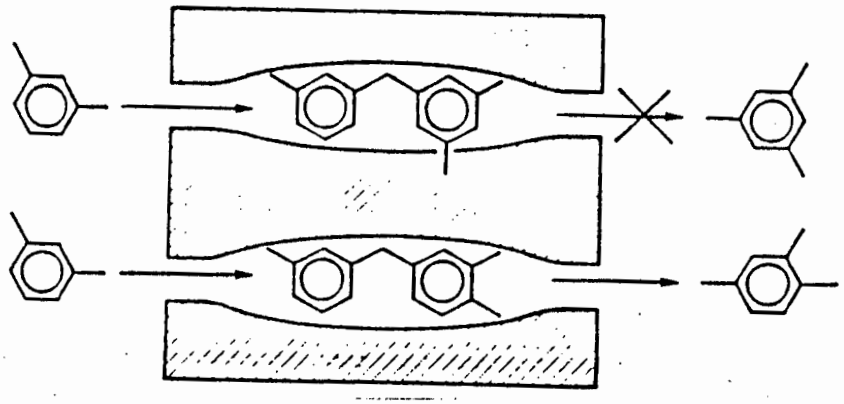

(c) Transition State Selectivity

catalyst are all involved in affecting the nature of product molecules. Due to its shape selective nature ZSM-5 is used for numerous reactions such as methanol reaction, xylene isomerisation, toluene disproportionation, ethylbenzene synthesis and M-reforming.

1.2 Reaction of Oxygenates over HZSM-5 and Zeolite catalysts.

1.2.1 Carboxylic Acids

Acetic acid has been reacted over HZSM-5 under a variety of conditions[12,13,21] and it has been shown that the mechanism for oxygen removal shifts from decarboxylation (where the oxygen atoms are removed from the molecular structure via CO_2) to both decarboxylation and dehydration over the temperature range 316°C to 370°C[13]. Decarboxylation results in lower hydrocarbon yields than those achieved from methanol dehydration[13] since carbon atoms are lost through CO_2. The main hydrocarbon products were isobutene and aromatics with their selectivities dependent on temperature and conversion. Typical product distributions are shown in Table 1.1.

Acetic acid reacted over ZSM-5 in a fixed bed configuration results in rapid deactivation of the catalyst with conversions dropping from 100% to 71.4% in 1.3 hours[13]. It was observed that periodic regenerations allowed consistently high conversions of >90 % to be maintained in a fluidised bed configuration[13] and that catalyst regeneration in fixed bed configuration resulted in the restoration of initial high activity[21]. When methanol was co-fed with the acid in fixed bed reactors deactivation was minimal and the main mechanism for oxygen removal was dehydration[13]. The

Table 1.1 Hydrocarbons from acetic acid conversion

Reaction conditions		
T (°C)	371	316
Conversion %	30[a]	8[a]
TOS (hr)	-	1.5
Hydrocarbon Distribution (wt%)	[c]	[d]
Methane	0.4	-
Ethane	0.1	-
Ethene	0.4	0.6
Propane	0.9	-
Propene	3.3	1.8
i-Butane	1.0	-
n-Butane	0.6	-
Butenes	71.5[b]	17.1[e]
i-Pentane	0.1	-
n-Pentane	-	-
Pentenes	0.4	-
C_6+ Aliphatics	-	-
Benzene	<0.1	
Toluene	2.0	
Ethylbenzene	0.5	
Xylenes	5.1	
C_9^+ Aromatics	11.4	
C_{10}+ Aromatics	11.4	
C_{11}+ Aromatics	2.2	
Aromatics	-	80.5

[a] LHSV = 1, [b] 93 % i-butene

[c] Carbon Selectivity %: CO_2 (41.2); Hydrocarbons (57.6)

[d] Carbon Selectivity %: CO (1.7); CO_2 (32.9); Acetone (33.4); Hydrocarbons (29.2).

[e] >95% isobutene

mechanism of acetic acid conversion to hydrocarbons is complex[21] (summarised in Figure 1.10) and has been referred to as the ketonisation of the acid to acetone followed by aldolisation and cracking reactions to hydrocarbons[12,13,20,21].

Much work has been done on finding the mechanism of and intermediates in the ketonisation of acetic acid over metal oxide catalysts[15-18]. Over Chromia[16,17] the reaction is proposed to take between two surface species: an acylium ion (formed by the dehydration function) and an acetate ion (formed by the dehydrogenation function) represented by:

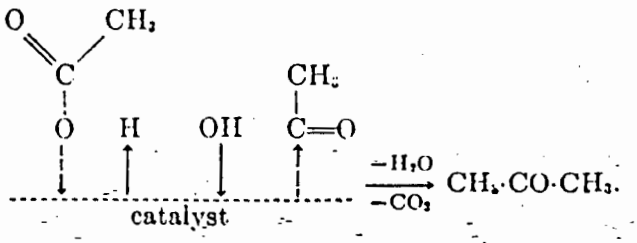

Figure 1.11 Reaction Intermediates of acetic acid conversion over chromia

An electron shift through the oxygen at the surface of the acetate ion allows the CH_3^- ion to leave and attack the acylium ion at the carbon atom in a classic nucleophilic addition reaction. On Anatase TiO_2 surfaces[18] the reaction involves two surface species: an acetate ion and an adsorbed intact acid molecule reacting via a ketene intermediate. The strength of the adsorped acid molecule/catalyst interaction was evidenced by the desorption of only reaction products at

Figure 1.10 Simplified oxygenate reaction mechanisms

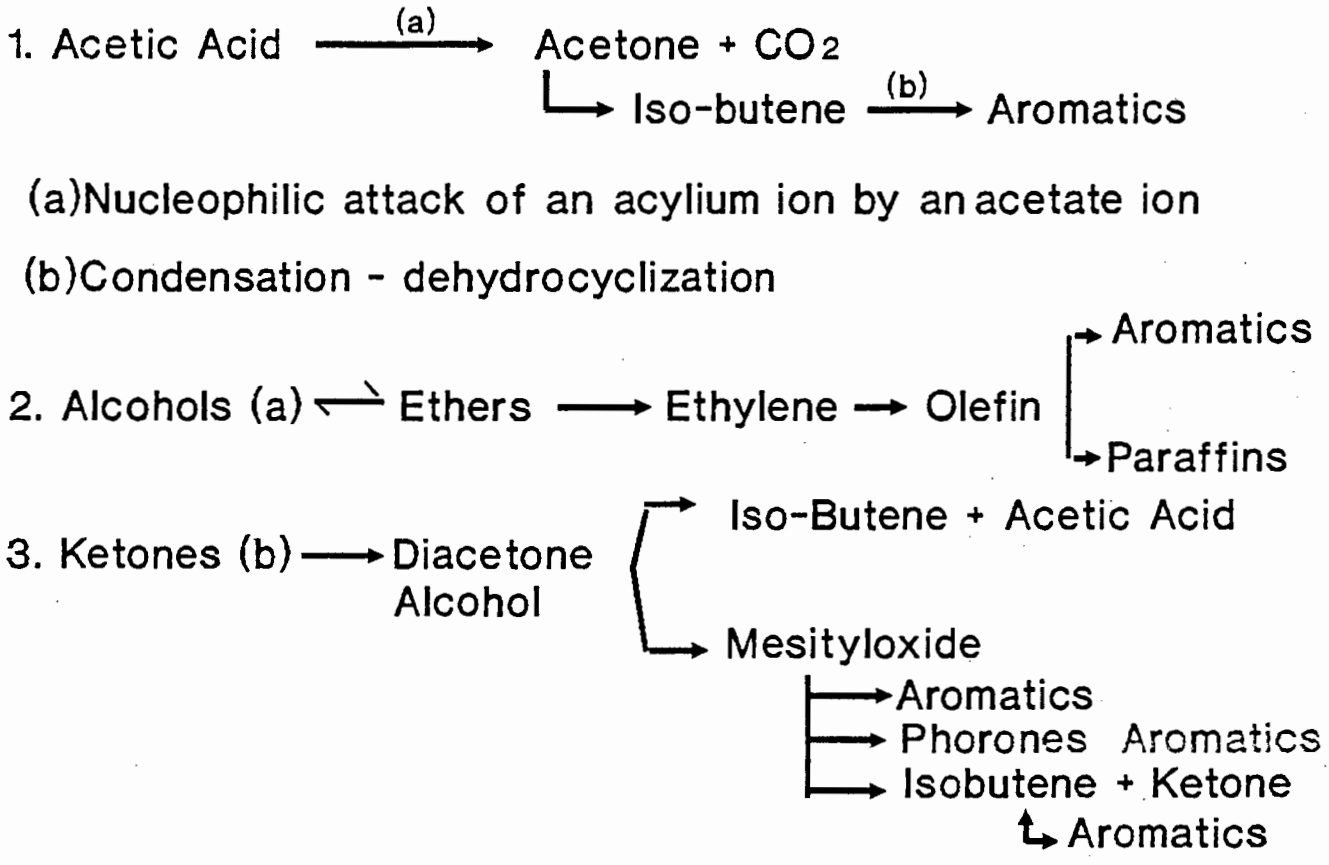

(a) Chang et al[97]

(b) Kubelkova et al[98]

temperatures > 250°C and that the acetate species only completely decomposed above 350°C. Over Iron Oxide[15], labelled acetic acid showed that ketene formation, prior to acetone formation, occurred and this explained the resultant product spectrum. Below 400°C the reaction involved the interaction of two adsorbed molecules of acetic acid, one forming the ketene intermediate.

The reaction mechanism over zeolites has been postulated to involve two surface species[13,20] one of which, the acetate ion which is formed from the acylium ion, causes dehydroxylation[13]. This has been disproved by the successful regeneration of HZSM-5 deactivated after acetic acid reaction[22]. Thus it seems likely that an adsorbed acid molecule (Figure 1.12) is more likely to replace the acetate ion in the reaction[21], a fact that has been investigated and found to be the most probable species at 150°C[19].

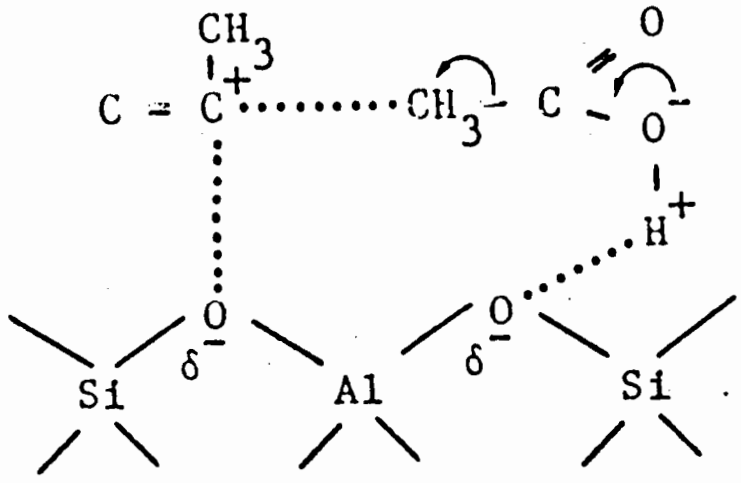

Figure 1.12 Formation of acetone via an acylium ion and an adsorped acid molecule over HZSM-5

The adsorption of acid and subsequent temperature programmed desorption showed that the H:C:O ratios of the desorbed products are the same as that of the parent acid indicating the adsorption of the molecule intact[19]. Indeed the strength of the adsorbed acid molecule is reflected in an IR study[20] that showed that bands of intact molecules and acetate ions were still present at 320°C, the former disappearing at 400°C. It was concluded that the transformation of acetic acid to aromatics occurs at temperatures between 320°C and 400°C[21]. On NaHY, acetic acid is sorped intact[14] with small amounts being converted to acetate and water. Complete transformation of the adsorped acid molecules to acetate ions occurred at 350°C and the acetate ion remains stable to 400°C. At 350°C the adsorption of acetic acid caused the complete disappearance of zeolitic hydroxyl bands and no change was observed in the crystal structure as indicated by XRD.

The primary product in acetic acid conversion is acetone and carbon dioxide[21] of which the former further reacts via aldolisation to diacetone alcohol and then dehydration to mesityloxide. This mechanism is very similar to that of acid catalysed conversion of acetone. The distribution of secondary products can occur either from isobutene condensation-dehydrocyclisation reactions, the acid catalysed dehydration of isophorone, condensation of acetone with mesityloxide to mesitylene and the formation of alkylphenols via a complex dehydrodemethylation reaction[21]. The distribution of aromatics is similar to that from methanol and acetone conversion illustrating that the isobutene route could be the more dominant[21]. The deactivation of the catalyst on reaction with acetic acid has not been investigated thoroughly and the dehydroxylation theory[13] has been proved invalid since the catalyst is regenerable. It is possible that reaction intermediates block the acid sites.

1.2.2 Alcohols

Alcohols have become of interest as a reactant for fuels production since the advent of the Mobil MTG process and the possibility of producing synfuels from biomass. HZSM-5 is an efficient catalyst for converting methanol, ethanol and butanol to hydrocarbons. A point of contention still remains over the formation of the first C-C bond in methanol to hydrocarbons[23] but the reaction of higher alcohols is less difficult to understand as the acid catalysed dehydration reaction to the corresponding alkene is well documented. However it has been postulated that the branched hydrocarbon products in methanol and ethanol conversion can be explained via an acid catalysed dehydration of two alcohol molecules to the corresponding ether[23]. Thus the possibility exists of a parallel reaction for ethanol and butanol:

1) Dehydration of the alcohol to the alkene[23] and
2) Dehydration of two alcohol molecules to the ether[23,29].

Reaction 2) has not been recorded by many researchers, especially for higher alcohols (C_2-C_4), and is probably due to the ease of and thus preferential formation of the resultant carbenium ions i.e. reaction 1). Diethylether was formed in significant quantities on a steam treated HZSM-5[26] catalyst but it is most likely to react rapidly to an alkene.

Co-feeding benzene with ethanol and ethene has been used to study reaction precursors[24]. Large increases in ethylbenzene and the absence of methylbenzenes were recorded for both ethanol and ethene below 300°C indicating that the ethene is the reactive component up to 300°C. The significant increase in the production of i-propylbenzene during ethene conversion with benzene was attributed to the formation of a reactive C_3 intermediate from the cracking of larger

molecules rather than the methylation of an ethene molecule. No i-propylbenzene was formed when ethanol was reacted with benzene. An ethanol feed gave lower gasoline yields (23 wt%) than ethene feed (51.3 wt%) under the same conditions even though the high yields of ethene obtained fron ethanol conversion was expected to give a similar product. It was concluded that ethanol partially blocks oligomerisation sites and completely blocks cracking sites below 300°C such that it is not safe to assume that ethanol is instantly dehydrated to ethene[24]. In the study of isobutanol over HZSM-5 two reaction regimes were identified[25]: 1) the formation of the ether between 45-70°C and 2) the complete dehydration above 125°C to the butene and water. Butene was formed either from the adsorbed ether or from the dehydration of the surface alkoxide species. The concentration of alcohol on the catalyst affected the reaction pathway, low concentrations promoting the oligomerisation of butene to longer hydrocarbon chains and subsequently deactivating the catalyst. An excess of the alcohol allows the surface alkoxide species to react with alcohol to form the ether preventing oligomerisation. Typical product distributions are shown in Table 1.2.

Catalysts acidified by different methods lead to product distributions that differ widely in the ethene/aromatic ratios for ethanol conversion[27]. This has been attributed to poor protonation of the zeolite[28]. However a catalyst having a high conversion for ethanol also gave a high conversion for ethene indicating that the first reaction step for ethanol is to the alkene. The effect of temperature on the conversion of ethanol shows that ethene is the primary product formed below 300°C but at higher temperatures the formation of longer aliphatic chains takes place with aromatics becoming significant at >350°C[23]. Chaudhuri et al.[29] found that a minimum ethene yield and a maximum aromatic yield occurred with temperature during ethanol

Table 1.2 Hydrocarbons from Ethanol[23] and t-Butanol[12] conversion

Reaction conditions			
T (°C)	250	300	371
Conversion %	100	100	100
Reference	23	23	12
Hydrocarbon Distribution (wt%)			
Ethanol	0.44	-	-
Diethyl ether	0.02	-	-
Aliphatics			
C_2	98.8	46.0	1.2
C_3	-	9.2	19.9
C_4	0.59	18.2	27.7
C_5	0.06	13.4	7.8
C_{6+}	0.07	10.2	7.6
Cyclics			
C_5	-	0.1	-
methyl C_5	-	-	-
C_7	-	0.3	-
Aromatics			
Benzene	-	-	3.3
Toluene	-	0.2	11.6
Ethylbenzene	-	0.2	1.3
p-Xylene	-	0.5	12.4
o-Xylene	-	0.1	-
m-,p-,Ethylbenzene	-	1.6	-
1,2,4-Trimethylbenzene	-	-	-
C_{9+}	-	-	7.1

conversion. A maximum in liquid hydrocarbon product was found at 400°C and for aromatics the maximum occurred at 450°C[30]. Above this temperature cracking of the heavy products resulted in their decrease. The aliphatic yields varied possibly due to the complex reaction scheme involving oligomerisation and cracking. Since these changes in product spectrum were completely reversible it was implied that the decrease in hydrocarbons heavier than ethene was due to the increasing importance of cracking reactions and the decrease in the surface concentration of primary and secondary products[29].

The selectivity to hydrocarbons heavier than ethene increases with the number of Brönsted sites[30] and suggests that the distance between the sites is important for the increase in the reaction rate as it allows easier access of reactants to each other. The amount of coke produced was proportional to the mass % of aromatics in the product[29] and the deactivation of the catalyst was due to coke deposition since n-hexane adsorption values dropped and the activity returned after decoking[27]. The aromatic content of the product changed with time-on-stream, trimethylbenzenes and C_{10+} aromatics increasing relative to C_6, C_7, and C_8 aromatics. Numerous factors affect the aromatic selectivity but generally the amount of aromatics increase with temperature but decrease with decreasing residence time.

Increasing pressure was found to make the dehydration of ethanol more difficult[30] but the selectivity of the product increases towards a heavier hydrocarbon. The thermodynamics of the reaction

	C_2H_5OH	->	$C_2H_4 + H_2O$	-> Higher hydrocarbons
ΔH_f	90 cal/g			-400 cal/g

indicates that the overall reaction of ethanol to hydrocarbons is exothermic.

The adsorption and TPD of alcohols[31,32], especially ethanol, have shown that in the primary alcohol series methanol, ethanol, propanol and butanol, the amount of catalyst pore space filled increases with increasing alkyl group length. This is due to the hydrophobicity of the catalyst. Methanol and ethanol desorb unreacted with methanol peaking at 127°C and ethanol at 97°C and 157°C. The first ethanol peak is due to excess physisorbed ethanol and 10 % of the ethanol reacts to form ethene and water. Propanol has two desorption states at 107°C and 167°C with 40% reacting to the dehydrated products. The high temperature peaks for ethanol and propanol were associated with a 1:1 ratio of alcohol to framework aluminium, indicative of strong interaction with the acidic sites. The following scheme:

$$HROH + ZOH \underset{k_{-1}}{\overset{k_1}{\rightleftharpoons}} HROH_2^+ + ZO^-$$

$$HROH_2^+ + ZO^- \overset{k_{21}}{\rightleftharpoons} HR^+ + H_2O + ZO^-$$

$$HR^+ + ZO^- \rightleftharpoons R + ZOH$$

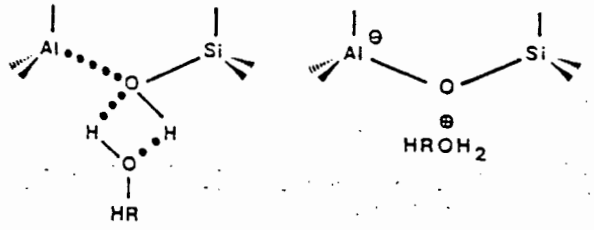

Figure 1.13 Reaction mechanism of alcohols with hydroxyl groups

was postulated[31] as the reaction of the alcohol with the hydroxyl group, the adsorbed oxonium ions decomposing either by reverse proton transfer or dehydration depending on the stability of the carbenium ion. Ethanol desorbs at a higher temperature on HZSM-5 (198°C) than on silicalite (67°C) indicating the strong interaction with acid sites[34]. In Table 1.3 the average activation energies for ethanol is compared for HZSM-5 and silicalite[34] and it can be seen that molecules with a dipole moment are strongly bound to an acidic surface. There was no evidence of reaction up to 180°C when all the ethanol had desorbed.

Table 1.3 Activation energies of alcohols adsorped on ZSM-5.

	Ethanol	Butanol	
HZSM-5[a]	-2.9	-23.7	J/g cat
HZSM-5[b]	-8.8	-18.8	J/g cat

a - Si/Al= ∞

b - Si/Al= 38

Water is a byproduct of the alcohol dehydration and its effect on the reaction is varied. Increasing the water content of the alcohol feed results in more ethene being produced[35] but also caused a loss in activity of the catalyst after regeneration due to the hydrothermal nature of the water. This causes the change in Al(IV) sites to octahedral Al(VI) sites. Changing the water content from 4 to 15 wt% decreased the catalyst life by half[30], attributed to a decrease in crystal structure, while an increase in the C_2-C_4 olefins at the expense of higher aliphatics and aromatics was noticed. An increase in the aromatic content

with an increase in water/ethanol ratio up to 1 was recorded[36] and no catalyst deactivation occurred for 50 hours. This was due to the water preventing the build up of large aromatic molecules, known to be coke precursors, by displacing the light aromatic molecules. It seems that the effect of water is temperature dependent with high temperature causing dealumination with a resultant loss in catalyst activity whereas at lower temperatures the effect is more toward competitive reaction between the water and other reaction intermediates with surface bound species.

1.2.3 Ketones

The reaction of ketones, especially acetone (DMK), over acidic zeolite catalysts has been investigated fairly extensively. Acetone can yield isobutene very selectively[50,55,60] but such selectivity from other ketones such as Methyl-Ethyl-Ketone (MEK) and Diethyl Ketone (DEK) does not occur. This has been explained to be due to the decreasing importance of aldolisation and the increase in intramolecular dehydration in the sequence DMK, MEK and DEK[55]. Certainly the difference in the product spectrum of DMK and DEK has been explained due to the primary reaction steps that lead to different surface intermediates[50,53,55].

A number of reaction conditions have been studied and typical product distributions are listed in Table 1.4[12,50,51].

The reaction mechanism for acetone conversion is complex[51] and has been generally described as a series of aldolisation and dehydration steps occuring after the protonisation of the acetone molecule[48,49,53,57] to the enol form, a mechanism assumed to be similar as that found in homogeneous media[49]. A theoretical study[58] was undertaken to examine the

interactions of ketones, acetone, methyl-ethyl-ketone and diethyl ketone, with the hydroxyl groups in zeolites. This interaction results in the protonated form of the ketone and leads to a transfer of electron density from the ketone to the zeolite and a polarisation of the molecule. These effects cause a weakening of the molecular C=O and C-H bonds and the zeolite O-H bonds. The C-C bonds in the molecule are strengthened. The overall effect is to increase the reactivity of the ketone in the following order DMK < MEK < DEK. Figure 1.12 shows a mechanism that has been followed by IR[54], TPC[53,57] and NH_3 reaction of adsorbed acetone[57] techniques.

The presence of mesityloxide (MO) in the product at low temperatures[12], the fact that MO produces more isobutene than DMK and diacetone alcohol (DAA)[53] and that MO, DMK and DAA all result in deactivation of the catalyst[53] with MO deactivating more rapidly than acetone[51] tend to support this mechanism. Certainly the formation of a protonated acetone molecule[54] and the production of MO from DMK[53] are evident.

This enol form of acetone has been shown to form an interaction with zeolite hydroxyl groups whose IR bands decrease on the adsorption of acetone[49,59]. The weakened state of the C=O band and other IR evidence[54] indicate that the adsorbed acetone is in equilibrium with its protonated form even though the quantity of the latter is small. The enol reacts with a physisorbed acetone molecule to produce DAA, feasible due to the stronger basic nature of acetone than the zeolite hydroxyl groups which allows it to abstract a proton from the enol[54]. Thus the formation of DAA occurs with rapid dehydration to MO[49]. Isobutene can be formed via 1) the cracking of DAA, 2) from the dehydration of MO[53,57] or 3) via the cracking of a higher condensate that, in addition to isobutene, yields a strongly bound oxygen-

Table 1.4 Hydrocarbons from acetone conversion

Reaction conditions		
T (°C)	250	329
Conversion %	3.9[a]	24.5[a]
Carbon Selectivity %		
Diacetone	3.5	0.1
Mesityl Oxide	27.3	1.2
Isophorone	-	5.3
Other O-compounds	6.0	<0.1
CO + CO_2	-	10.0
Hydrocarbons	63.2	83.4
Hydrocarbon Distribution (wt%)		
Methane	-	0.2
Ethane	-	0.4
Ethene	<0.1	1.2
Propane	-	1.9
Propene	2.5	4.2
Butanes	-	0.1
Butenes	19.1	83.3
Pentanes	-	-
Pentenes	-	-
C_6+ Aliphatics	19.1	1.6
Benzene	-	-
Toluene	-	0.1
Ethylbenzene	-	-
Xylenes	-	2.1
Trimethylbenzenes	59.3[b]	4.6
C_9^+ Aromatics	-	0.3
C_{10}+ Aromatics	-	-
C_{11}+ Aromatics	-	-

[a] LHSV = 8, [b] 1,3,5-Trimethylbenzene

containing species[50]. Isobutene has been shown to consist of three carbon atoms from one acetone molecule and a methyl group from another[48]. The formation of isobutene from MO is accompanied by the release of CO_2 which involves only the carbonyl carbon[48]. Other hydrocarbon products are a result of oligomerisation, cracking, cyclisation and methylation reactions of isobutene. This sequence of reactions is terminated by co-adsorbing NH_3 at 150°C[57] which also suppresses the formation of CO_2 and acetone.

The conversion of acetone results in rapid deactivation of HZSM-5[50,60] that changes the product selectivity, reduces the catalyst void volume and the number of free hydroxyl groups whilst the amount of coke increases[50]. Cejka et al.[60] observed that deactivation affects the selectivity of acetone conversion. An initially active ZSM-5 (Si/Al = 13.6) catalyst (100% conversion at 350°C and WHSV = 0.7 h^{-1}) results in a product of 80 wt% aromatics but this changes to 4 wt% aromatics and 75.8 wt% isobutene as the conversion decreased to a steady state value of 5%. The selectivity for the deactivated catalyst was similar to that of a high Si/Al (600) catalyst, which exhibited low initial conversions of < 9%, but after a similar time-on-stream it had twice the amount of carbonaceous residue. The nature of this deactivation has been ascribed to an unsaturated ketonic surface species [50,53] that bridges acidic sites and blocks pore channels. This species is not found in the coke deposits formed from isobutene and DEK reaction and seems to form around a temperature of 250°C[53]. Its formation has coincided with the release of isobutene[50]. This species is thermally stable up to 500°C and its coverage of the hydroxyl groups makes it a reasonable cause for deactivation. Its formation has been found to be more intense in the conversion of MO than for acetone and it is likely that it is produced from condensation products formed from the reaction of MO with DMK[53]. The co-feeding of water

prevents rapid deactivation of the catalyst when reacting acetone possibly by preventing the condensation steps by shifting the equilibrium, for example:

$$DAA \quad <===> \quad MO + H_2O$$

and causing the cracking of DAA to isobutene to dominate[50,51] and preventing the formation of higher condensation products.

The Temperature-programmed-desorption and conversion of DMK, MEK and DEK over HZSM-5 showed a decrease in the temperature of initial reaction and an increase in the amount of adsorbed ketone reacted[55]. This is observed both in theoretical modelling[58] and ketone reactions in an integral reactor[59]. Condensation products occurred for DMK and MEK over HZSM-5 but dehydration starts to play a role for MEK and is the only reaction mechanism for DEK. A comparison of the reaction products for DMK and MEK conversion over HZSM-5 at 250°C and 300°C, shown in Table 1.5, reflects the different reaction mechanisms. The conversion of MEK was higher than DMK under the same reaction conditions and MEK, at temperatures > 250°C, does not yield, compared to DMK, selectively any hydrocarbon but relatively large amounts of aromatics were produced. Other oxygen containing compounds are produced over both acetone (< 15 wt%) and MEK (< 10 wt%) but these were not specified. An increase in the amount of adsorbed ketone resulted in no change in the product spectrum or ratios except that at higher coverages the condensation reaction was favoured for MEK. Over silica-alumina[52] MEK was reacted at 400°C to see if the mechanism for acetone conversion applied to MEK. It was found that condensation of MEK occurred through the methyl group only as propanoic acid was the only acid isolated. Table 1.6 gives the product distribution.

Table 1.5 Hydrocarbon distribution from acetone and MEK over ZSM-5 at 250°C and 300°C and WHSV = 11.3 h^{-1}.

Ketone	Acetone[a]		MEK[b]	
Temperature °C	300	350	300	350
Aliphatics (wt%)				
C_2	0.6	0.8	2.6	3.3
C_3	2.7	1.3	6.6	6.1
C_4	77.5	68.2	9.5	10.7
C_5	-	-	8.5	4.3
C5=	-	-	19.2	6.6
C_6	-	-	-	-
Aromatics (wt%)				
A_6	-	6.3	3.4	14.7
A_7	1.9	3.9	6.3	10.7
A_8	13.8	15.5	29.9	31.4
A_9	3.4	4.0	13.9	12.3
Conversion %	38.9	41.7	65.2	97.1

Ref. Nedomova et al[59]

[a] O-Compounds < 15 wt%

[b] O-Compounds < 10 wt%

Table 1.6 Hydrocarbons from of methyl-ethyl-ketone conversion over silica-alumina at 400°C. (LHSV = 2 h^{-1})

Product	Moles per mole MEK Reacted
Water	0.44
CO_2	0.16
CO	0.02
Propionic Acid	0.09
C_4 Hydrocarbons	0.17
C_5 Hydrocarbons	0.13
C_6 Hydrocarbons	0.16
Coke + Condensation Products	0.19

1.3 Alkene Oligomerisation

Many substances of great utility have been produced by the polymerisation of simple molecules. Of importance in this work is that related to gaseous olefins, difficult to store and transport, which are converted to liquid fuels. Acid catalysts are the key for this process.

It is only in the last thirty years that polymerisation of olefins to liquid fuels has gained importance although the reaction has been known for a lot longer. The catalysts used are of the acidic type with sulphuric and phosphoric acid being the most widely used initially. Certain oxides particularly clays and certain synthetic silica-alumina composites are very active catalysts due to the presence of acidic protons.

The theoretical understanding of the polymerisation process has lagged behind the commercialisation of it but at present there is a reasonable understanding of the mechanism[8]. It now seems possible to classify polymerisation into free radical and ionic, the latter being further divided into cationic and anionic. Anionic, catalysed by basic substances such as metallic sodium, and free radical polymerisation will not be dealt with in this work.

The theory of cationic polymerisation considers the catalyst to be an acid of the Brönsted type. Many catalysts require a "co-catalyst" which induces the Brönsted nature of the catalyst. Examples of catalysts, co-catalysts and the idealised Brönsted acid formed are[8]:

$AlCl_3$	BF_3	SO_3	SiO_2-Al_2O_3	Catalyst
HCl	HF	H_2O	HOH	Co-catalyst
$HAlCl_4$	HBF_4	H_2SO_4	$HAl(OSi=)_4$	Brönsted Acid

In cationic polymerisation the reaction procedes via the formation of a carbonium ion R^+ or protonated olefin[8]. This is the most widely accepted mechanism and the initial carbonium ion is formed by the addition of a proton from the catalyst to the alkene double bond[9].

Besides polymerisation there are numerous reactions that the carbonium ion can undertake leading to a variety of products. The two types of cationic polymerisation, pure and conjunct polymerisation will be given greater consideration here.

1.3.1 Pure Polymerisation

This consists of product alkenes having integral multiples of the monomer alkene. For propene under conditions yielding

pure polymerisation very little dimer is found and trimerisation occurs readily. A liquid product of about 50% nonenes, 25% dodecenes and less than 5% hexenes was formed over solid phosphoric acid at 160°C and 10 atmospheres. The reason for the low yield in hexenes and high yield of nonene lies in the relative reactivity of the tertiary hexyl carbonium ion (XVII) over the secondary propyl ion (XVI)[9].

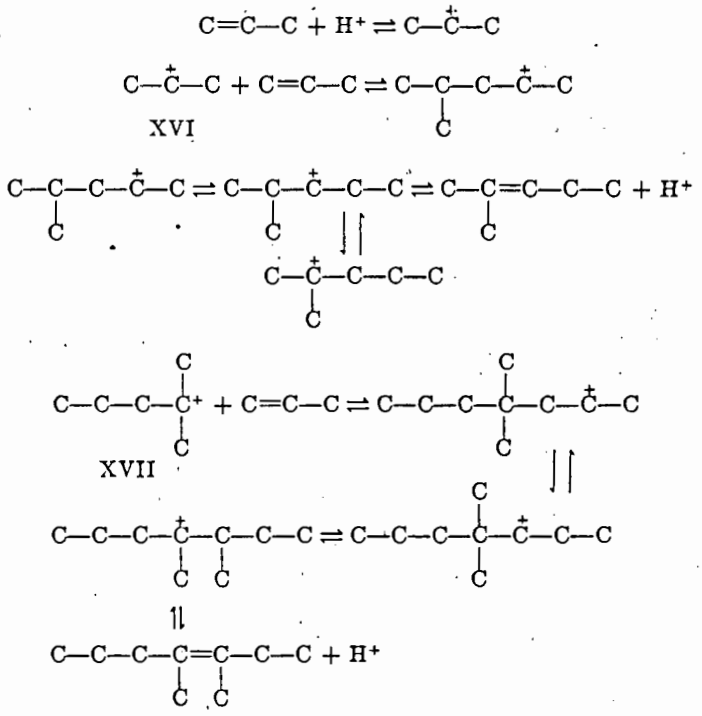

Figure 1.14 Reaction mechanism of propene over acid catalysts

1.3.2 Conjunct Polymerisation

This type yields a complex mixture of alkanes, alkenes, cycloalkanes, cycloalkenes, cycloalkadienes and aromatics in some cases[8]. The products do not necessarily have carbon numbers that are integral multiples of the monomer alkene.

It is evident that the reactions which occur when olefins are reacted over acid catalysts under many conditions are not simple. The products can be accounted for by looking at all the separate reactions that are catalysed by acids, namely[8]:

1) Initiation by proton addition

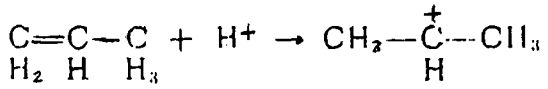

2) Propagation by olefin addition

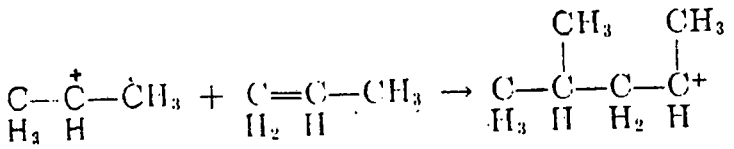

3) Chain termination by proton expulsion

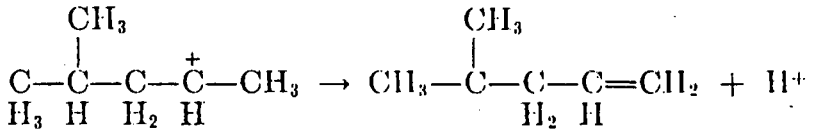

4) Chain termination by proton transfer

$$C_8H_{17}^+ + C_4H_8 \rightarrow C_8H_{16} + C_4H_9^+$$

5) Chain termination by addition of a hydride ion

$$C_8H_{17}^+ + RH \rightarrow C_8H_{18} + R^+$$

6) Depolymerisation

$$2C_5H_{10} \xrightarrow{H^+} C_{10}H_{21}^+ \rightarrow C_6H_{12} + C_4H_8 + H^+$$

....

7) Isomerisation

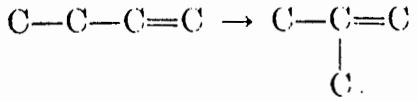

8) Hydrogen exchange

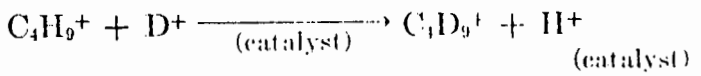

9) Cyclization

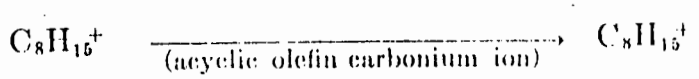

10) Loss of a hydride ion - from large carbonium ions

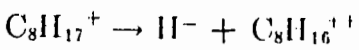

Much work has been done on the oligomerisation of propene over HZSM-5[87-90]. The nature of the product is dependent on a number of factors namely the process conditions and the shape selective nature of the catalyst itself. The reaction has been shown to proceed sequentially by reaction to oligomers followed by cracking and copolymerisation[87]. This results in a changing product distribution with time and temperature. The effect of pressure is to increase the molecular weight of the product. Temperature has the same effect by increasing the oligomerisation rate until about 300°C when cracking becomes significant[87]. The structural nature of the product is determined by the pore size of the catalyst. In this instance HZSM-5 produces mainly methyl branched olefins for high carbon number chains whilst for

low carbon numbers (C_4,C_5) the isomer distribution is approximately at equilibrium. Conversions of >90% for a WHSV = 12 h^{-1}, temperature = 250°C and pressure = 50 Bar has been reported for HZSM-5 with a Si/Al = 35. A typical product distribution[85] is shown in Figure 1.15.

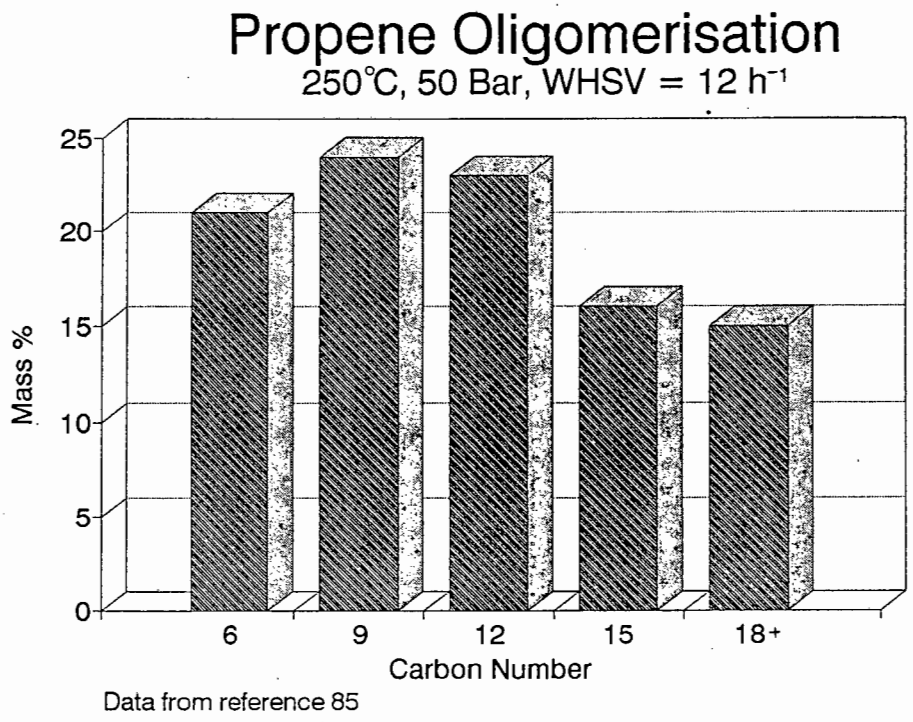

Figure 1.15 Typical propene oligomerisation product distribution

1.4 Hexane Cracking

The use of zeolites for cracking reactions is well known and their improvement over previous amorphous silica aluminas is vast[62] possibly due to the difference in the strength in the Brönsted acidity. However in zeolites the presence of channels allows most, if not all, the sites to come into contact with the reacting material providing the geometries of both are compatible.

Specifically for n-hexane cracking over HZSM-5, the use of this reaction allows the determination of crystallinity and it is used for shape selective characterisation in the constraint index test. There are two mechanisms for alkane cracking:

1) The protonation of a feed alkane molecule across a C-C bond or a C-H bond to form a penta-coordinated carbonium ion that subsequently cracks to another alkane and carbenium ion, the latter cracking via ß-scission to an alkene and a smaller carbenium ion[63].

2) The protonation of a product alkene to tri-coordinated carbenium ions that abstract hydrogens from feed alkanes, which form new carbenium ions that crack to an alkane and another carbenium species[63].

The extent of these reactions depends on the temperature, nature of the alkane feed (branched or linear), conversion and catalyst pore size. The transition state of 2) is larger than 1) and is thought to prevail at high conversions when the amount of product alkenes is large or at low temperatures. Both 1) and 2) occur at Brönsted acid sites. However the adsorption of a product alkene to form a carbenium ion acts as a Lewis acid site as this can abstract a hydride (H^-) ion from a product molecule. This mechanism mainly occurs for branched alkane molecules[65].

It has been conclusively proven that Brönsted acid sites, associated with tetrahedral aluminium atoms, cause this reaction to occur but there are differences on whether the strength or the number of acid sites have more influence on the rate of reaction[11]. However it has been shown that catalytic activity decreases with increasing Si/Al ratio, increasing WHSV and decreasing temperature.

Table 1.7 Product distribution from n-hexane cracking over HZSM-5.

Reference	a	b
Temperature (°C)	500	500
WHSV h^{-1}	4	22.4
Conversion %	98	3.4
Product Distribution w%		
CH_4	10.1	5.2
C_2H_4	4.1	15.31
C_2H_6	15.3	12.58
C_3H_6	8.8	25.78
C_3H_8	33.4	19.45
C_4(iso)	2.4	1.2
C_4(normal)	4.1	4.6
C_4(olefins)	-	10.4
C_{5+}(aliphatics)	1.4	4.1
Aromatics	20.9	0.4

a - Borade et al[62]
b - Gielen et al[64]

olefins at the expense of aromatic products occurred. Certainly the effect of water is important in this work as most of the reactants undergo dehydration reaction and it is rare for most industrial feeds to be completely water free.

The interaction of water with catalysts has been studied[38,44,45,91] previously and it is evident that

interaction prevails between the water and the Brönsted acid site that is involved in all acid catalysed reactions.

Oligomerisation of ethene at room temperature (RT) was noticeably slower on a hydrated catalyst[38] the effect of water increasing with an increasing amount of hydrated sites. Bolis et al.[93] have shown, using I.R., TG/DTA and ^{13}C-NMR, that the chemisorption of ethene is strongly inhibited on a hydrated catalyst surface. When water and ethene are co-adsorbed, competition for the sites results in water being preferentially adsorbed. The reaction of ethene in the presence of water only resulted in a change in the ^{13}C-NMR spectrum at 250°C. In another study ethene reacted rapidly at room temperature to form a polymeric species that cracks at higher temperatures to paraffins which then leave the surface. In the presence of water these sites are partially neutralised. Thus any olefins formed via cracking can leave the surface and appear in the product. Adsorption of ethene on a hydrated surface followed by heating showed no spectrum change until 240°C.

Water has been postulated to exist as H_3O^+ ions at low coverages but forming clusters when more than one molecule per site occurs[45]. The low heat of adsorption (12.1 kcal/mol) means that this adsorbed species is easily removed. Aronson et al.[31] showed that evacuation at RT could remove all adsorbed water in 1.5 hours but also reported that evacuation at RT resulted in 0.7 molecules per site remaining on the surface. At higher temperatures water has a shorter retention time on the catalyst but can still exist in dynamic equilibrium with the acid site[44]. Thus it is still possible for water to interact with zeolite hydroxyl groups which have a strongly adsorbed molecule already associated with it.

High concentrations of water and high temperatures result in catalyst dealumination in which framework aluminium is removed from the structure. Under mild steaming conditions (10-40 minutes, P_{water}= 60-100 Torr, Temperatures = 450-530°C) it is possible for activity enhancement to be achieved for reactions such as alkane cracking[39,43,46] and xylene isomerisation[46]. These conditions result in a decrease in Brönsted acidity but an increased amount of extra framework aluminium. It is likely that the newly formed sites have a higher acidity due to the electron withdrawing effect of the hydrolysed aluminium species on a neighbouring Brönsted site. The nature of the extraframework aluminiun species is uncertain. Severe steaming (2-24 hours, >500°C, 1 atm. water) completely hydrolyses the aluminium and drastically decreases the number of acidic sites resulting in much lower activites. The change in diffusivities of the reactants and products due to the extraframework aluminium should not be ignored.

1.6 Objectives of Research

The aims of this work were:

1) To investigate the effect of co-feeding oxygenates on the oligomerisation of propene over ZSM-5 and

2) To investigate the hypothesis that the co-feeding of oxygenates results in the poisoning of the active sites of the catalyst by preferential adsorption relative to the propene.

2 EXPERIMENTAL

2.1 Catalyst Synthesis and Preparation

2.1.1 Hydrothermal Synthesis

All catalysts were synthesised with a Si/Al = 35 via a method[85] adapted from the patent by Argauer and Landolt (1972)[75]. The reagents used and their quantities for a volume of 250ml are listed in Table 2.1.

Table 2.1. Type, source and quantities of reagents for NaZSM-5 synthesis.

Reagent	Chemical Source and Purity	mass (grams)
TPABr	(Fluka) >98%	25.18
NaOH	(Merck) Pure	1.87
Water	Distilled	100
Ludox	(Dupont) 40 wt% SiO_2	31.84
$Al(OH)_3$	(BDH) Pure	0.4751

The TPABr was dissolved in minimal water in a 250ml Teflon beaker. $Al(OH)_3$ and NaOH were then mixed and boiled (to dissolve the $Al(OH)_3$) in a separate beaker before being added to the TPABr solution which was stirred using a Teflon coated magnet over a magnetic stirrer. The ludox was then added dropwise to the solution while stirring continued. The remaining water was then added.

The Teflon beaker containing the solution was transferred to an autoclave as shown in Figure 2.1 and agitated by a Teflon coated magnet rotated by stirrer controller. The autoclave was sealed and heated at 5°C/min until the final reaction temperature of 160°C was reached. The time period at the final temperature could be varied but typically a synthesis time of 72 hours was used[85].

2.1.2 Post Synthesis Treatments

2.1.2.1 Washing

After the autoclave cooled, the beaker was removed and the catalyst allowed to settle. The supernatant liquid was then decanted after which the catalyst was transferred to a 1 litre flask, washed with water and allowed to separate. The supernatant liquid was centrifuged to catch some suspended catalyst which was returned to the beaker. This procedure was carried out three times before the catalyst was dried in an oven at 90°C overnight.

2.1.2.2 Detemplation

Removal of the TPABr templating agent, which fills the pores of the synthesised catalyst, was carried out in a fixed bed stainless steel reactor as used in the oligomerisation reactions. The catalyst was loaded and heated under a nitrogen flow (60 ml/min) to 500°C and left for eight hours. Air was then introduced at 60 ml/min for a further twelve hours. The pretreatment of the catalyst with nitrogen at 500°C removed most of the organic material through pyrolysis and so reduced the heat from the exothermic oxidation of the template when oxygen is introduced. If pretreatment occurred

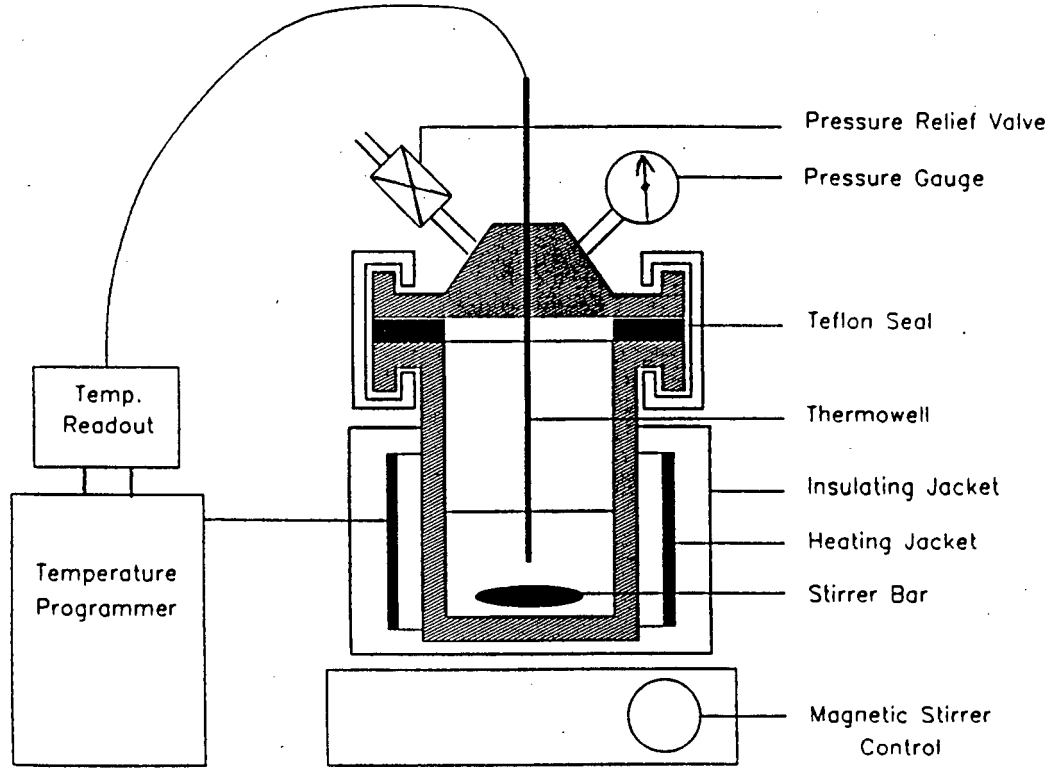

Figure 2.1 The magnetically stirred autoclave

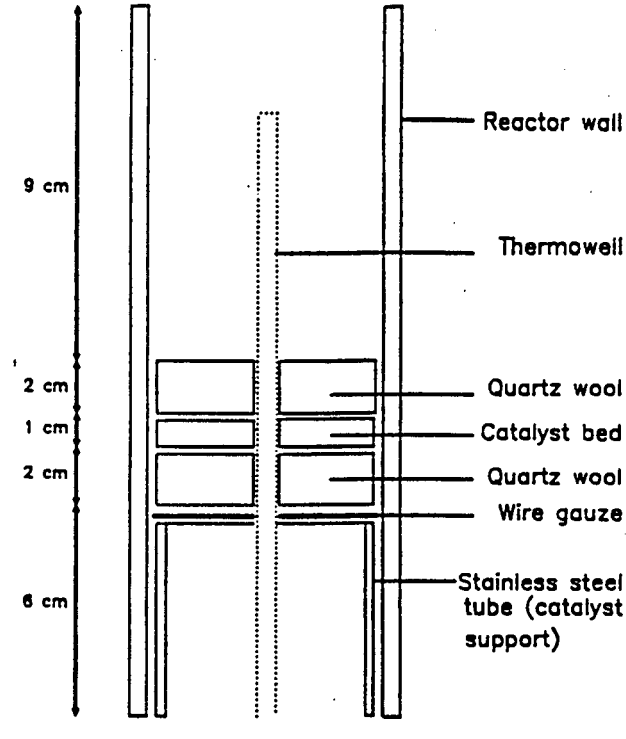

Figure 2.2 Schematic representation of a packed catalyst bed in reactor

with oxygen only, the rapid oxidative decomposition results in an exothermic effect that can result in a temperature increase of up to 30°C and as this decomposition coincides with a release of water the resultant steaming effect can produce dealumination of the zeolite structure[84].

2.1.2.3 Ion Exchange

After detemplation the catalyst was added to 800 ml of a 2 molar solution of ammonium nitrate (NH_4NO_3). The addition of the catalyst to the solution was done with care since the hydrophobic nature of the catalyst caused spitting and subsequent catalyst loss if undertaken quickly. A Teflon coated stirrer bar was added and the beaker placed on a magnetic stirrer-hotplate. The mixture was heated under reflux to 80°C and left for 24 hours. Ion exchange is necessary to remove the charge balancing Na^+ ions and replace them with NH_4^+ ions according to the equation:

$$Na^+\text{-ZSM-5} + NH_4NO_3 \rightarrow NH_4^+\text{-ZSM-5} + NaNO_3$$

2.1.2.4 Calcination

Prior to reaction the catalyst is activated to convert the ammonium form of the catalyst to the acidic proton form. This is illustrated below:

$$NH_4^+\text{-ZSM-5} \xrightarrow{heat} H^+\text{-ZSM-5} + NH_3(g)$$

Calcination was carried out in air, flowing at 30 ml/min, at 500°C overnight. The loading of the catalyst was similar for both the low and high pressure work and is shown in Figure 2.2.

2.1.3 Catalyst Coding

The terminology used was ZS(i) where:

Z - Zeolite
S - Synthesis
i - indicates the batch number and has values from 1 to 5.

2.2 Catalyst Characterisation

Catalysts were analysed using the following techniques:

- X-ray diffraction (XRD)
- Scanning electron microscopy (SEM)
- Atomic Absorption (AA)
- Ammonia Temperature Programmed Desorption (TPD)
- Thermogravimetric and Differential Thermal Analysis (TG/DTA)
- Magic angle spinning nuclear magnetic resonance (MAS NMR)

2.2.1 X-ray Diffraction (XRD)

A Phillips X-ray diffractometer with Cu-K radiation was used. Crystallinity was determined using the heights of the seven peaks[79] in the range, $5°<2\theta<25°$, to that of a reference (ZS3, Si/Al = 35). The range $44°<2\theta<48°$ was also scanned as this range distinguishes between ZSM-5 and ZSM-11. The parameters used for the diffractometer are listed in Table 2.2.

2.2.2 Scanning Electron Microscopy (SEM)

Micrographs of catalysts were taken using a Cambridge S200 scanning electron microscope. The samples were sprinkled on aluminium stubs covered with a water based glue and colloidal carbon mixture. After this they were coated with a thin Au/Pd film. SEM parameters are presented in Table 2.3.

Table 2.2 XRD parameters

voltage	40 kV	slits
current	30 mA	divergent 1°
range	4 x 10^3	receiving 1°
time constant	1	
scanning speed	2 (2 °/min)	

Table 2.3 SEM parameters for Cambridge S200.

Accelerating Voltage (kV)	15
Beam Current (μA)	250
Aperture	30
Resolution	9-10
Working Distance (mm)	10

2.2.3 Thermogravimetric/Differential Thermal Analyses (TG/DTA)

TG/DTA were carried out on a Stanton-Redcroft STA-780 Thermogravimetric Balance. Detemplations were carried out on as-synthesised ZSM-5, calcinations on ion-exchanged catalysts and decoking on post run samples. The conditions and atmospheres used are listed in Table 2.4.

The decoking of deactivated catalysts resulted in a mass loss during the nitrogen stage that was accorded to the loss of high molecular weight, non-graphitic hydrocarbons and an exothermic mass loss under flowing air which was due to the combustion of graphitic coke. Graphitic and non-graphitic are terms used merely to differentiate the two different regions and are not indicative of the nature of the coke.

Table 2.4 TG/DTA parameters.

	Detemplation	Calcination	Decoking
Catalyst mass (mg)	13	13	13
Temperatures °C			
Initial	RT	RT	RT
Final	500	500	600
Rate °C/min	10	10	10
Atmosphere			
Initial	Air	Air	N_2(90mins)
Final	Air	Air	Air(60min)
Flowrates ml/min	30	30	30

RT: Room Temperature

n-Hexane adsorption experiments were also carried out using TG/DTA. 13 mg of catalyst was loaded into the platinum crucible and calcined at 500°C in 30 ml/min of air for 2 hours. N_2 at the same flowrate was then introduced and the temperature cooled down to 70°C at which stage the N_2 stream was passed through a double stage saturator containing the hydrocarbon. The saturation temperature in the second stage was held at 20°C and the vapour was carried by the N_2 through heated lines to the catalyst. The weight gains that occurred were recorded on a dry mass basis.

2.2.4 Ammonia Temperature Programmed Desorption (TPD)

TPD experiments were carried out in a tubular quartz reactor. 0.25 g of catalyst was loaded into the quartz reactor tube and calcined at 500°C for 4 hours in air flowing at 60 ml/min. Ammonia (5% in helium) at 60 ml/min was adsorbed on the catalyst at 100°C for 1 hour before it was replaced by a pure helium stream at the same flowrate.

Desorption of the physisorbed ammonia was allowed to continue for 24 hours. Temperature programmed desorption of ammonia took place in 60 ml/min of helium with a heating rate of 10°C/min up to a temperature of 600°C and held for 45 minutes at that temperature. Ammonia was recorded by a thermal conductivity detector (TCD).

2.2.5 Elemental Analysis (AA)

The aluminium content was analysed using a Varian Spectra AA-30 spectrometer attached to a DS-15 data station. The catalyst sample was prepared by dissolving approximately 0.345 g of the ion-exchanged catalyst with 5 ml of 40 wt% HF, 5 ml of concentrated HCl and 20 ml of Boric Acid in a

polypropylene beaker. The final volume of 50 ml was made up with distilled water. The mass of catalyst was chosen to get an aluminium reading of between 50-100 ppm which was in the linear range of the machine. Calculations to determine the aluminium contents are detailed in Appendix C.

2.3 Reaction of Pure Oxygenate Compounds

2.3.1 Reactor System

The reaction system is shown in Figure 2.3. The reactor was a 20 mm I.D. borosilicate glass tube with a frit placed two thirds of the way down to support a glass wool plug on which the catalyst was placed. The catalyst was then in the middle of the heating zone. The reactor was attached to the stainless steel piping by 3/4" Cajon fittings using Viton high temperature O-rings.

Calcination was done in a flowing air stream at 30 ml/min at 500°C. Oxygenates were fed to the reactor via a Sage 341B Syringe Pump using a Hamilton 20 ml glass syringe with an airtight plunger and Lauer lock end. The line linking the pump to the reactor and the product line to the GC were heated to prevent reactant and product condensation respectively. Nitrogen was used as the carrier gas and was controlled at 30 ml/min by a Brooks 5850TR Nitrogen MFC. The products were analysed using an online HP5890 gas Chromatagraph with FID and a 60m x 0.253 mm DB Wax column linked to an HP3390 Integrator. The products were then condensed and the uncondensed fraction was sampled online for CO and CO_2 using a Varian 3700 Gas Chromatagraph with TCD and a 10′ x ¼" stainless steel Carbosieve S-II column. Light hydrocarbons were trapped in a glass sample loop and injected into a Gow-Mac GC with FID holding a 6m x ¼"

Figure 2.3 Pure oxygenate reaction system

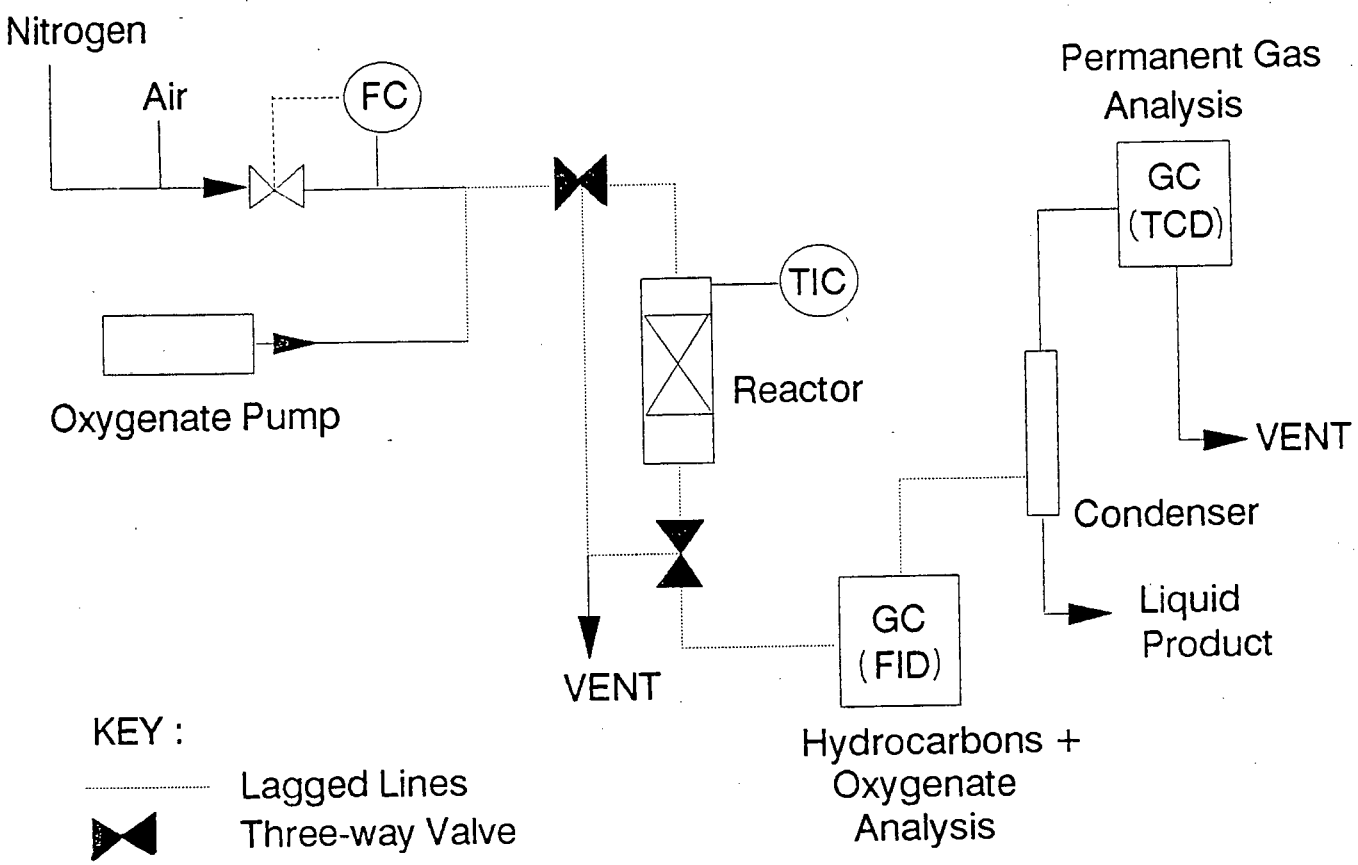

stainless steel Octane Porasil C column.

2.3.2 Reactants and Reaction Conditions

The oxygenates used and their source/purity are listed in Table 2.5. For the pure oxygenate experiments a WHSV = 1 h^{-1} was used for the following reaction temperatures:

Hexane Cracking	250°C
Acetone	250°C
MEK	250°C, 300°C
Ethanol	250°C, 300°C
n-Butanol	250°C, 300°C
Acetic Acid	250°C, 300°C, 350°C

In order to get the required WHSV the density of the oxygenate was obtained and the relevant flow setting on the syringe pump chosen to give a mass flow of approximately 1 g hr^{-1}. Then the same mass of catalyst was weighed out and loaded into the reactor tube.

Table 2.5 Reagent specifications.

Reagent	Chemical Source	Purity
Acetic Acid	Merck	99.8%
Methyl-Ethyl-Ketone	N.T.	Pure
Acetone	BDH	99.5%
Ethanol	BDH	99.5%
n-Butanol	Merck	99.5%
n-Hexane	Merck	99.0%

For hexane cracking studies 1 gram of catalyst was used and the lowest setting of 0.16 $mlhr^{-1}$ on the syringe pump was used when the oxygenates were co-fed. Hexane was contained in a double stage saturator maintained at ambient temperatures through which a N_2 stream at 60 ml/min was directed.

2.3.3 Product Analysis, Calibration Procedure and Estimation of Accuracy

The calibration was done in two stages, firstly the light hydrocarbons from C_1-C_4 and the permanent gases (CO, CO_2, N_2, O_2 and H_2) and then the liquid oxygenates and hydrocarbons. For all the compounds the following formula was used:

$$RF_i = \frac{W\%_i}{A_i} \times \frac{A_{ref}}{W\%_{ref}} \times RF_{ref}$$

where RF_i is the response factor of compound i relative to a reference whose response factor was chosen as 1. For the light hydrocarbons, permanent gases and the oxygenates, propane, nitrogen and n-hexane were the reference compounds respectively. Calibration gases for the light hydrocarbons were used and propane was chosen mainly because it was the tie component between the two bottles. The gas compounds were injected in amounts that lay within the detector's linear range and calibration runs were continued until five were obtained whose results differed from each other by less than 5%.

The calibration of the heavier compounds was more complicated. A 25ml volumetric flask was filled with 5 ml of four components of interest and the reference. The mass of

each 5 ml was noted to obtain a weight percent distribution for the mixture. 5 ml of this mixture was then pipetted into another 25 ml flask and diluted to the final volume by an oxygenate not in the original mixture and whose retention time differed from all the original compounds. This procedure was continued until the mass % of each of the compounds was < 1% of the diluted mass. Then small glass sample bottles with air tight lids, through which injection samples could be taken, were filled and stored in a fridge. Different samples from the various dilution stages were injected to test whether the final samples lay within the linear range of the detector. Again calibration runs were done until five results were obtained within 5% of each other. An average was then taken.

Hydrocarbons of carbon number > 5 generally have response factors very close to 1[96] and for the purpose of this work were assumed to be one, if not calculated separately. To cater for any complex hydrocarbon mixture a liquid sample from a propene oligomerisation run was injected and the product spectrum compared to that obtained for the same sample injected into a Varian GC calibrated for this product. The various hydrocarbon groupings were identified and the retention times noted. Selected aromatics eg benzene (C_6), toluene (C_7), xylenes and ethylbenzene (C_8), some C_9's, n-butyl- (C_{10}), n-pentyl- (C_{11}) and n-hexyl- (C_{12}) benzenes were injected to find retention times. These were used to identify aromatics in the reaction product, easily identified due to their strong intensity.

The accuracy of the calibration response factors is within 5% but including the assumptions of 1 for the hydrocarbons and errors in the injection and weighing of sample it could be slightly higher. Appendix A shows the calculations of conversions and selectivities based on a carbon balance since water could not be analysed.

2.4 Alkene Oligomerisation

2.4.1 Reactor System

The apparatus used for the propene oligomerisation work is shown in Figure 2.4. Liquified propene from a Cadac cylinder was fed to the reactor at 5 MPa via a Lewa FLM1 high pressure diaphragm pump. The feed was dried over 3Å molecular sieve prior to the pumping stage and in order to prevent cavitation, the pump head was cooled by a flowing glycol stream at -12°C. It was necessary to heat the backpressure regulator due to the cooling effects resulting from the flashing of unreacted feed. A stainless steel reactor of 18 mm I.D. was used and placed in an externally lagged brass block heated by 4 cartridge heating elements connected to a PI controller. Catalyst bed temperatures were recorded by a thermocouple placed axially in the reactor from the bottom. Liquid products were collected in a condenser cooled by the glycol stream from the pump head and gas samples were trapped in a glass sample loop. Measurement of off-gas rates was done using a wetgas flowmeter.

The introduction of oxygenates at high pressure was a difficult problem to solve, especially finding a method where the quantity of oxygenate was known and consistently injected. A single-stage high pressure saturator was used firstly in a 'reverse' configuration Figure 2.5 (a), where liquid was forced through the outlet by positive displacement using a high pressure nitrogen source on the inlet side, and finally using the saturator in the conventional way Figure 2.5 (b) by flowing a low rate N_2 gas stream through the liquid and injecting the wet gas into the propene stream. The first method was not consistent in the quantity injected into the feed and also low quantities of

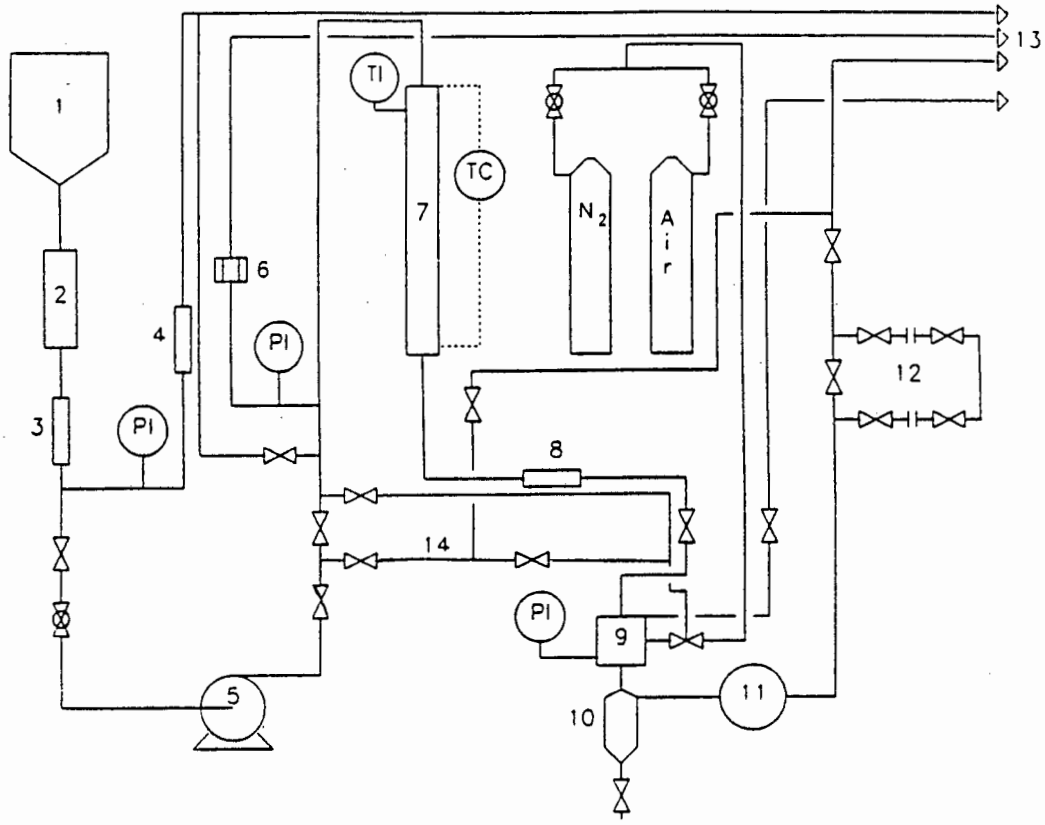

1. Feed cylinder
2. Molecular sieves (3 Å)
3. 0.5 μm filter
4. Pressure relief valve
5. High pressure diaphragm pump
6. Bursting disk
7. Reactor
8. 0.5 μm filter
9. Back pressure regulator
10. Liquid catchpot
11. Wet gas flowmeter
12. Gas sampling loop
13. Flare lines
14. Bypass line

PI Pressure Indicator
TI Temp. Indicator
TC Temp. Controller

Figure 2.4 High pressure oligomerisation rig

Figure 2.5 High pressure saturators

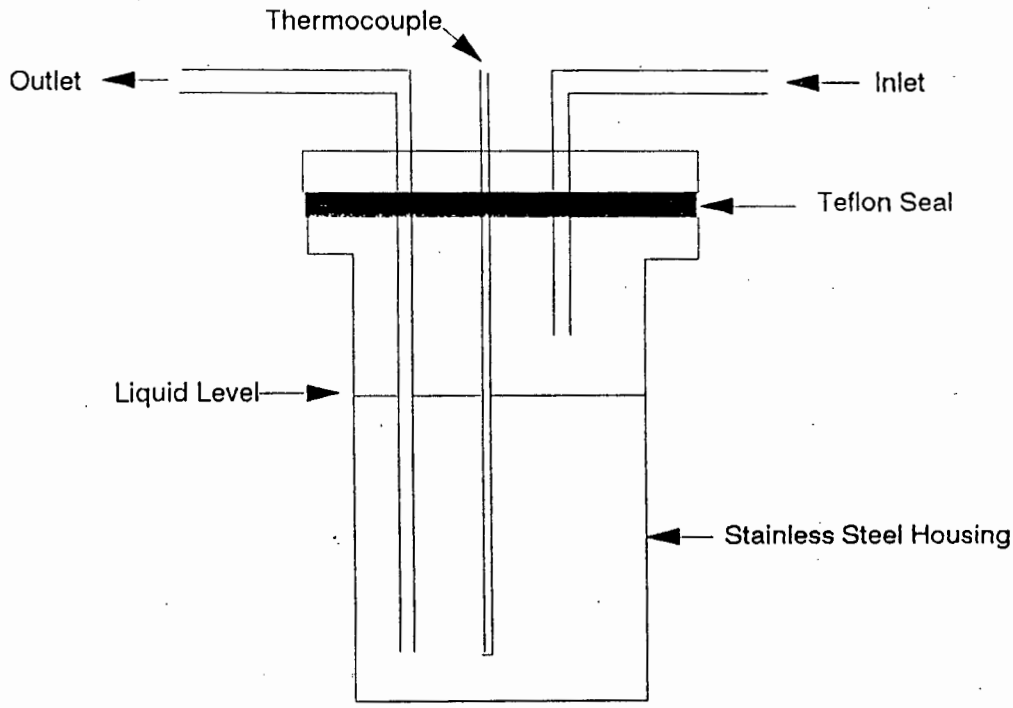

(a) Reverse configuration

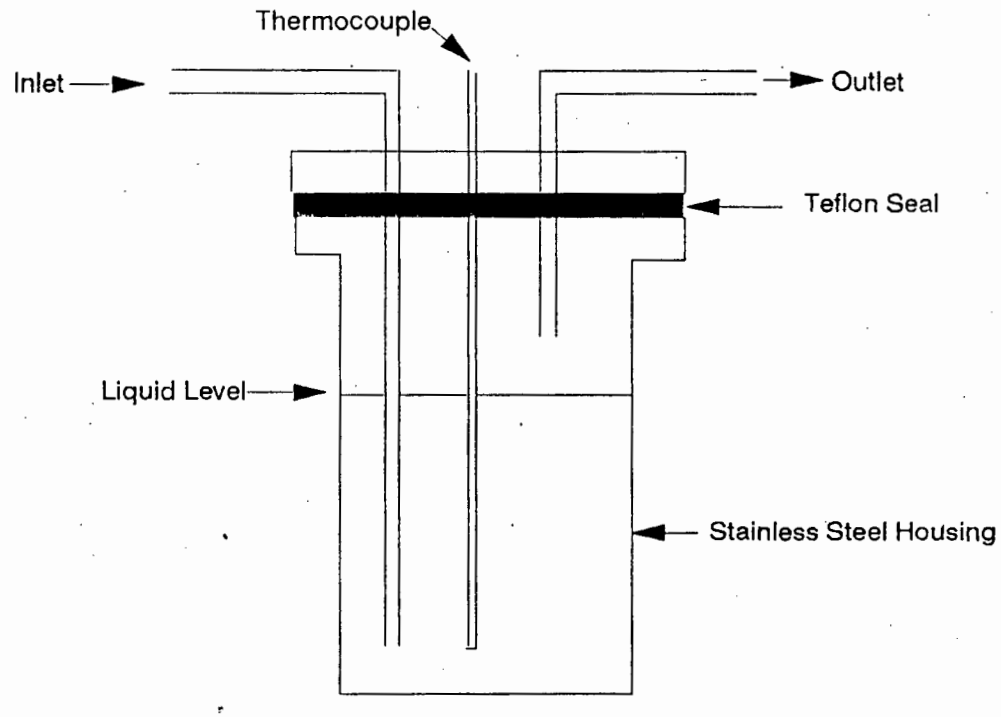

(b) Normal configuration

oxygenate < 10 wt% could not be achieved. The second method also had its disadvantages, namely:

1) Dilution of the propene feed with N_2, and
2) Difficulty in determining the quantity of oxygenate injected.

However reasonable consistency and low concentrations of the oxygenates were its advantages.

Liquid products were analysed on a Varian 3600 gas chromatograph with FID. A 0.351 mm I.D., 30 m fused silica megabore column coated with a 1.5 micron film of DB-1 (100% methylpolysiloxane) was used. The gas products were analysed on the Gow-Mac GC as described in section 2.3.1.

2.4.2 Reactants and Reaction Conditions

2.4.2.1 Pure Propene Feed

The reaction of propene took place at 250°C, 50 Bar and a WHSV of 12 h^{-1}. The feed composition was 86 wt% propene and 14 wt% propane. It was pumped in a liquid phase to the reactor where a preheat zone ensured gasification before the catalyst bed. The calculation of the WHSV and conversion is shown in Appendix E.

2.4.2.2 Co-feeding Oxygenates

The reaction conditions are similar to those for the normal propene oligiomerisation reactions. The nitrogen carrier stream was fed in at a rate of 2.5 ml/min and the high temperature saturator was kept at 90°C for each oxygenate.

Thus the mass % of each oxygenate fed varied according to its relative partial pressure at 90°C and 50 Bar.

2.4.3 Analysis

The tail-gas analysis was done through a Gow Mac GC with FID holding a 6m x ¼" stainless steel Octane Porosil C column as mentioned in Section 2.3.1.

Liquid products were analysed on a Varian gas chromatograph detailed in Section 2.4.1.

Appendix E shows how the conversion of propene was calculated for oligomerisation reactions both with and without the co-feeding of oxygenates. In the case of co-feeding oxygenates the volume of tail-gas, as measured by the wet gas flowmeter, was corrected for the flow of nitrogen diluent. This was done by multiplying the flow by the time period of interest and subtracting this from the total measured volume.

3. RESULTS

3.1 Catalyst Characterisation

The five catalyst batches used in this work were subjected to the various analytical procedures as outlined in the experimental section. The results can be seen in Table 3.1.

An accurate method for identification and determination of ZSM-5 crystallinity has been developed using IR spectroscopy[68]. The optical density ratio of two bands at 450 and 550 cm^{-1} have been used in this respect. The 450 cm^{-1} band corresponds to the asymmetric stretching, symmetric stretching and the bending modes of the $Si(AlO_4)$ tetrahedra. The 550 cm^{-1} band is structure sensitive resulting from the double five-membered rings in the primary unit and thus help in rapid identification of zeolites containing five-membered rings (Figure 1.2). It has been shown that the IR crystallinity varies from the XRD crystallinity by 2-3%[68]. The optical densities for the 550 and 450 cm^{-1} peaks were obtained by integrating (from the baseline) between 635-520 cm^{-1} and 480-440 cm^{-1} respectively. Values for the optical density ratio of approximately 0.8[68-70] indicated a well crystallised sample. The ratios obtained in this work indicate that the catalysts were of a high crystallinity (Table 3.1). Examples of the spectra for a fresh and regenerated catalyst are shown in Appendix I.

Organic structure-directing templates (e.g. TPA) are occluded into the ZSM-5 framework intact and can only be removed via thermal degradation[76]. Pure tetraalkylammonium salts decompose below 300°C[77,78] but due to its incorporation into the framework its stability is increased above 400°C. Calcination in air has shown exothermic DTA peaks between 400°C and 450°C[76,79,72]. The weight lost for a

Table 3.1 Catalyst characterisation results

CATALYST	a) Si/Al	b) Relative Crystallinity %	c) Optical Density ratio	d) Ammonia TPD mmol/g	e) Hexane Adsorption wt %	f) TG/DTA Detemplation wt% H2O	f) TG/DTA Detemplation wt% TPA	g) TG/DTA Calcination wt% H2O	g) TG/DTA Calcination wt% NH3	h) Oligomerisation Conversion %
ZS1	29.1	97.0	0.78	0.6514	8.0	2.0	9.5	2.0	4.5	92.0
ZS2	28.3	95.0	0.74	0.6984	8.5	2.1	9.3	2.0	3.2	97.0
ZS3	29.2	100.0	0.76	0.6523	7.5	1.9	10.1	2.0	4.8	98.0
ZS4	30.0	96.0	0.75	0.6312	7.9	2.9	9.1	2.1	4.3	91.0
ZS5	33.1	100.0	0.76	0.6424	8.0	2.0	15.0	3.0	4.5	95.0

a) Determined from AA Spectrometry
b) Summation of 7 XRD peaks wrt ZS3 as a reference
c) Ratio of 550cm-1/450cm-1 peaks
d)-g) Dry mass basis
h) Propene at 250°C and 50 Bar

Table 3.2 Regenerated catalyst characterisation results

Oxygenate Reacted	Catalyst	Temperature °C	a) Relative Crystallinity %	b) Optical Density Ratio	Ammonia TPD mmol/g	c) TG/DTA Decoke wt % N-G	c) TG/DTA Decoke wt % G
ACETIC ACID	ZS2	350 300 250	94 - -	0.81 - -	0.6921 - -	5.9 5.9 6.9	4.7 2.1 0.0
BUTANOL	ZS2	300 250	92 -	- -	0.6801 -	8.8 9.5	0.0 0.0
ETHANOL	ZS1	300 250	- -	- -	- -	5.9 11.6	0.9 0.7
MEK	ZS3	300 250	100 -	- -	0.6543 -	6.7 4.3	0.8 0.0
ACETONE	ZS3	250	-	-	-	9.3	0.9

a) Summation of 7 XRD peaks wrt ZS3 as a reference
b) Ratio of 550cm-1/450cm-1 peaks
c) Dry mass basis (N-G = Non-Graphitic; G = Graphitic)

100% crystalline material consists of between 2-4 mass% water, accompanied by a large endotherm centered at 127°C, and 7.6-12 mass% TPA^+ (mass lost between 300-600°C[72,81,82]). All the synthesised catalyst detemplations featured exothermic peaks at approximately 450°C and lost between 9-11 mass% TPA. A typical detemplation plot is shown in Figure 3.1.

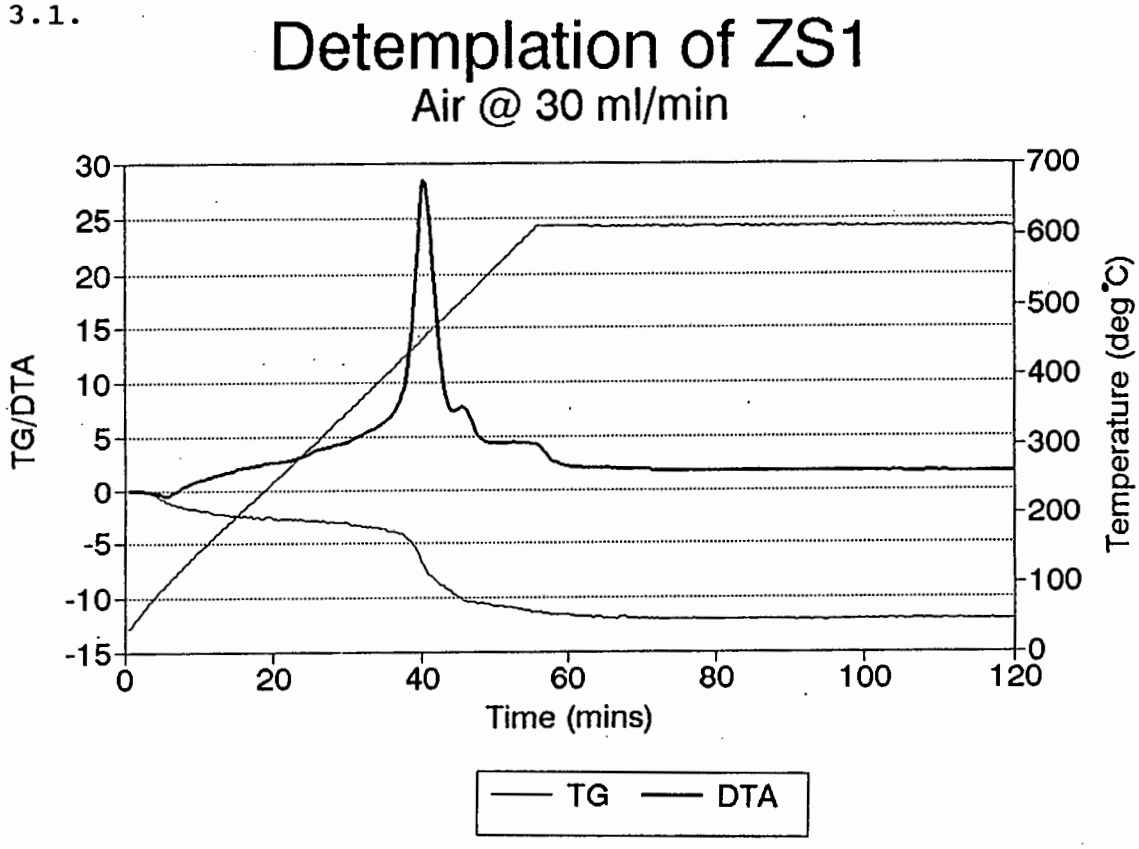

Figure 3.1 Typical detemplation curve of as-synthesised NaZSM-5

^{27}Al MAS-NMR is a valuable tool for probing the coordination, quantity and location of Al atoms. Al is present in the framework in tetrahedral coordination and also outside the framework in ionic or uncharged form with octahedral and tetrahedral coordination. Tetrahedral Al lies between 40-70 ppm[71] whilst octahedral Al is found at approximately 0 ppm[72]. Framework and non-framework tetrahedral Al are found at approximately 60 and 50 ppm respectively. The spectrum of ZS1 (Appendix F) is

representative of all five synthesised catalysts and shows that all the catalysts had tetrahedral aluminium and no extra-framework octahedral aluminium.

The inherent periodicity of a crystal lattice enables it to be used as a diffraction grating for X-rays whose wavelength is comparable to the interatomic spacings. Thus a unique 'fingerprint' pattern (Appendix G) is generated for each crystal structure and for ZSM-5 this can be used not only for identification but also as an indication of crystallinity. In this work the crystallinity was calculated on the intensities of seven peaks[79] using catalyst ZS3 as a reference of 100%. The XRD patterns are the same as those found in the literature[73,74,75,85].

SEM micrographs (Figures 3.3 (a) to (e)) indicate that the catalysts are conglomerates of very small crystals. TPD (Figure 3.2 and Table 3.1) indicated a high degree of ion exchange and values were comparable to those in the literature[92].

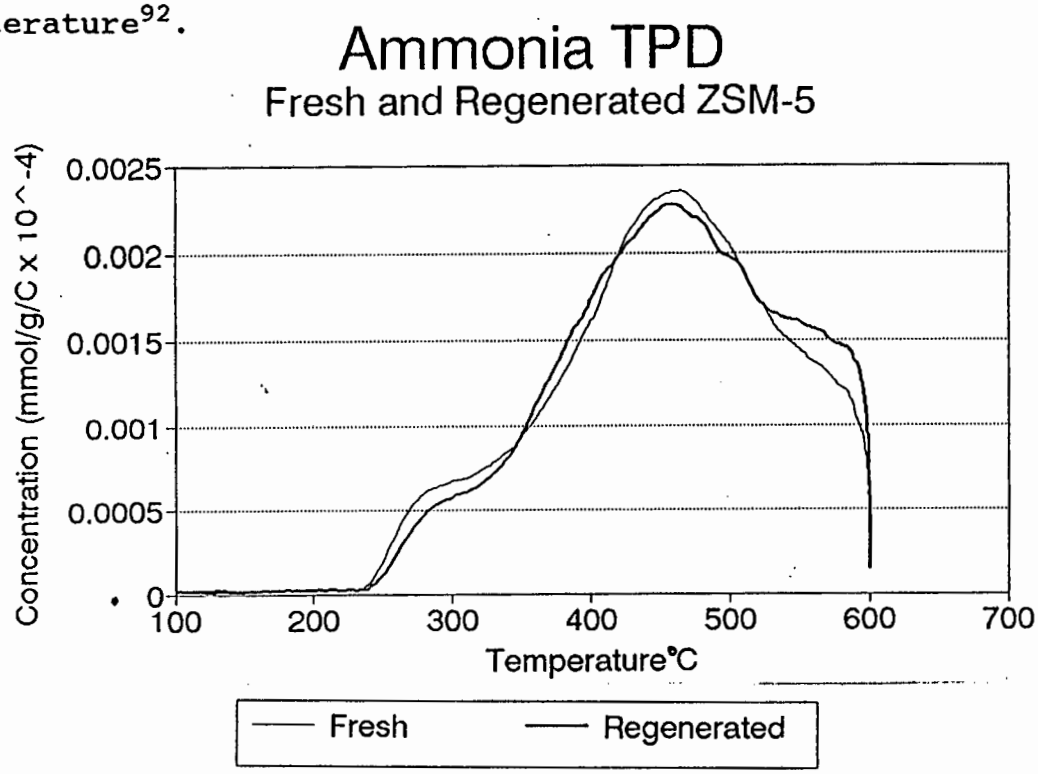

Figure 3.2 Typical TPD curve of fresh and regenerated ZSM-5

Figure 3.3 Electron micrographs of ion-exchanged and regenerated (oxygenate, hours on line and reaction temperature indicated) ZSM-5

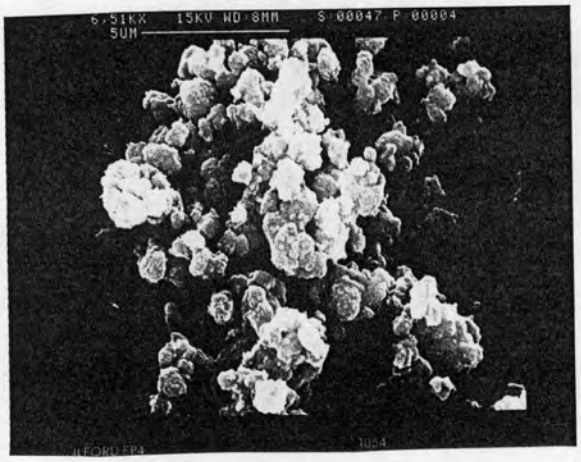

(a) ZS1

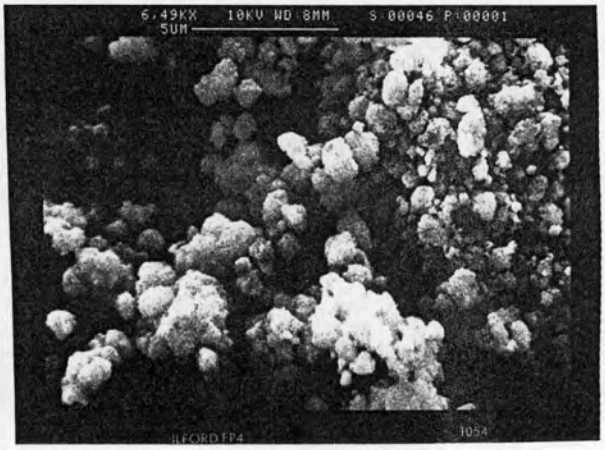

(b) ZS2

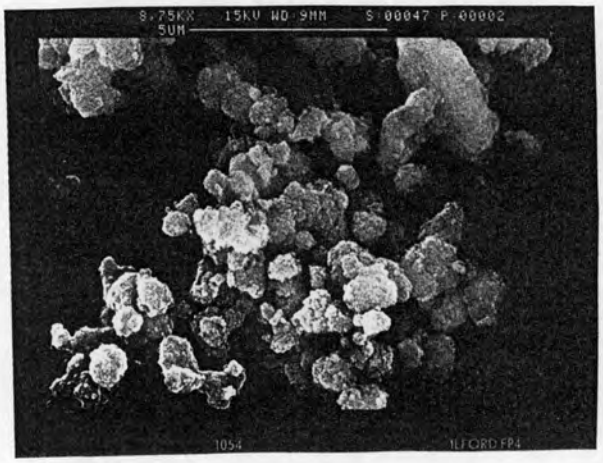

(c) ZS3

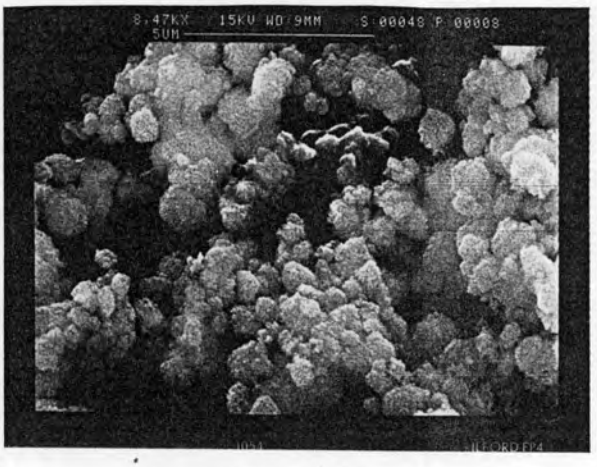

(d) ZS4

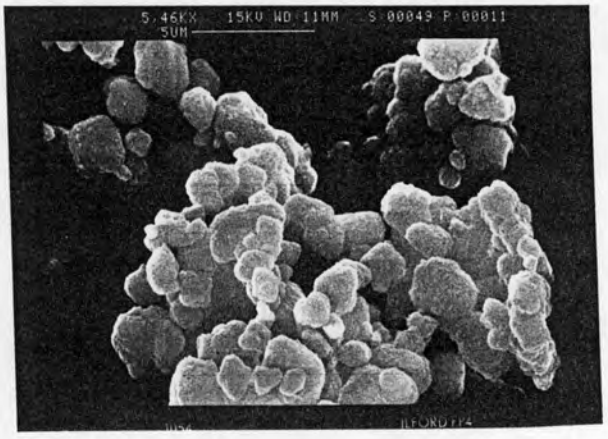

(e) ZS5

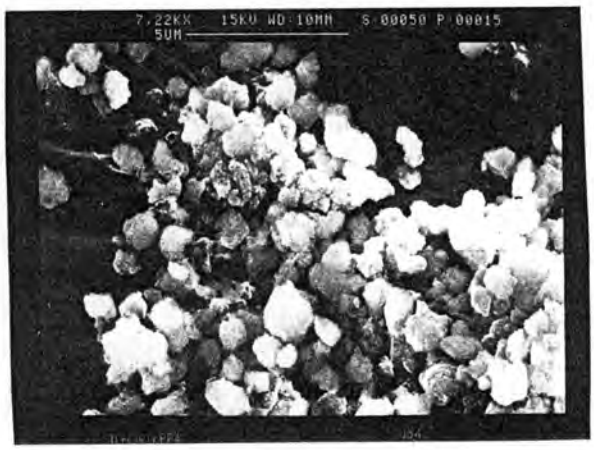

(f) Acetic acid, 10 hours at 350°C

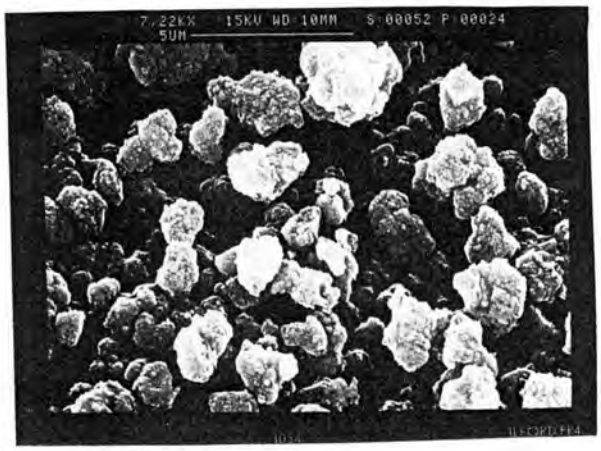

(g) n-Butanol, 10 hours at 300°C

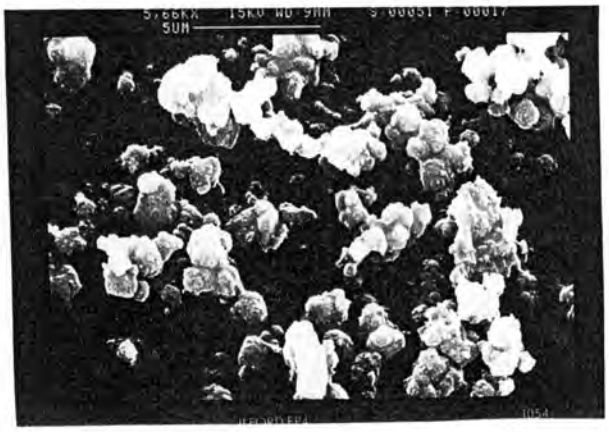

(h) MEK, 10 hours at 300°C

3.2 Propene Oligomerisation in the absence of Oxygenates.

Propene Oligomerisation reactions were carried out on all the catalyst batches to ensure a consistent high activity over a long run time (12 hours) so that differences in activity and/or selectivity between the pure propene and propene + oxygenate oligomerisation results are due to the effect of the oxygenate and not the catalyst. The results are indicated in Table 3.1 and Appendix J represents typical conversion vs run time and product selectivity data.

Before each run when co-feeding of oxygenates was to occur, the nitrogen carrier gas was passed through the reactor bed before it was contacted with the oxygenate in the saturator. The nitrogen had a dilution effect on the reaction as it lowered the conversions (see the oligomerisation during co-feeding results in later sections compared to pure propene oligomerisation represented in Appendix J) but did not affect the selectivity. Normal activity was restored after removing the nitrogen. Mass balances were not conducted due to the equipment lacking facilities for calibration by an internal standard and identifying an oxygenate peak in an oligomerisation product from a chromatograph is impossible.

3.3 Carboxylic Acids.

3.3.1 Reaction of Pure Acetic Acid over HZSM-5

The initial conversions (Based on a carbon balance - see Appendix A) for acetic acid increased with reaction temperature (Table 3.3). Reaction at 300°C and 350°C caused rapid deactivation (Figures 3.4 and 3.6) with the conversions levelling out after approximately 4 hours and 7 hours respectively. Reaction at 250°C produced very low

Table 3.3 Pure oxygenate reaction results

OXYGENATE		CONVERSION t=0*	CONVERSION t=1/2*	SELECTIVITY %							
				Aliphatic Butenes	Aliphatic Others	Aromatic	CO	CO2	Acetic Acid	Propanoic Acid	Acetone
Acetic	1	4.0	0.8	0.1	0.03	22.3	-	65.1	-	-	4.9
	2	28.0	4.0	13.9	2.66	9.9	0.2	17.0	-	-	55.0
	3	99.0	21.0	0.26	0.26	76.2	3.0	20.2	-	-	-
Butanol	1	100.0	100.0	2.82	75.7	21.5	-	-	-	-	-
	2	100.0	100.0	2.84	31.2	66	-	-	-	-	-
Ethanol	1	100.0	100.0	5.81	75.7	18.5	-	-	-	-	-
	2	100.0	100.0	3.18	13.62	83.2	-	-	-	-	-
MEK	1	73.0	32.0	2.11	32.9	29.4	0.07	0.16	15.1	18.4	0.9
	2	96.0	33.0	1.47	21.4	75.5	0.2	0.6	0.03	0.07	0.6
Acetone	1	90.1	48.4	5.69	59.81	26.3	0.03	0.4	7.56	-	-

* t = Normalised Time-On-Stream (t=1 corresponds to a run length of 10 hours)
1 = 250°C
2 = 300°C
3 = 350°C

Table 3.4 Pure oxygenate reaction product - aliphatics selectivity

Component	Temperature °C	Aliphatics Selectivity % a) Total	C1+C2	C3	C4 b)	C5+C6	C7	C8	C9	C10+
Acetic Acid	300	13.55	0.00	0.00	0.31	0.00	0.00	8.33	0.00	4.91
	350	0.53	0.06	0.15	0.26	0.06	0.00	0.00	0.00	0.00
Ethanol	250	80.68	11.10	0.00	4.68	7.41	5.09	1.82	12.96	31.80
	300	15.61	0.00	1.66	4.44	1.50	0.60	0.47	0.37	3.40
n-Butanol	250	77.75	0.00	0.12	1.35	7.29	3.42	2.64	8.79	49.33
	300	34.06	0.00	0.37	2.11	3.63	1.12	1.44	5.37	17.15
MEK	250	35.97	0.24	0.00	0.76	16.46	0.53	0.00	0.41	15.45
	300	22.82	0.34	0.00	0.60	2.42	0.24	0.40	2.44	14.90
Acetone	250	65.50	0.14	0.00	5.69	11.54	1.02	21.74	14.16	11.21

a) Selectivity after NTOS=1
b) Excluding butenes

conversions (< 4%) and thus the deactivation was difficult to monitor. The product spectrum at 300°C (Figure 3.5) showed that the amount of aromatics, the only hydrocarbon present in significant quantities, decreased with time on stream similar to that for the conversion. The selectivity (defined in Appendix A) to acetone, carbon dioxide and carbon monoxide increased with a drop in catalyst activity (as found by Chang et al.[13] and Servotte et al.[21]) indicating a series type nature for this reaction. At 350°C (Figure 3.7) a similar pattern was seen. The amount of product butenes is low at both temperatures due to its rapid conversion to higher hydrocarbon products. Analysis of the non-condensable products for 350°C (Appendix K) showed that isobutene was the predominant component for both reaction temperatures. Its selectivity (light hydrocarbons selectivity - see Appendix B) with respect to the other light compounds increased with TOS. Very small amounts of ethane, propane, propene and butanes were produced of which propene is the next most abundent. As mentioned above the lack of equipment that could use an internal standard, the use of relative response factors and low weight hourly space velocities made the calculation of mass balances impossible for the pure oxygenate reactions.

3.3.2 Influence of Acetic Acid on Catalyst Properties

As can be seen in Table 3.2, Figure 3.3 and Appendix H reaction of acetic acid did not result in a loss of acidity or structure as indicated by ammonia TPD and XRD. Thus no dehydroxylation and no change in crystal structure by dealumination occurred. SEM (Figure 3.1 (f)) did not indicate a change in catalyst morphology and TG/DTA (Table 3.2) showed that only non-graphitic coke was produced at 250°C whilst increasing amounts of graphitic coke was produced at 300°C and 350°C. The total amount of coke

increased with reaction temperature and so did product selectivity to aromatics which are coke precursors[50].

3.3.3 Co-feeding trace Acetic Acid with Propene in Oligomerisation Reactions.

The co-feeding of acetic acid inhibited the reaction of propene at oligomerisation conditions. Figures 3.8 (a)-(b) show how the conversion and the liquid hydrocarbon production rate were affected by the insertion of trace acetic acid in the feed. Appendix L shows the effect of oxygenates on the bed temperature and propene mass % (in the tail gas) during propene oligomerisation. An important fact to note is that even after withdrawal of the oxygenate no resumption of the original activity occurred indicating that the acid has a irreversible effect on the catalyst. Figure 3.9 (a) shows that the selectivity for the reaction was not influenced by the acid.

In one propene oligiomerisation run in which an excess of acid was introduced (· 20 %) the catalyst was completely deactivated and the product liquid analysed on a HP 5890 Series 2 GC, fitted with a mass spectrometer detector, showed that only acetic acid was present with no trace of any other compounds.

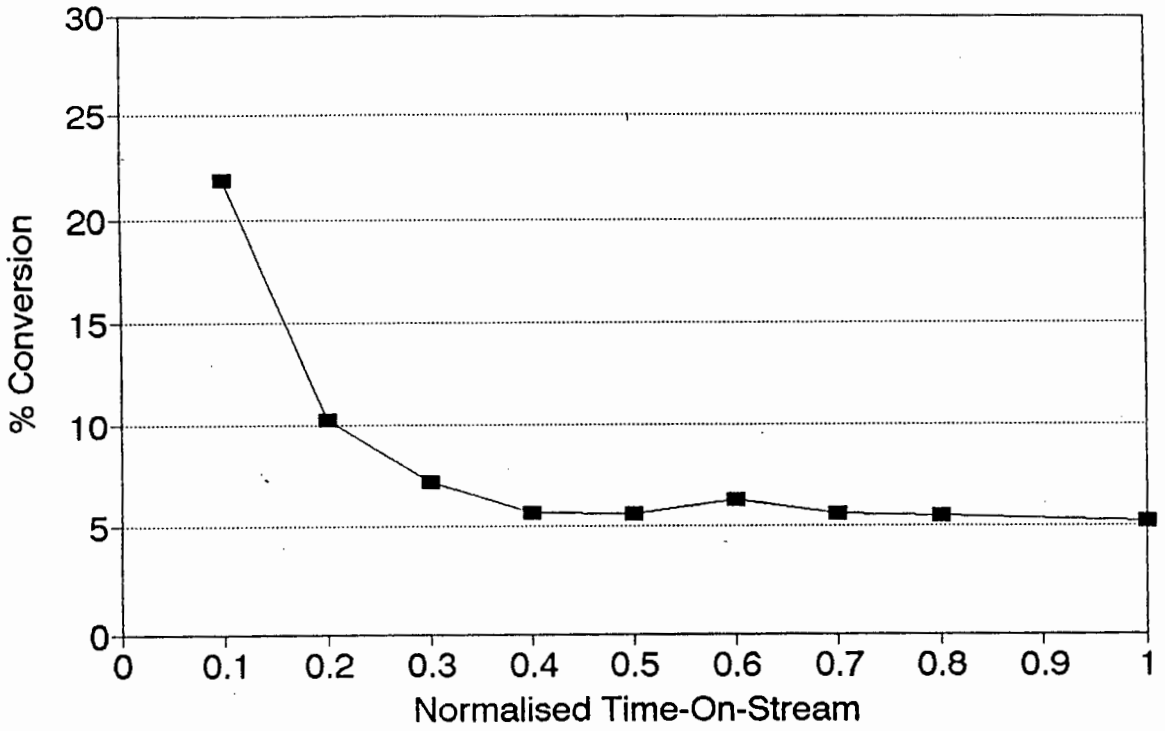

Figure 3.4 Conversion of acetic acid at 300°C

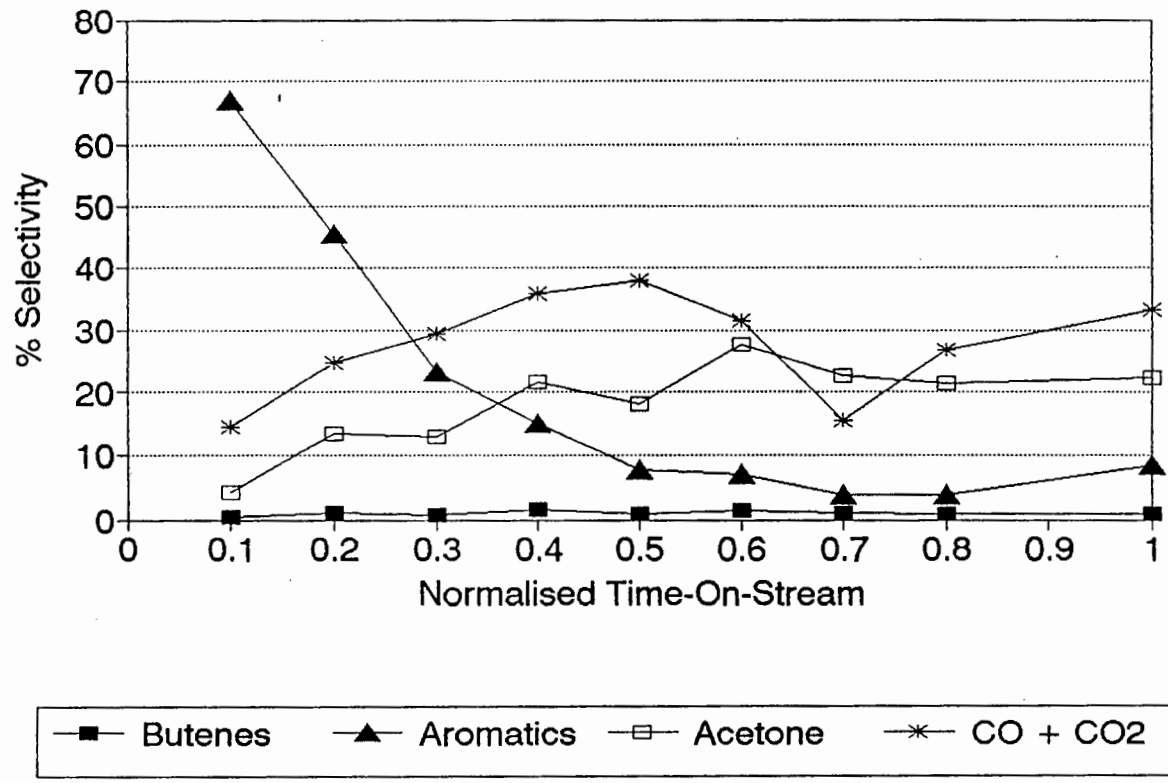

Figure 3.5 Product selectivity for acetic acid conversion at 300°C

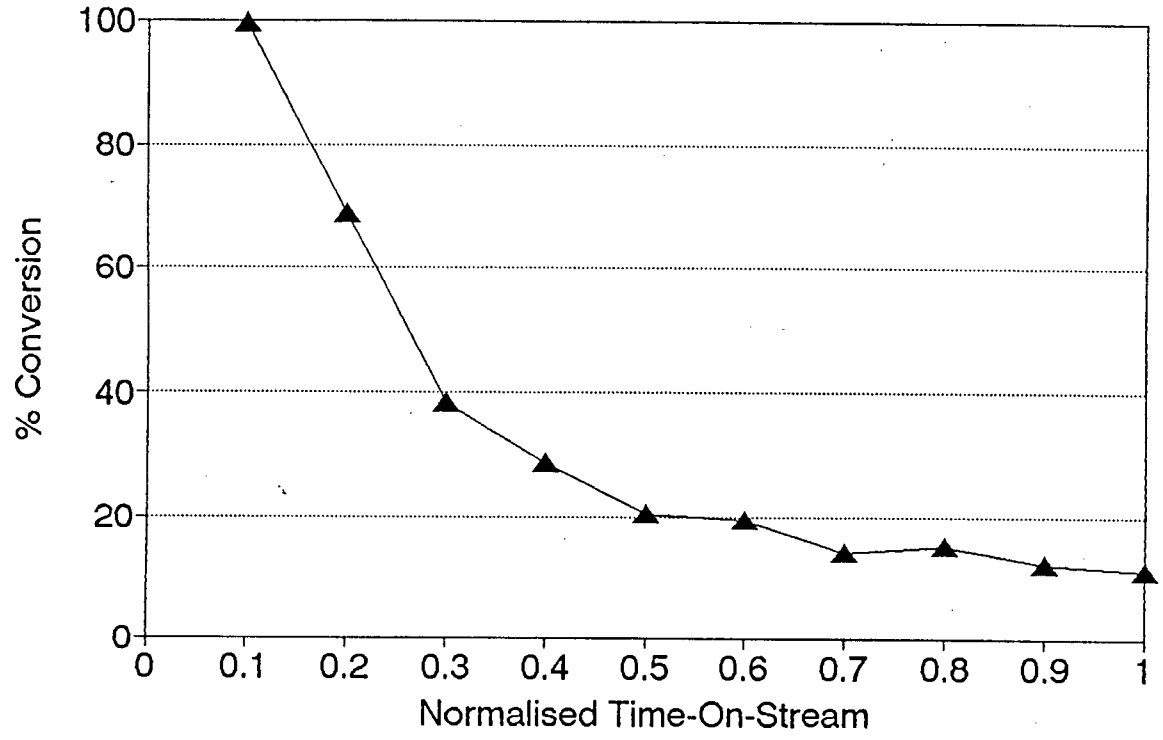

Figure 3.6 Conversion of acetic acid at 350°C

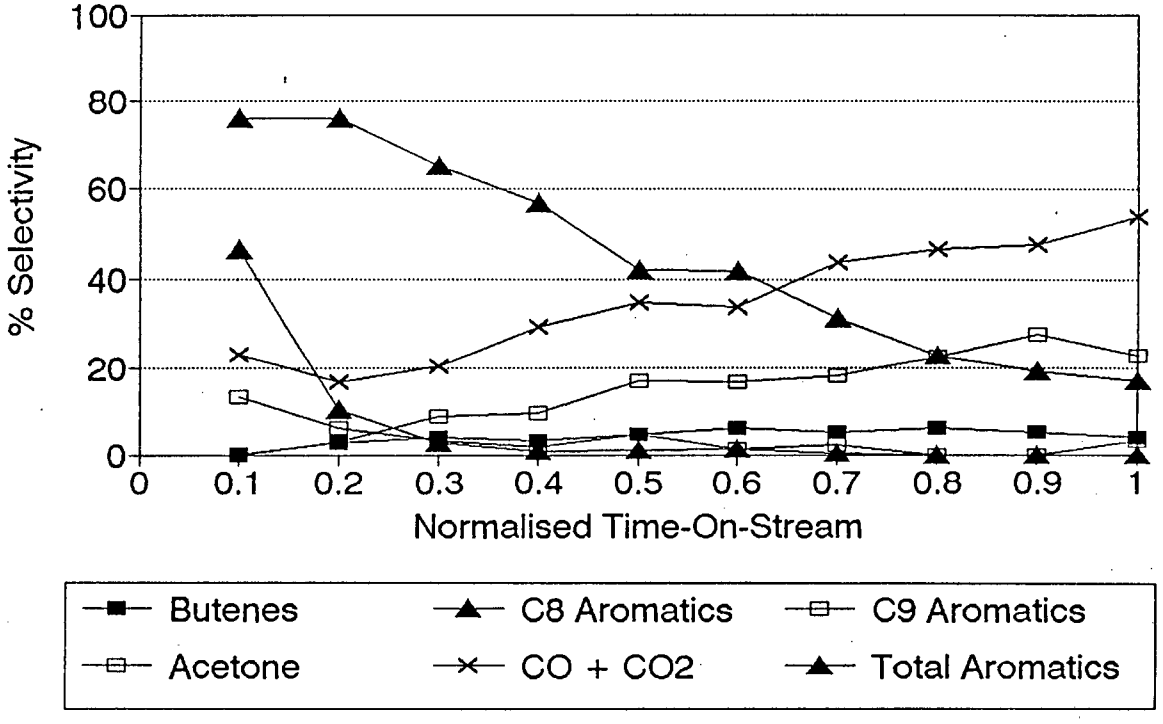

Figure 3.7 Product selectivity for acetic acid conversion at 350°C

Figure 3.8 Propene oligomerisation results co-feeding acetic acid

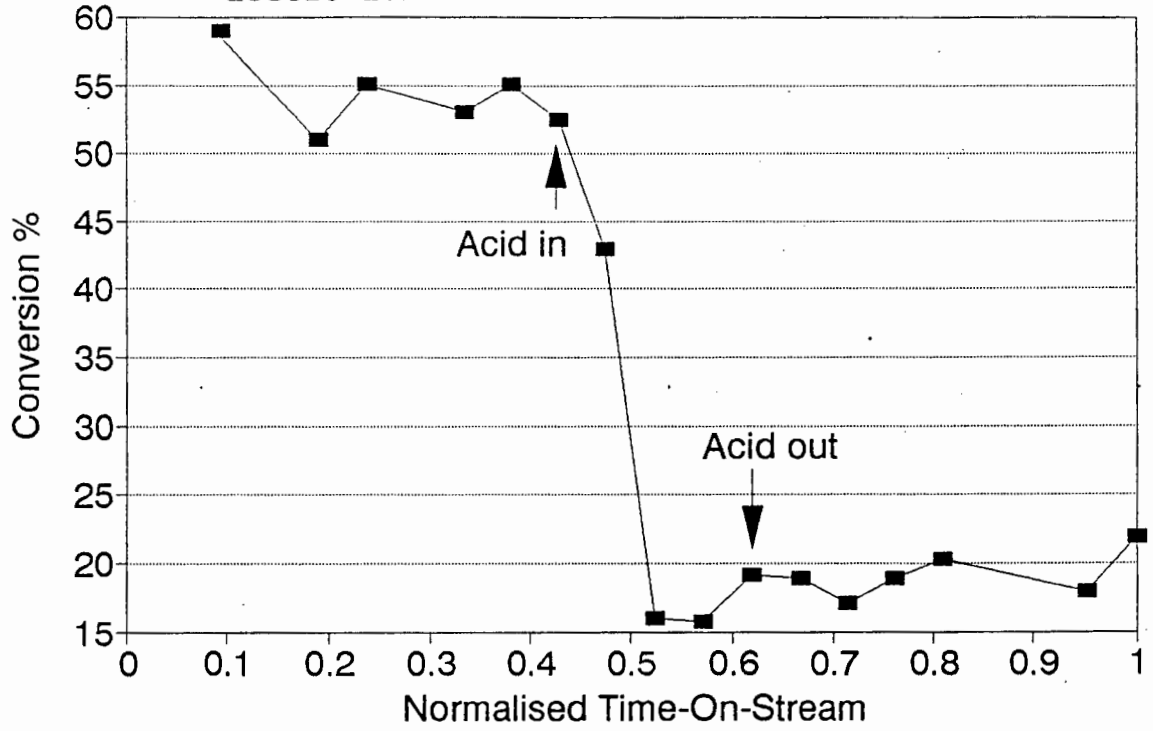

(a) Conversion vs NTOS

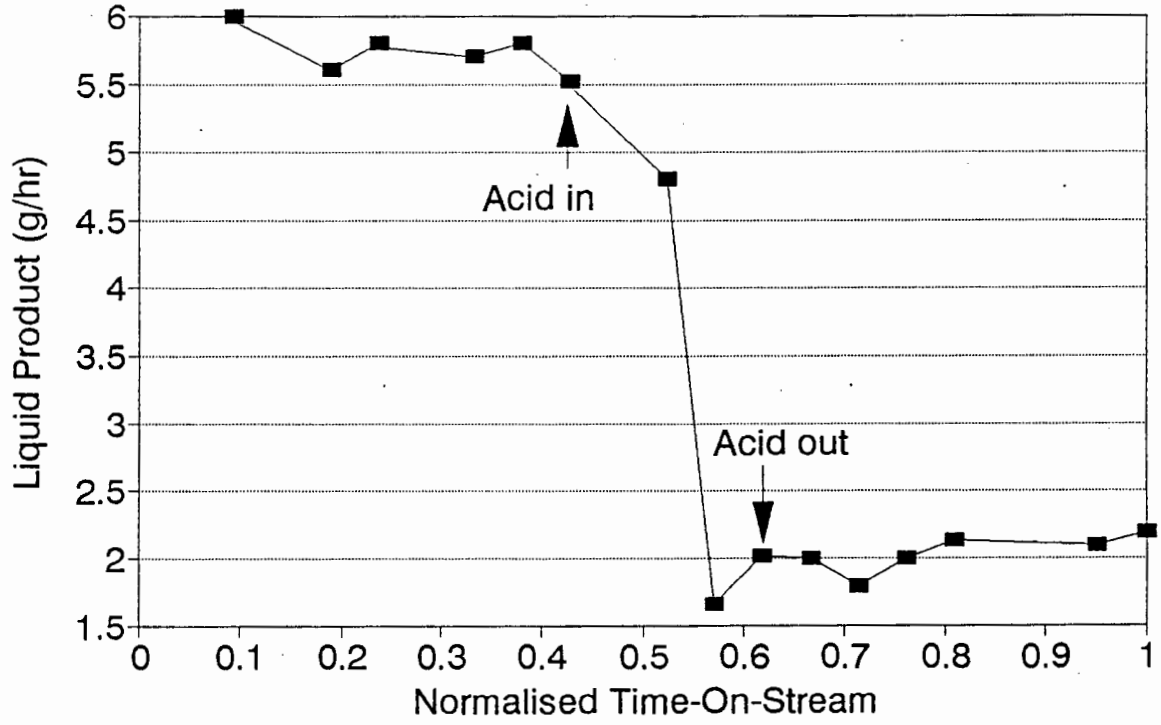

(b) Liquid product (g/hr) vs NTOS

Figure 3.9 Liquid product spectra for propene oligomerisation during co-feeding of:

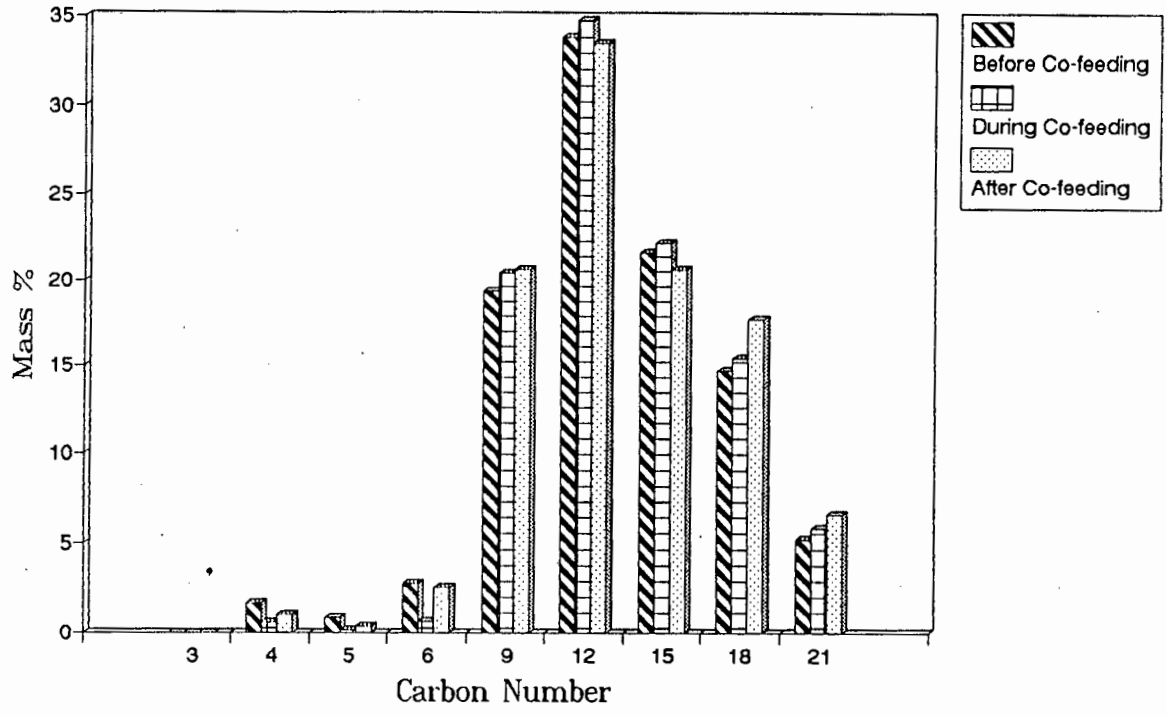

(a) Acetic acid

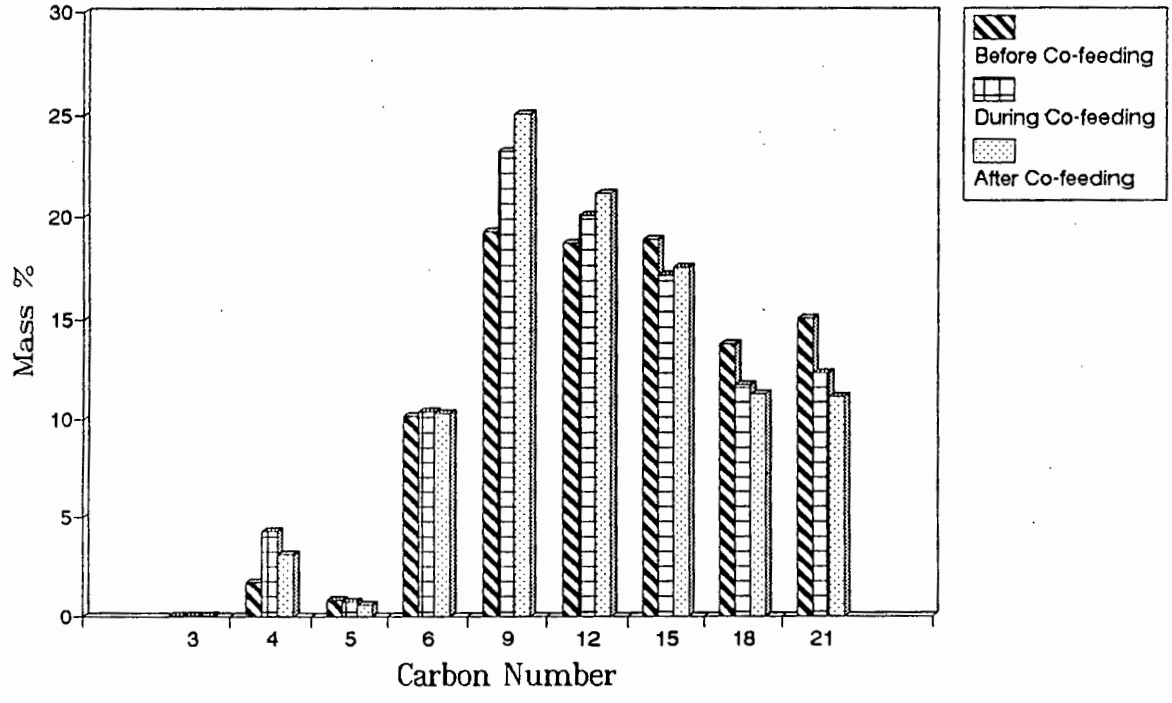

(b) Water

3.4 Alcohols.

3.4.1 Reaction of Pure Alcohols over HZSM-5

3.4.1.1 Ethanol

At 250°C there was a preponderance of aliphatic compounds during the time-on-stream and the percentage selectivity to these compounds increased slightly with TOS (Figure 3.10). The opposite was true for the aromatic products which which were roughly between 10-25 % of the aliphatic product and their selectivity decreased with time. The amount of butenes recorded reached a maximum after a normalised time of 0.4 after which it decreased. The analysis of the non-condensable products (Appendix K) showed that the predominant product was ethene with the butenes not showing the trend seen in the bulk product analysis. All the other products decreased with time except that of ethene which increased and then plateaued after 0.3-0.4 normalised time. This is possibly due to the deactivation of the catalyst resulting from coke formation which has been reported elsewhere[27,29,30]. Conversion, however, remained at 100% for the entire run and there was no evidence of combustion reactions since no CO_2 and CO was recorded. Cracking was not significant as little methane was found.

At 300°C there was a reversal in the relative ratios of aromatics and aliphatics with the former being produced in the greater quantities (Figure 3.11). Selectivities to both aromatics and aliphatics remained fairly constant at 87 wt% and 16 wt% respectively. Only after a normalised time of 0.8 was there any indication of deactivation as seen by the drop in aromatic selectivity. The proportion of butenes analysed in the non-condensable product (Appendix L) remained

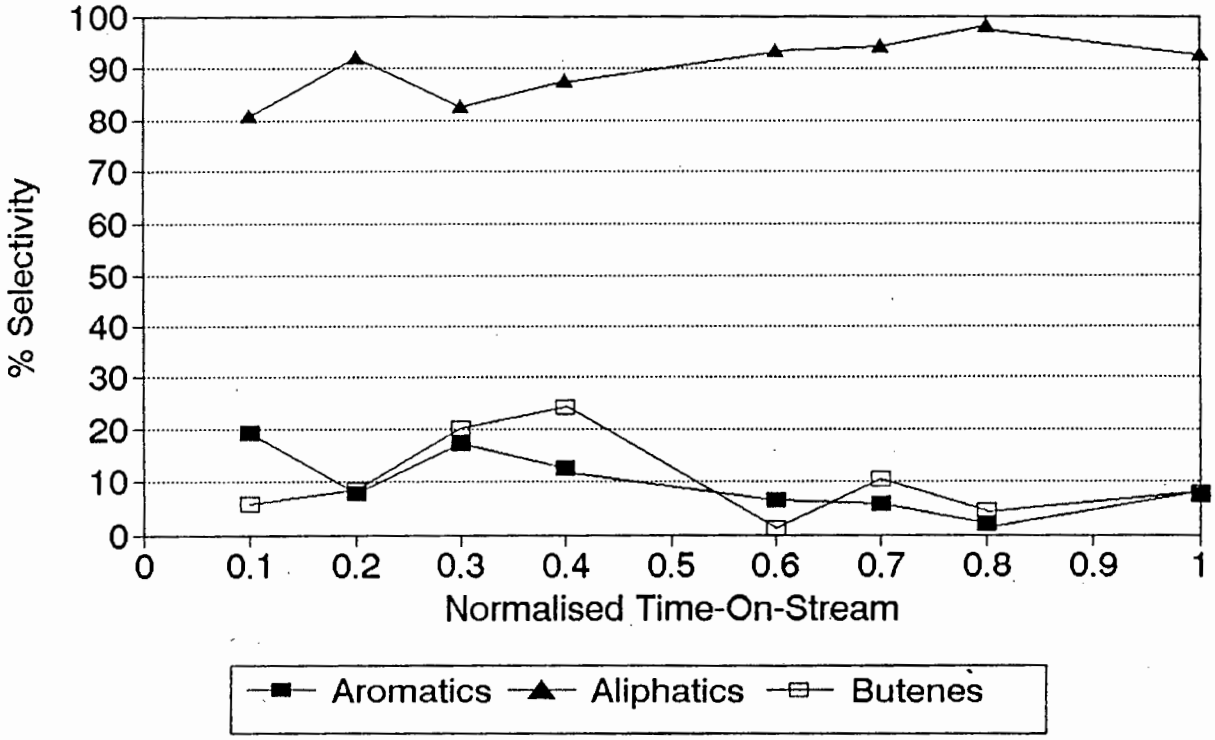

Figure 3.10 Product selectivity for ethanol conversion at 250°C

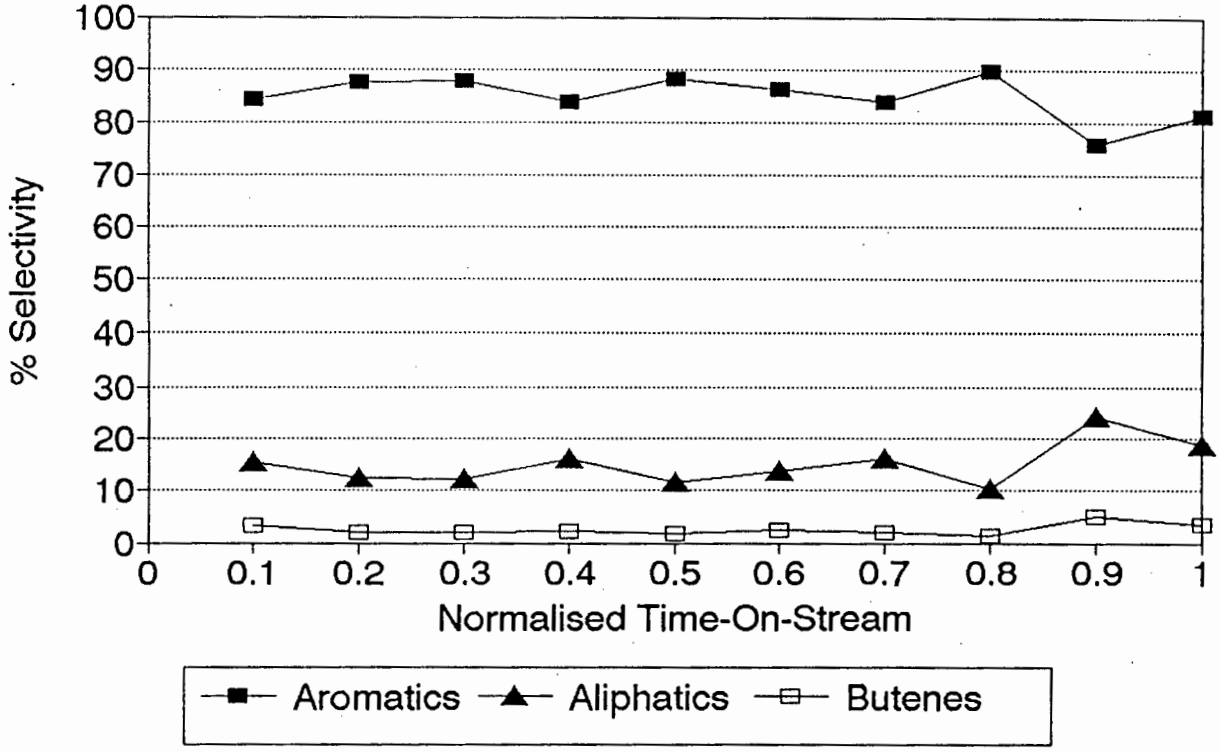

Figure 3.11 Product selectivity for ethanol conversion at 300°C

constant until the onset of deactivation after which it increased slightly. The C_3-C_4 paraffins were the most dominant products whilst ethene, propene and the C_4 olefins all remained at less than 10%. Conversion was 100 % for the entire run.

3.4.1.2 n-Butanol

Selectivity to aliphatic products was greater than that to aromatics at 250°C and the aliphatic content increased almost immediately (Figure 3.12). The similarity of the reaction products of ethanol and n-butanol at 250°C indicates that the reaction mechanism is similar. At 300°C the ratio of aromatics to aliphatics (Figure 3.13) inverted as with ethanol, and their selectivities remained fairly static over the run time.

The C_4 olefins were the main non-condensable hydrocarbons at 250°C (Appendix K) and their selectivity increased with time. No methane was detected, the amount of C_4 paraffins dropped with time and propene remained constant. For both ethanol and n-butanol the corresponding alkene was the most abundant light hydrocarbon. The light hydrocarbons at 300°C (Appendix K) showed that the C_4 components are the most abundant. An inversion at NTOS=0.4 occurred with the C_4 paraffin/C_4 olefin ratio, changing from >1 to <1. A similar event also occurred for the propane/propene ratio with the unsaturated hydrocarbon becoming more abundent with time. These trends indicate a drop in catalyst activity that is not reflected in the bulk product analysis i.e. a drop in the aromatic content. Unlike ethene in ethanol conversion, the butenes remain the most abundant hydrocarbon in the non-condensable phase possibly because the dehydration steps are so fast that the further reaction steps of the alkene are rate determining.

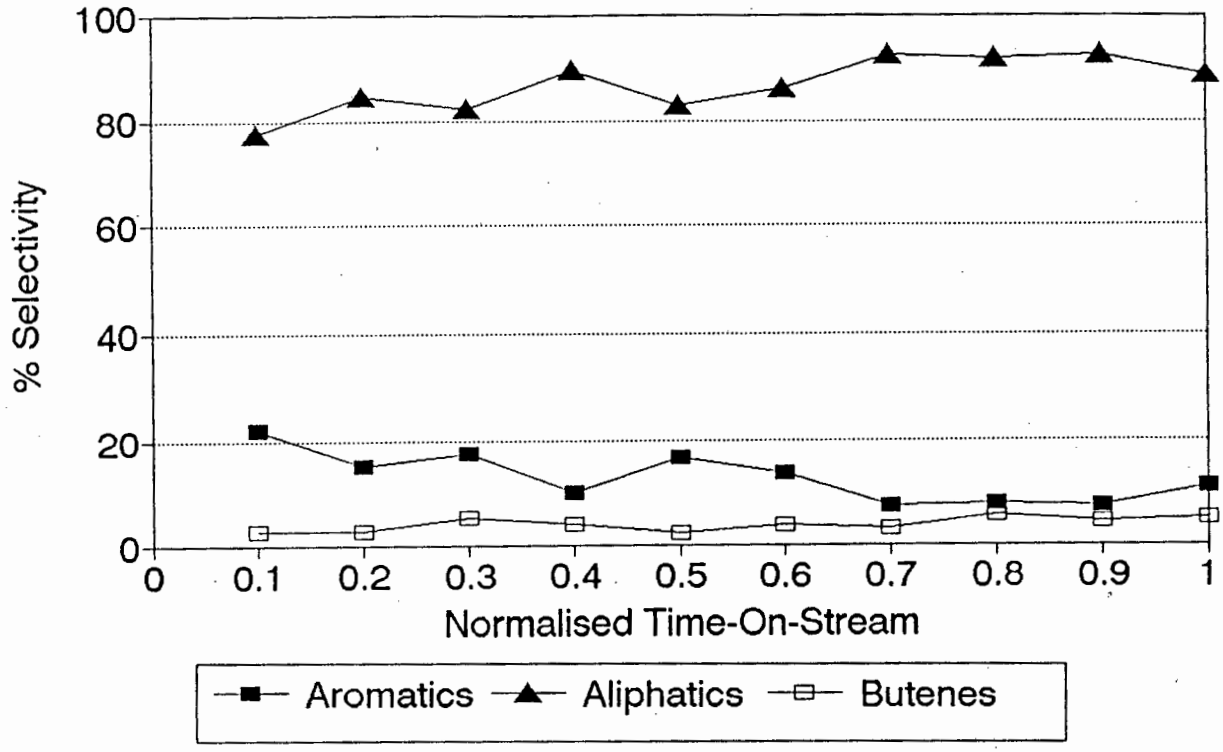

Figure 3.12 Product selectivity for n-butanol conversion at 250°C

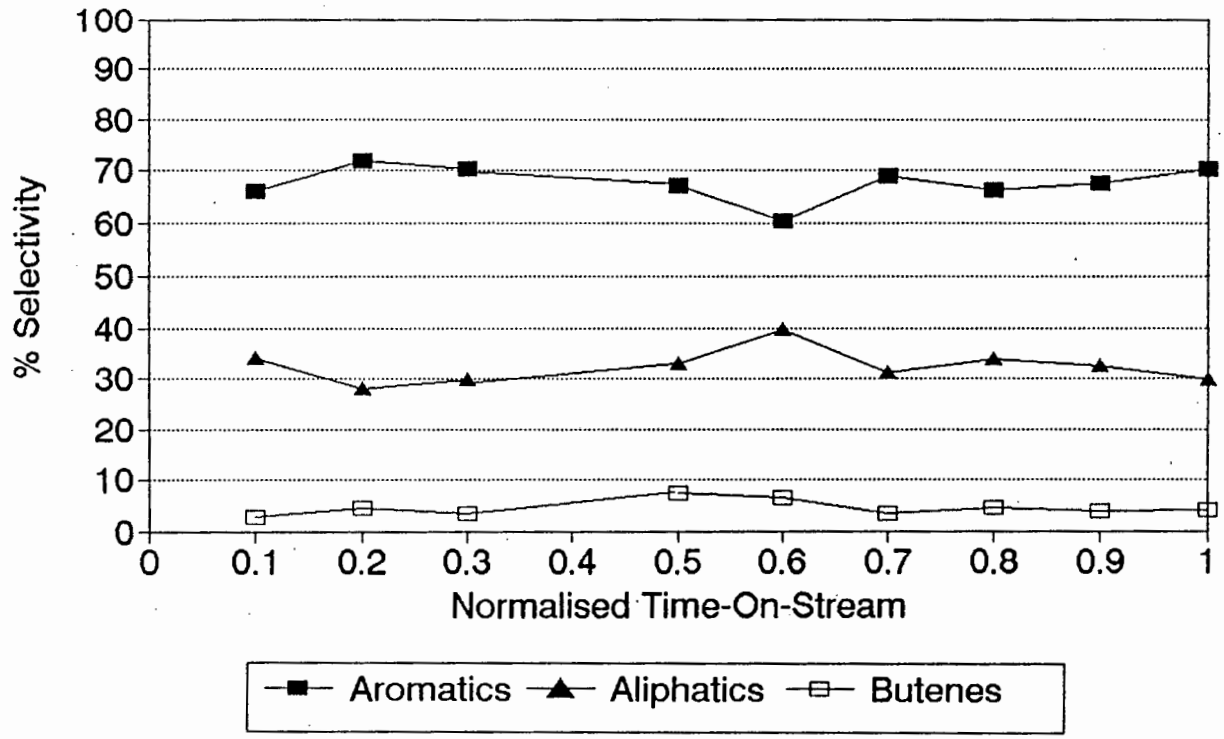

Figure 3.13 Product selectivity for n-butanol conversion at 300°C

3.4.2 Influence of Alcohols on Catalyst Properties

The reaction of alcohols (only catalyst reacting with n-butanol was analysed) resulted in coking of the catalyst. TPD and XRD of the spent catalyst (Table 3.2 and Appendix H) showed no evidence of reduced acidity or crystallinity. TG/DTA (Table 3.2) showed the amount of coke produced from alcohols over HZSM-5. There is a decrease in the mass of non-graphitic coke with temperature which indicates that some of the high boiling products formed could desorb from the catalyst at 300°C and not at 250°C. Ethanol produced small and insignificant amounts of non-graphitic coke. Figure 3.3 (g) indicated that the morphology of the regenerated catalyst was the same as the fresh catalyst.

3.4.3 Co-feeding trace Alcohols with Propene in Oligomerisation Reactions

3.4.3.1 Ethanol

The introduction of ethanol into the propene feed stream showed a similar effect to that seen by acetic acid with one important difference. Although the conversion, bed temperature, propene mass % in the tailgas and the liquid production rate all decreased during the cofeeding, the effect was less dramatic than that for the acid and once the ethanol was removed the original values for the above properties were restored. This can be seen in Figures 3.14 (a)-(b) and Appendix L.

3.4.3.2 n-Butanol

The introduction of n-butanol into the propene feed caused a

similar result to that of ethanol although the effect was less intense. It should be noted that the activity for the reaction decreased on co-feeding the alcohol but returned to the pre-cofeeding values on its removal from the alkene feed. These results are shown in Figures 3.15 (a)-(b) and Appendix L.

Figure 3.14 Propene oligomerisation results co-feeding ethanol

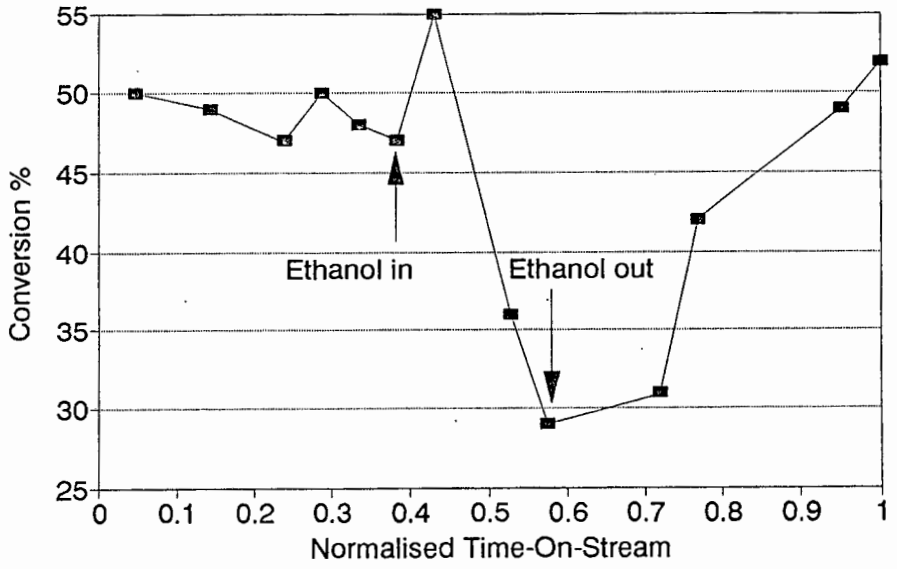

(a) Conversion vs NTOS

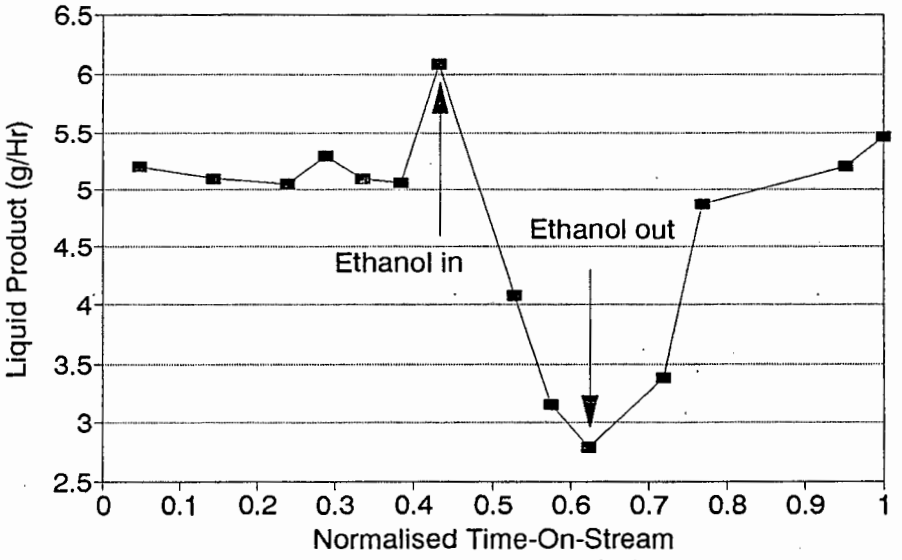

(b) Liquid product (g/hr) vs NTOS

Figure 3.15 Propene oligomerisation results co-feeding n-butanol

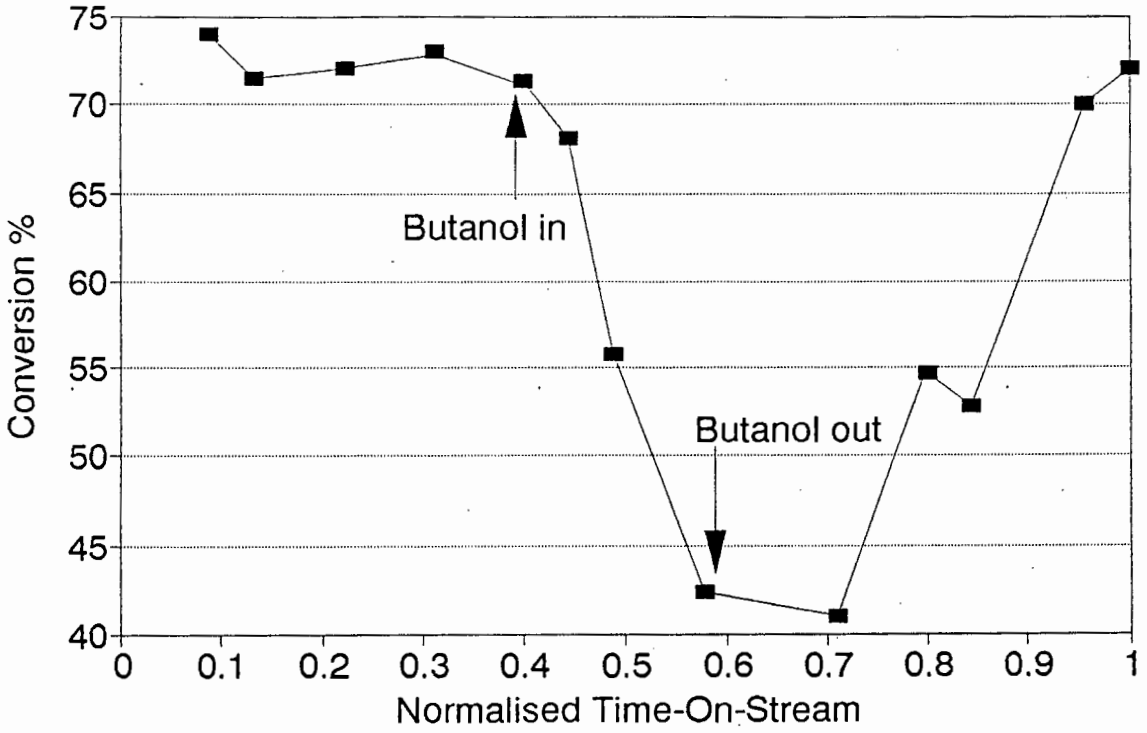

(a) Conversion vs NTOS

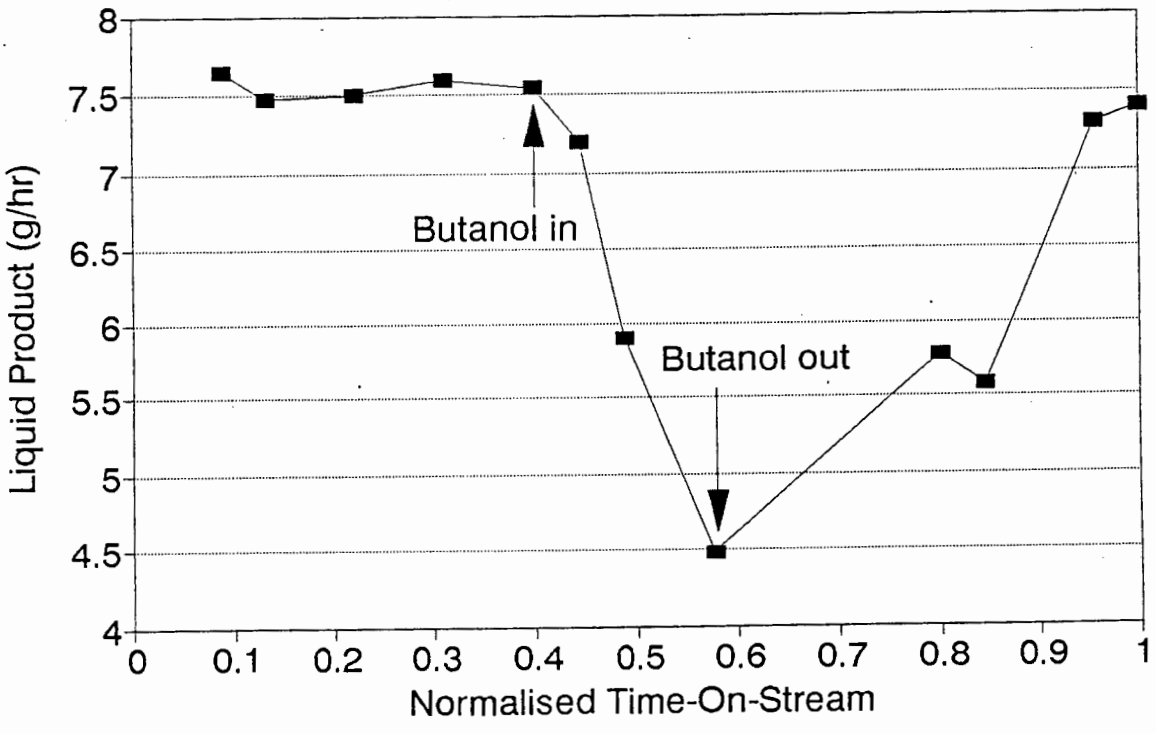

(b) Liquid product (g/hr) vs NTOS

3.5 Carbonyl Compounds

3.5.1 Reaction of Pure Ketones over HZSM-5

3.5.1.1. Acetone

Conversion of acetone over H-ZSM-5 at 250°C produced a decrease in activity with time-on-stream (Figure 3.16) and has been observed previously[50,51,60]. Although initially rapid the conversion levels out at approximately 50 %. There were small amounts of aromatics produced and no CO and CO_2. There was a high selectivity to C_8's which seemed to increase at the expense of the other products (Figure 3.17). The light hydrocarbons (Appendix L) were predominantly butenes which comprised mainly isobutene (>75%). The C_1-C_3 fraction was very small.

3.5.1.2 Methyl-Ethyl-Ketone

The conversion of MEK at 250°C produced a large amount of acetic and propanoic acid (Figure 3.19). Thus it was not surprising to see a large amount of aromatics in the product as acetic acid conversion involves a high selectivity to aromatics[12,13,21]. The activity of the catalyst dropped significantly from 73 % to 17 % in 10 hours (Figure 3.18). The selectivity for acetic acid remained fairly constant over the run time but that for propanoic acid increased slightly. Aromatic production also decreased with time.

At 300°C the aromatic content of the product increased dramatically over that at 250°C becoming the most dominant product (Figure 3.21). However selectivity to aromatics decreased with time and the production of acetic and

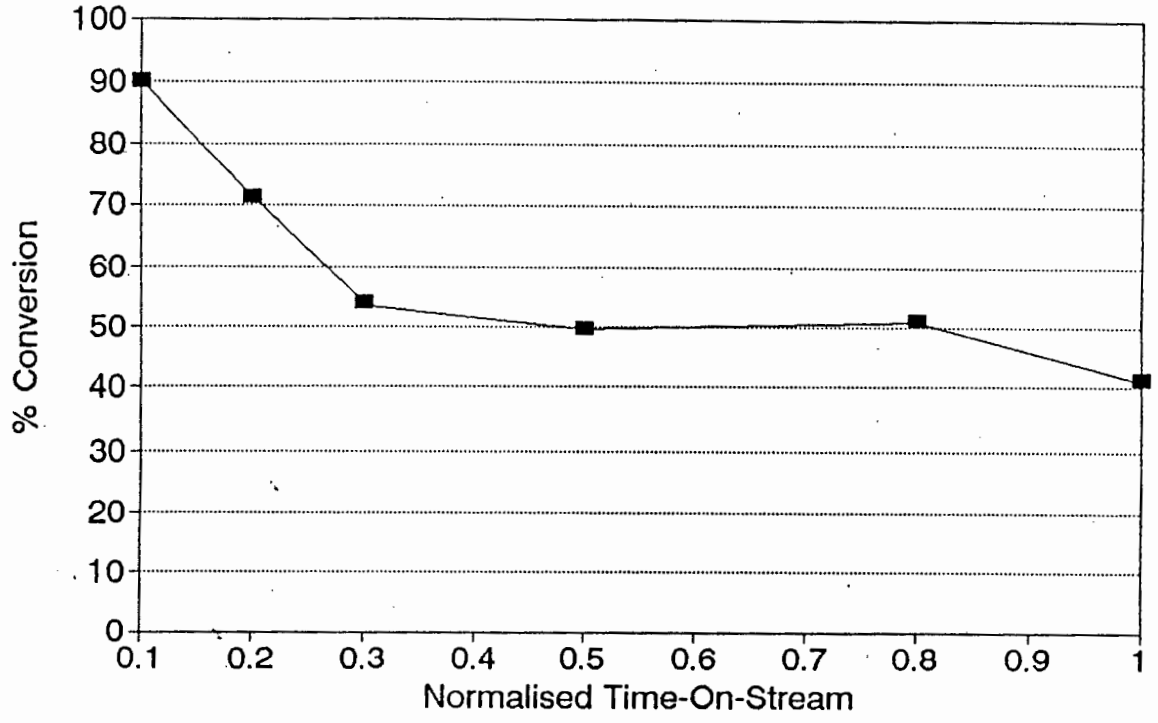

Figure 3.16 Conversion of acetone at 250°C

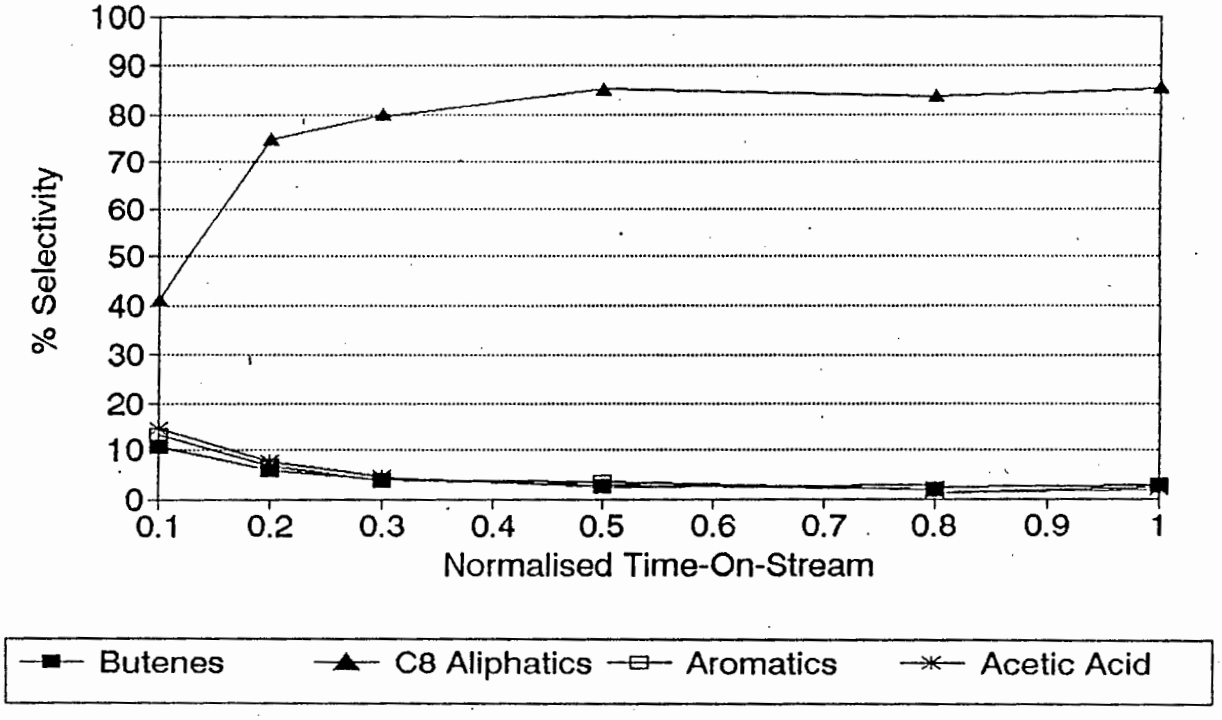

Figure 3.17 Product selectivity for acetone reaction at 250°C

propanoic acid increased. The amount of carbon dioxide and carbon monoxide produced was small compared to that of acetic acid. Conversion dropped from approximately 96 % to 13 % (Figure 3.20) during the run and this was reflected in the drop in aromatic yields.

The light hydrocarbon spectra for both temperatures (Appendix L) were dominated by the C_3-C_4 olefins, with the butenes more abundant initially. Isopentene was not selectively produced at 250°C as previously reported[59] but the large aromatic content of the product at 300°C has been observed[59].

3.5.2 Influence of Ketones on Catalyst Properties

Ketones caused the catalysts (only catalysts reacting with MEK were analysed) to deactivate but no change occurred in the acidity or cystallinity (Table 3.2 and Appendix H) of the spent catalyst. The production of acids from both acetone and methyl-ethyl-ketone may have been part of the deactivation process but this did not affect the above catalyst characteristics. TG/DTA (Table 3.2) showed that a small amount (0.8 wt%) of graphitic coke was produced and the total coke content of the catalyst increased with reaction temperature. Figure 3.3 (h) indicated no change in catalyst morphology.

3.5.3 Cofeeding trace Ketones with Propene in Oligomerisation Reactions

3.5.3.1 Acetone

The cofeeding of acetone decreased the activity for propene

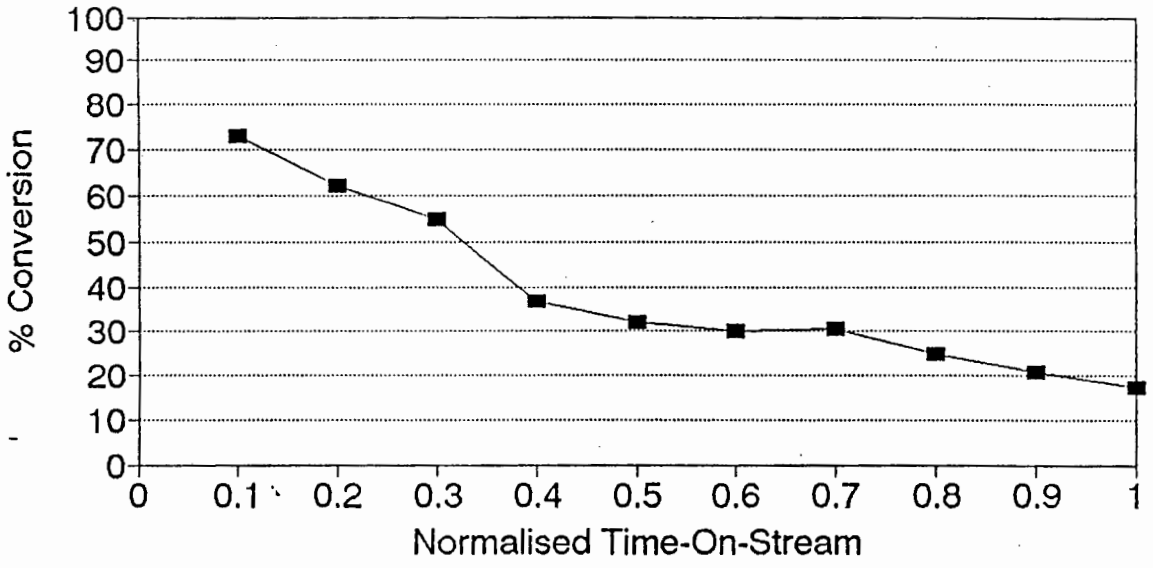

3.18 Conversion of methyl-ethyl-ketone at 250°C

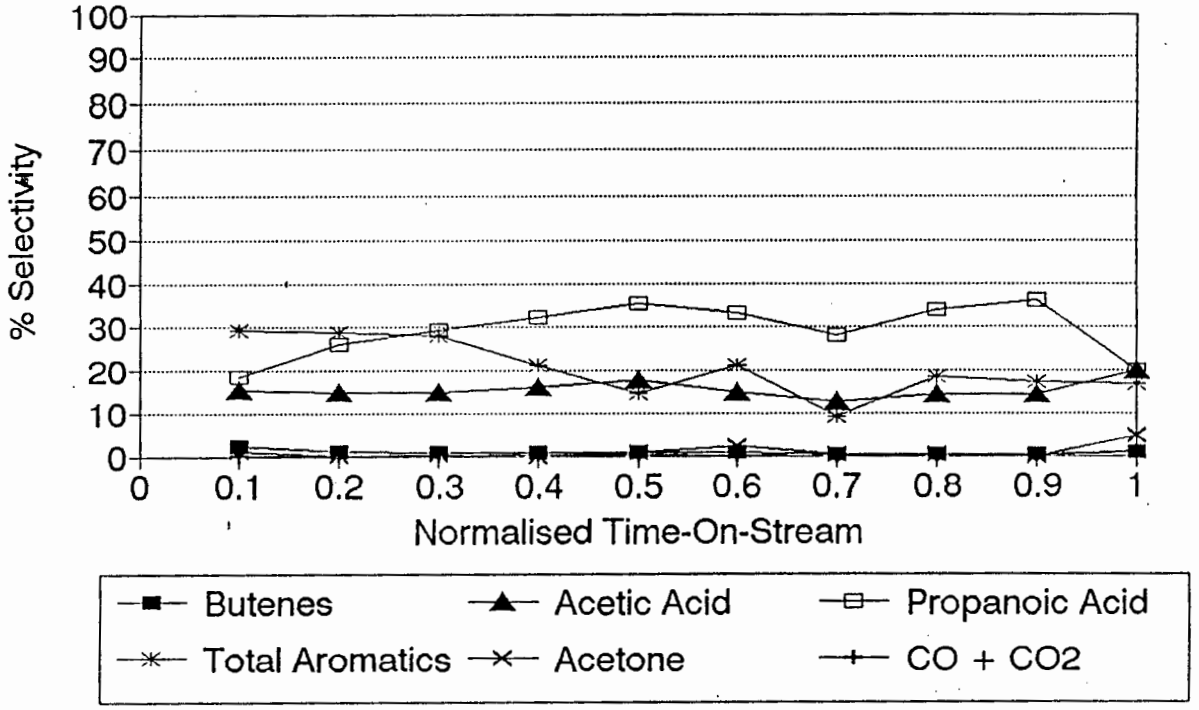

Figure 3.19 Product selectivity for methyl-ethyl-ketone at 250°C

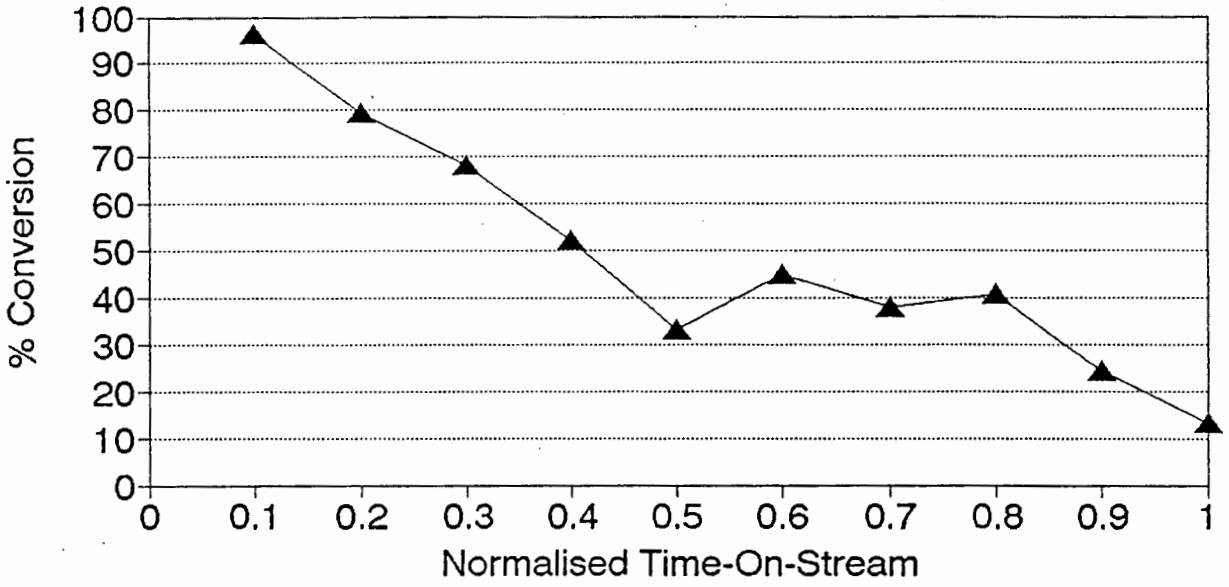

3.20 Conversion of methyl-ethyl-ketone at 300°C

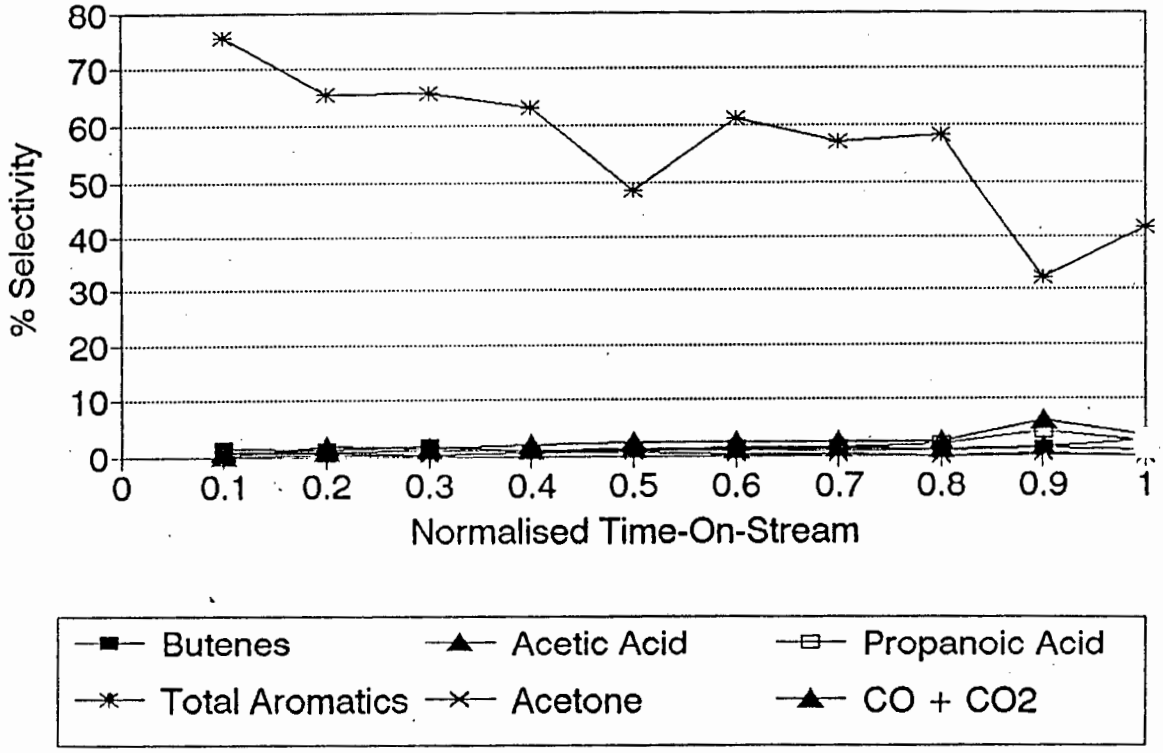

Figure 3.21 Product selectivity for methyl-ethyl-ketone at 300°C

oligomerisation (Figures 3.22 (a)-(b) and Appendix L). The selectivity was not affected but the activity of the catalyst was reduced on removal of the oxygenate relative to that before the cofeeding of the acetone started.

3.5.3.2 Methyl-Ethyl-Ketone

Methyl-ethyl-ketone also reduced the activity for propene conversion to a slightly greater extent than that of acetone (Figures 3.23 (a)-(b) and Appendix L). However the effect of both ketones was less than that for acetic acid. A permanent reduction in the activity was observed for MEK on its removal from the feed stream.

3.6 Water

3.6.1 Cofeeding trace Water with Propene in Oligomerisation Reactions.

Water was used as a cofeed because it is a by-product from all the above pure oxygenate reactions which undergo dehydration and/or condensation reactions at some stage of their conversion to hydrocarbons. Compared to the other oxygenates a relatively small drop in activity was noted which was reversible (Figures 3.24 (a)-(b) and Appendix L). In a propene oligomerisation run in which a large amount of water was cofed (· 20%) the reaction was completely stopped but returned to the original activity once the water was removed from the feed stream. GC-MS analysis of the products indicated trace amounts of 1- and 2-propanol to be present in the water.

Figure 3.22 Propene oligomerisation results co-feeding acetone

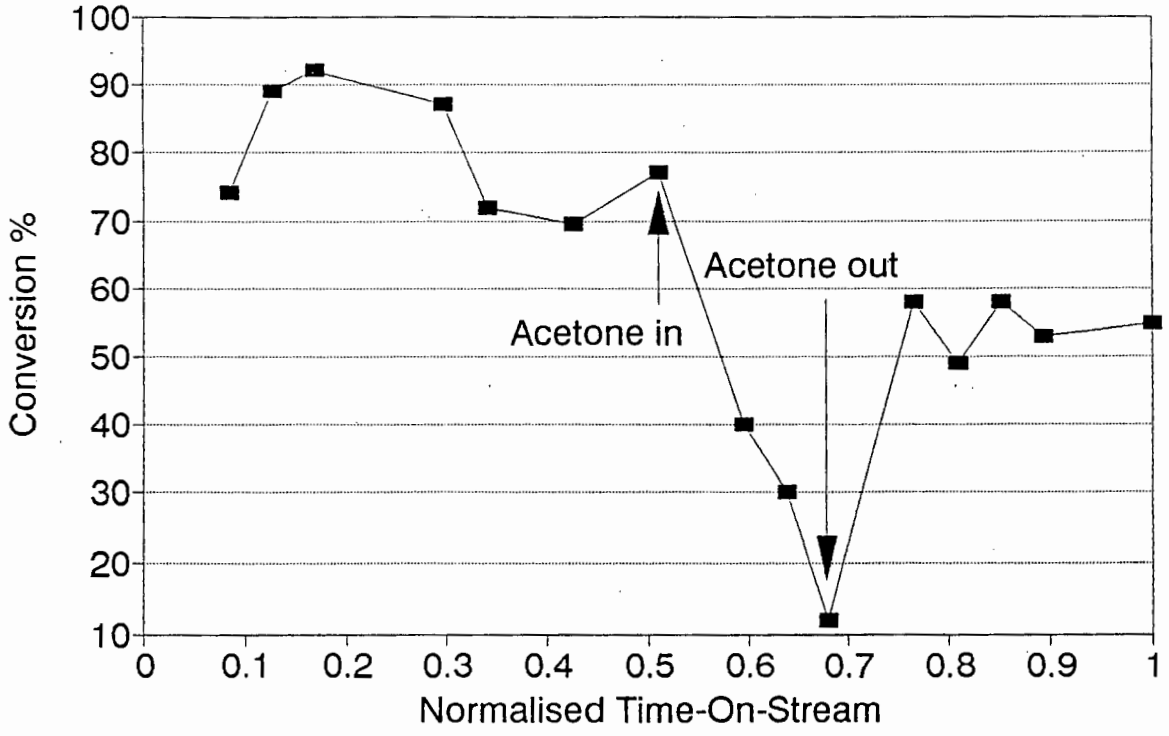

(a) Conversion vs NTOS

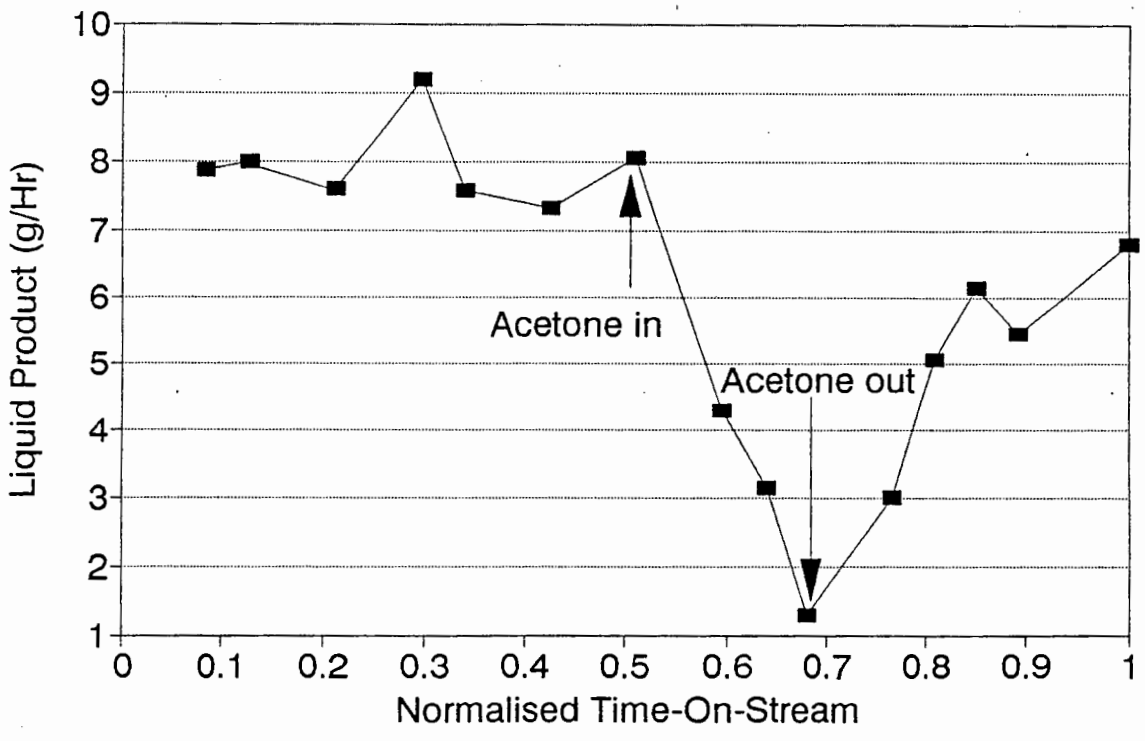

(b) Liquid product (g/hr) vs NTOS

Figure 3.23 Propene oligomerisation results co-feeding methyl-ethyl-ketone

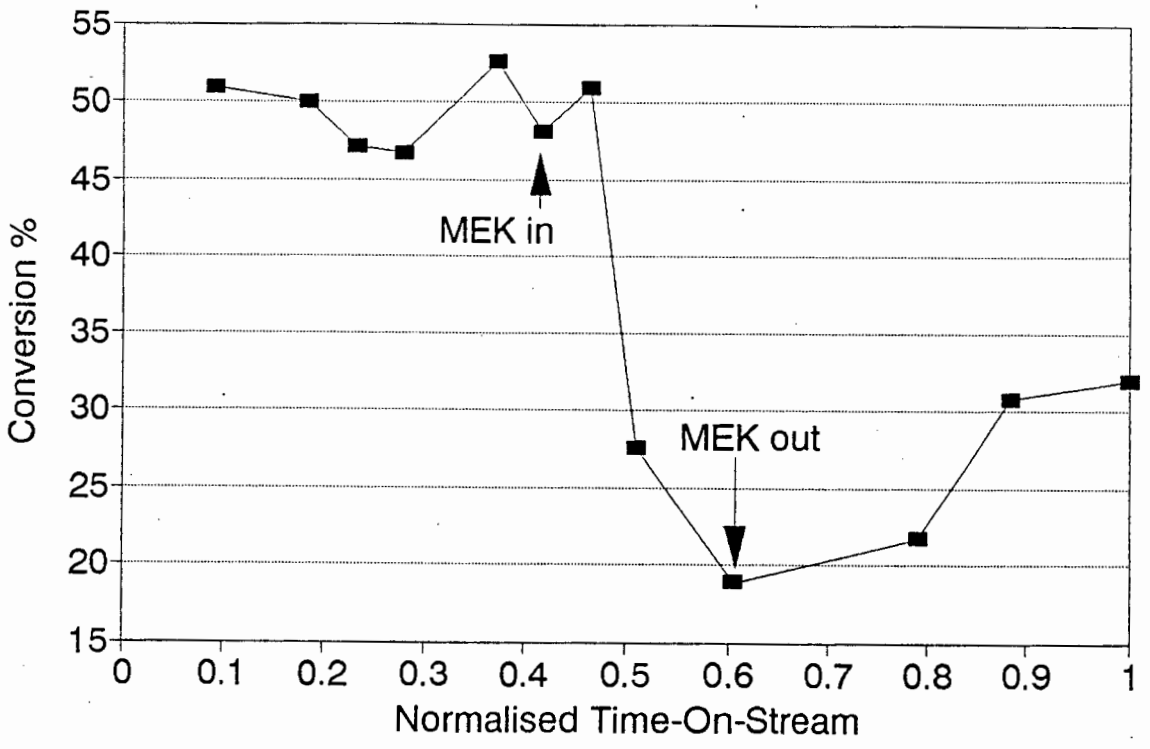

(a) Conversion vs NTOS

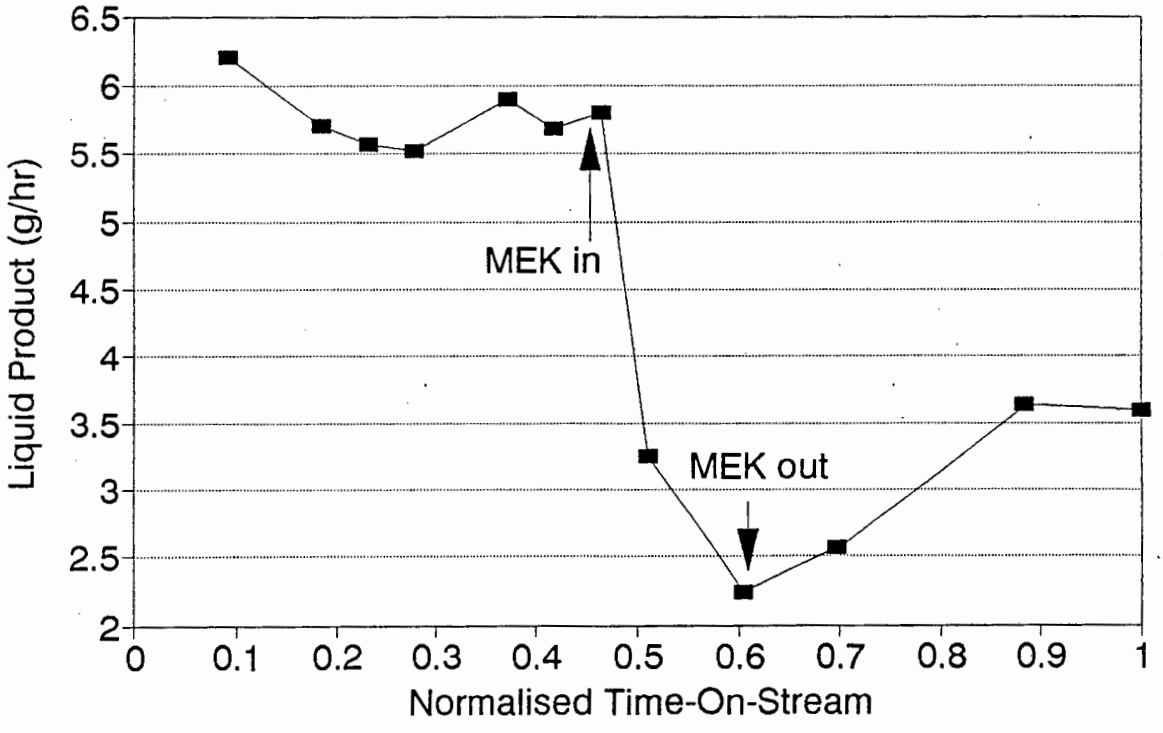

(b) Liquid product (g/hr) vs NTOS

Figure 3.24 Propene oligomerisation results co-feeding water

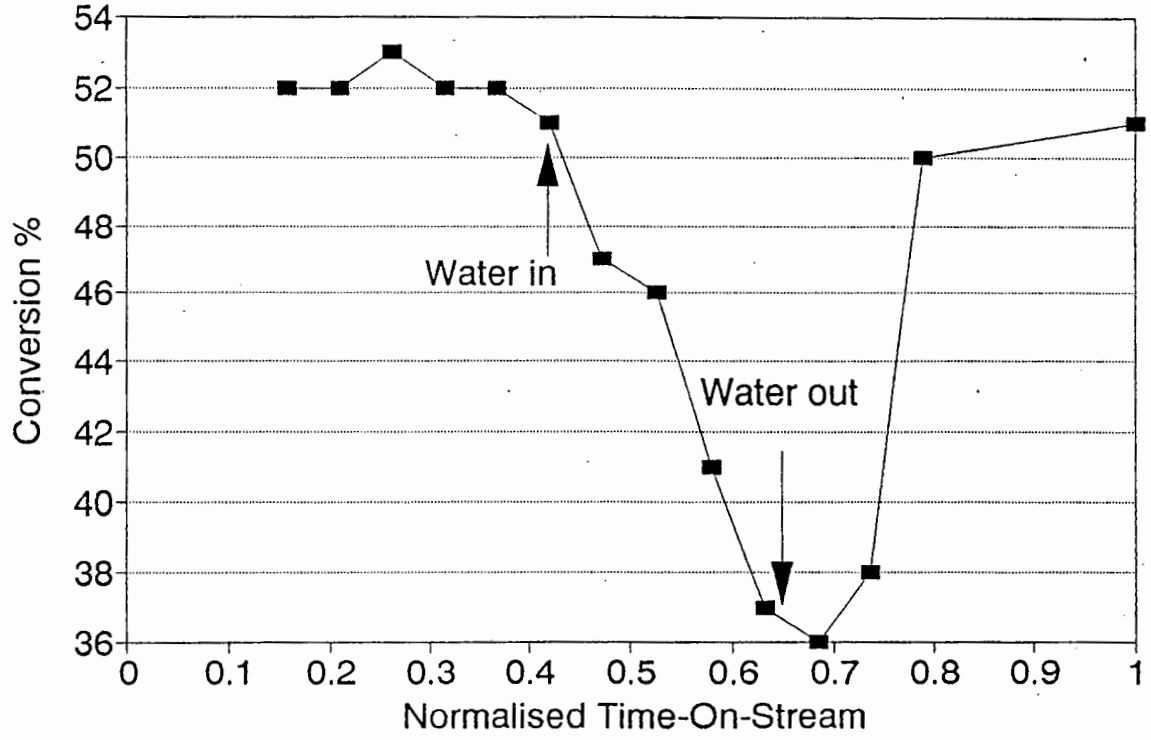

(a) Conversion vs NTOS

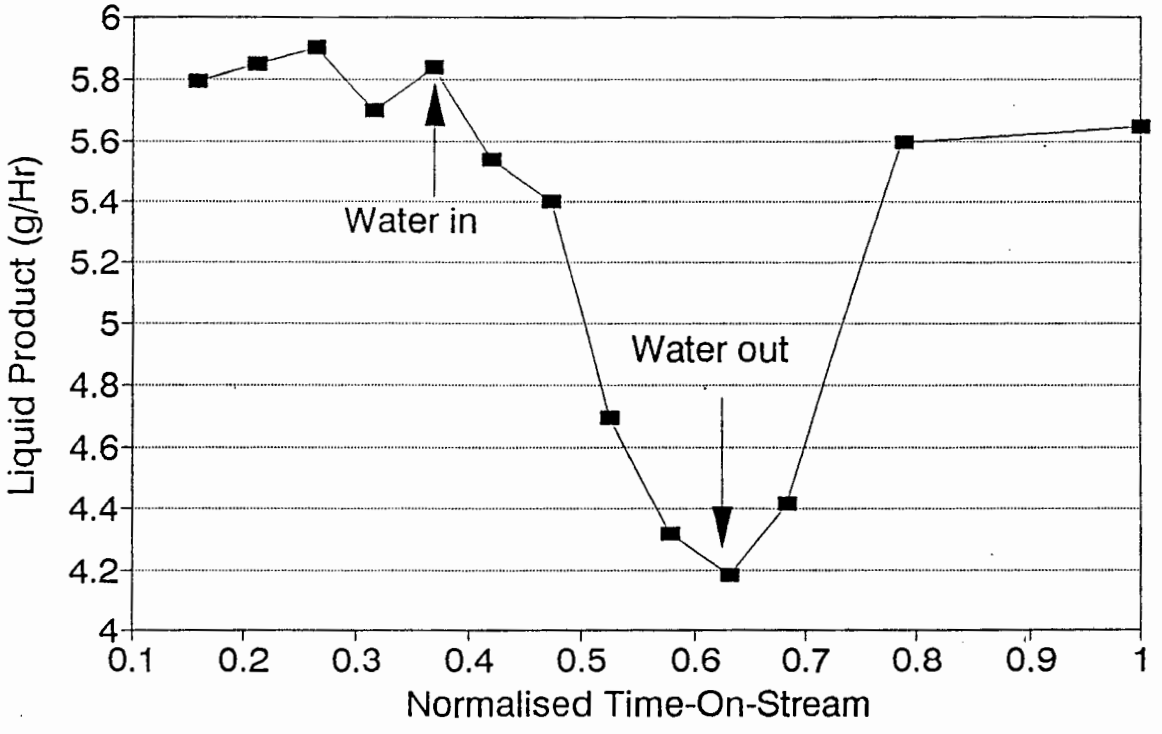

(b) Liquid product (g/hr) vs NTOS

3.7 Hexane Cracking

The conversion of hexane was based on the gaseous products sampled after the product condensor and thus can only be used in relative sense. Table 3.5 shows a typical product distribution of hexane cracking at 250°C over HZSM-5.

Table 3.5. Typical product distribution of n-hexane cracking at 250°C.

Component	Mass %
Methane	0.00
Ethane	0.15
Propane	4.98
Propene	0.74
Isobutane	6.33
n-Butane	5.16
1-Butene	0.00
Isobutene	0.62
Trans-2-butene	0.00
Cis-2-butene	2.28
C_5	2.56
Hexane	77.18

3.7.1 Co-feeding Acetic Acid

The introduction of acetic acid suppressed the production of C_1-C_5 hydrocarbons (Table 3.6). There was no recovery in activity after the acid was removed and this prevented any paraffin/olefin and isobutane/n-butane ratios from being calculated (Table 3.7). During co-feeding of acetic acid

some products of acetic acid conversion, e.g. carbon dioxide and trace aromatics, were noticed but even these decreased with time-on-stream. Acetic acid was still present in the reaction product for a couple of hours after its removal from the feed stream.

3.7.2 n-Butanol

Co-feeding n-Butanol showed an increase in the activity of the catalyst (Table 3.6). However the product spectrum showed a large increase in the C_4 olefins during the co-feeding period which would reduce the mass % of hexane in the product. Since the conversion of hexane was based on the percentage of unreacted hexane this resulted in an increased conversion. The extra C_4 olefins produced from the dehydration of butanol and the presence of some aromatics in the bulk product analysis indicated that the alcohol did react on the acid sites. On removing the butanol from the feed the activity of the catalyst returned to the value attained before its introduction. Table 3.7 shows that the propane/propene ratio decreased during co-feeding whilst the isobutane/n-butane ratio was constant.

Table 3.6. n-Hexane conversion before, during and after the co-feeding of oxygenates.

	Water	Butanol	Acetic Acid
Before	25.37	22.80	27.36
During	6.78	30.20	1.30
After	25.92	24.01	0.94

3.7.3 Water

Water reduced the hexane cracking activity of the catalyst but, unlike that of acetic acid, the activity returned on withdrawal of the water from the feed (Table 3.6). The product spectrum did change during the co-feeding stage with more propene and less butenes formed. However the effect was not permanent. Table 3.7 indicates that the propane/propene ratio decreases, the butane/butene ratio increases and the isobutane/n-butane ratio stays constant during co-feeding.

Table 3.7. Paraffin/Olefin ratios for n-Hexane cracking.

	Before	During	After
Water			
$C_3/C_3=$	5.85	4.07	5.70
$C_4/C_4=$	3.73	8.84	3.04
iC_4/nC_4	1.25	1.08	1.22
n-Butanol			
$C_3/C_3=$	6.69	1.59	5.19
$C_4/C_4=$	3.96	1.3	2.70
iC_4/nC_4	1.23	1.23	1.15
Acetic Acid			
$C_3/C_3=$	6.70		
$C_4/C_4=$	4.45		
iC_4/nC_4	1.33		

$C_3/C_3=$ - wt% Propane/wt% Propene
$C_4/C_4=$ - wt% Butanes/wt% Butenes
iC_4/nC_4 - wt% isobutane/wt% n-butane

4. DISCUSSION

4.1 Propene Oligomerisation in the absence of Oxygenates.

The catalysts synthesised were subjected to propene oligomerisation reactions as part of the characterisation process. Thus only those catalysts producing high conversions (>80%) for long run times (>15 hrs) were selected. The conversions and selectivities were consistent with those reported by Schwarz[85] and TG/DTA showed that the non-graphitic coke (36 wt%) was completely removed by 350°C and no graphitic coke was produced. Thus any deviation from normal oligomerisation activity and/or selectivity can only be due to the effect of co-feeding oxygenates.

4.2 Carboxylic Acids.

The reaction of acetic acid over HZSM-5 showed a dramatic decrease in activity over a ten hour run. This deactivation phenomenon has been recorded by other researchers[13,21] and has been attributed to the dehydroxylation of the catalyst on the formation of an intermediate acetate species[13] or by the formation of unsaturated ketonic species that bridge the acidic sites. In this research the activity of the catalyst was restored after calcination in air at 500°C, consistent with the results of Servotte et al.[21] and not with those of Chang et al.[13]. Initial conversions for pure acetic acid reaction were very low at 250°C, approximately 4%. Servotte et al.[21] recorded, at a similar temperature, complete conversion but at a much lower WHSV (0.11 h^{-1}). The initial conversions increase to 22 % at 300°C and 100 % at 350°C. Chang et al.[13] reported a 71.4% conversion at 371°C (WHSV = 1 hr^{-1}) and Servotte et al.[21] observed a 92% conversion after approximately 15 minutes of reaction. Since the rate

of deactivation is high and the time delay between starting the reaction and the first sample is not indicated it is difficult to compare the present results with their work.

The major reaction products from acetic acid were aromatic in nature with a large selectivity to xylenes and ethylbenzene. Isobutene was the predominant light olefin and the large selectivities to carbon dioxide (65.1% and 20.2% at 250°C and 350°C respectively) indicated that oxygen removal was through decarboxylation. This was an important indication of the catalyst activity since low CO_2 yields corresponded to low conversion levels. This was evident at 250°C. From the product spectrum (Figures 3.5 and 3.7), the series reaction postulated by Servotte et al.[21] is supported by the increase in selectivity to primary products at low conversions. Deactivation is not caused by any change in the physical properties of the catalyst (no changes in the structure of H-Y were observed after reaction with acetic acid at 400°C[14]) and since the conversion at typical oligomerisation temperatures is low it is postulated here that coking by reaction intermediates and/or products causes the loss of activity.

A number of authors studying ketonisation of acetic acid over metal catalysts[15-18] showed the reaction occurred through two surface species and only at relatively high temperatures. Similarly the acetate ion formed on HNaY[14] was very stable and only decomposed at 400°C with the complete transformation of adsorbed acid to acetate ions occurring at 350°C. Servotte at al.[21] proposed a pathway for the formation of aromatics from acetone either via:

1) acid catalysed aldolisation and dehydration reactions into isophorone which subsequently convert to aromatics or

2) isobutene condensation and dehydrocyclisation.

The proportion of isobutene in the light hydrocarbons was high (> 75%) and the presence of mesityl oxide in the product seemed to indicate that this route is more likely. Kubelkova et al.[50] showed that isobutene contributes little to catalyst deactivation and that deactivation due to acetone conversion was due to the presence of an unsaturated ketonic species bridging the hydroxyl groups. As the catalysts reacted at 350°C were black after reaction it is possible that deactivation is due to the formation of hydrocarbons blocking the acid sites. However at 250°C the low activity may be due to the stability of the acylium and acetate ions or the adsorbed acid molecule. At 300°C the strong acid sites were possibly the only sites involved in the reaction thus giving intermediate conversions.

The activity for propene oligomerisation and n-hexane cracking, two reactions occurring over Bronsted acid sites, irreversibly decreased during co-feeding the acetic acid. The significant and detrimental effect of acetic acid in the propene feed on catalyst actitvity for oligomerisation reactions is postulated, since selectivity is not affected, to be the result of one or more of the following:

1) Loss in catalyst crystallinity
2) Loss in catalyst acidity (dehydroxylation)
3) Dealumination
4) Competitive adsorption with propene for the acid sites.

Figure 3.9 shows the liquid product analysis for the three stages of the reaction: before, during and then after the co-feeding. Very little difference can be seen. Post reaction analysis of the catalysts show that options 1), 2) and 3) are not significant. On the basis of the strength of acid bonding to hydroxyl groups it is very likely that the acetic acid competes for acid sites and, at the temperatures concerned, remains adsorbed excluding the sites from further

interaction with propene. Propene reacts via the classic carbenium ion mechanism, these ions are relatively unstable and easy to displace from the acid site. However, the strength of acetic acid interaction on metal catalysts[18], HNaY[14] and HZSM-5[21], whether as an adsorbed molecule or as an acetate ion, is great as indicated by the temperatures above which the adsorbed molecules are removed (> 250°C). Romotowski et al.[20] found that even under evacuated conditions, transformations of acetic acid on the catalyst occurred at temperatures between 320°C and 400°C much higher than typical oligomerisation temperatures. Parker[19] found that acetic acid was strongly adsorbed on HZSM-5 at 150°C with only partial transfer of the zeolitic proton. She found a one-to-one interaction between acetic acid and the zeolitic acid sites and thermal-desorption/mass spectometry showed evidence of reaction products above 240°C. This also supports the low conversion results in this work for the pure acetic acid feed at 250°C. However it should be noted that since aromatics desorb at high temperatures the initial conversions at 250°C could be higher since they would not appear in the reaction product.

The postulation that acetic acid causes dehydroxylation is not observed in this study and in the work of Servotte et al.[11] where regeneration of the catalyst resulted in the original activity. Indeed Chang et al.[13] also noted that repeated regeneration of catalyst in a fluidised bed configuration resulted in the return of high activities. In this study TPD of regenerated catalyst (Figure 3.2) indicates that both the quantity and distribution of the acid sites is the same as that of the fresh catalyst. Acetic acid has been identified as causing an irreversible decrease in conversion for propene oligomerisation. This may be due to particularly strong adsorption caused by dual site hydrogen bonding between the acetic acid and the zeolite involving interactions between the carbonyl oxygen and the

framework proton as well as the acetic acid proton and the framework oxygen (Figure 4.1). The bond angles and lengths involved in the approach of an acetic acid molecule to the surface hydroxyls and the framework oxygen are similar to those of the acid dimer and are consistent with the proposed strong adsorption.

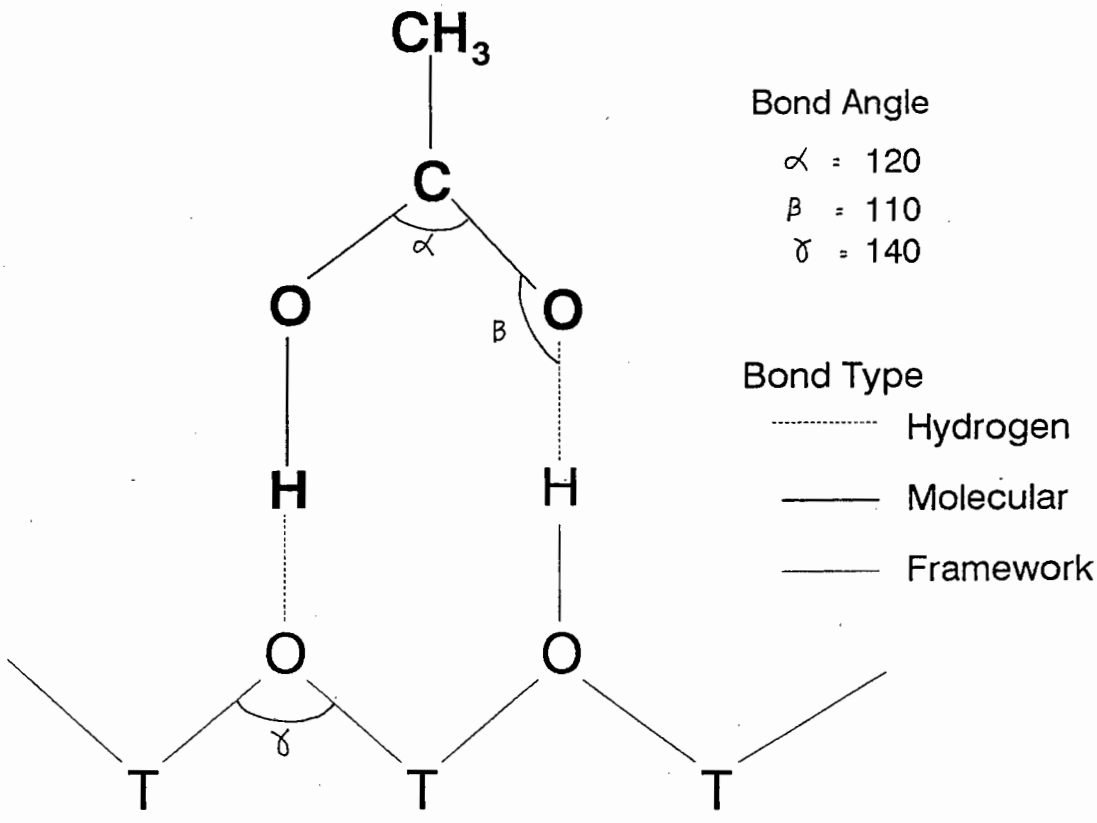

Figure 4.1 Schematic of adsorbed acetic acid on HZSM-5

4.3 Alcohols

The conversion of ethanol was complete at 250°C and 300°C and no ethanol was recorded in the GC analysis of the reaction product or in the liquid product analysed by mass spectrometry and ^{1}H-NMR (Figure 4.2). The latter was undertaken in case the ethanol peak was covered by hydrocarbons in the GC spectrum. In this work no diethyl

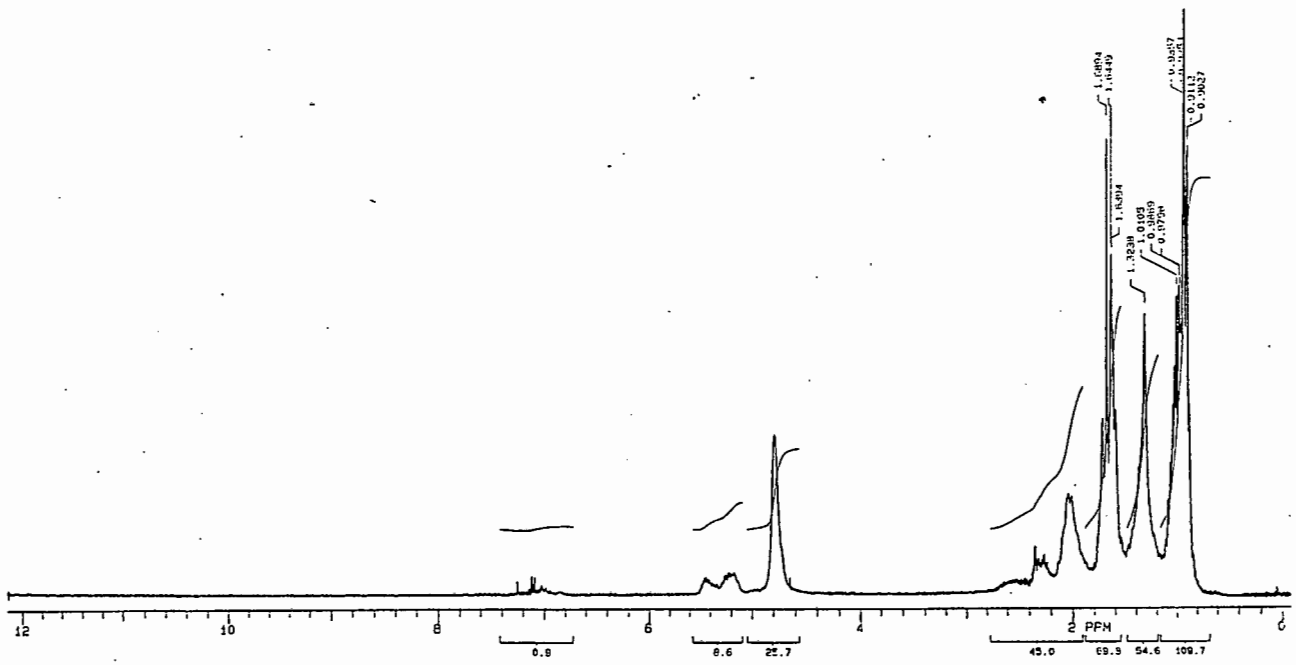

Figure 4.2 H^+-NMR spectrum of liquid product from ethanol conversion at 250°C

ether was recorded at 250°C and 300°C. These results are consistent with the work of Derouane et al.[23] and Chaudhuri et al.[29]. The former found that the diethyl ether and ethanol ^{13}C-NMR resonance peaks disappeared between 150°C and 250°C. The amount of aromatics in the product increased with reaction temperature from approximately 20% (NTOS=0.1) at 250°C to 85% at 300°C, a relationship observed in other work[23,29,30,36]. The increase in ethene selectivity and the decrease in n-hexane adsorption has been associated with deactivation[27,30] of ZSM-5 for ethanol conversion. Regeneration in air at 550°C[30] and 400°C[27] resulted in the restoration of the original activity and n-hexane adsorption capacity. Slight deactivation of the catalyst at 250°C from

coking can be monitored by the increase in the ethene (Appendix K (c)) and the decrease in the product aromatics. Chaudhuri et al.[29] found a linear relationship between the selectivity to aromatic molecules and the concentration of coke on the catalyst. However, at 300°C these indicators of catalyst deactivation were not observed. It is through the formation of coke deposits that the activity of the catalyst decreases. TG/DTA showed that the amount of non-graphitic coke was higher at 250°C (11.6 wt%) compared to 300°C (5.9 wt%) but the amount of graphitic coke was approximately the same 300°C (0.9 wt%) and 250°C (0.7 wt%). The slight deactivation at 250°C is probably due to high boiling point hydrocarbons that cannot be desorbed at 250°C but are removed at 300°C possibly by the steam distillative release of heavy hydrocarbon products by water of dehydration[36]. This would also account, in part, to the increase in aromatic products at 300°C.

The co-feeding of ethanol with propene resulted in a drop in the activity for propene oligomerisation. However the effect was much less than that for acetic acid during co-feeding, the original activity was restored on removing the ethanol. Product distributions were not affected by the drop in conversion. Ethanol does interact strongly with zeolite Brönsted acid sites[31,32,33] (Figure 1.12), either as a hydrogen bonded molecule or as an ion pair, as indicated by the heat of adsorption data of ethanol from aqueous solutions over ZSM-5 (-8.8 J/g_{cat}) compared to silicalite (-2.9 J/g_{cat}). The heat of adsorption of alcohols (21-26 kcal/mol) is higher than that for propene (10 kcal/mol) on 5Å Zeolite. Ethanol desorbs intact, except for a small amount (10%) which reacts to ethene and water[31,32], at relatively high temperatures, 170°C (Aronson et al.[31]), 195°C (Li-feng et al.[33]). Thus the drop in activity in propene oligomerisation is postulated to be due to the competition between ethanol and propene for the active site.

Water of reaction did not effect the selectivity for ethanol conversion and an ethanol feed containing 4 wt% water did not result in any structural damage to the catalyst[30]. Oudejans et al.[36] observed no activity decrease over 50 hours for an ethanol/water feed of mole ratio 0.37 over ZSM-5 at 300°C.

As in the case of ethanol, n-butanol was completely converted over HZSM-5 at 250°C and 300°C. The product distribution at 250°C for both alcohols were similar indicating a similar reaction mechanism[12]. In this study the C_4 olefins, a mixture of isomers that results from dehydration of butanol[37], dominated the light hydrocarbons at 250°C and increased with time-on-stream indicating, using the same argument as above for ethanol conversion, slight deactivation. Dehydration was the method of removing oxygen from the alcohol, water was collected as an aqueous phase and analysed on GC Mass Spectrometer, but the reaction mechanism via either an ether or directly to the alkene was not ascertained. At 300°C C_4 paraffins were the most dominant product in the light hydrocarbon gas until after a normalised time of 0.4 when the olefins became more selectively formed. This is in contrast to ethanol conversion at the same temperature where no increase in ethene was observed and no deactivation occurred. The aromatic selectivity for n-butanol conversion at 300°C was lower (70%) than the corresponding value (85%) for ethanol. According to Chaudhuri et al.[29] this should result in a lower coke content. TG/DTA showed that the quantity of coke produced by reacting ethanol and n-butanol was approximately the same (10-11 wt%) but ethanol conversion resulted in the formation of small amounts of graphitic coke (~ 1 wt%). This graphitic coke did not produce any activity and selectivity difference between ethanol and n-butanol conversion at 250°C. The decreased activity and aromatic selectivity for n-butanol at 300°C compared to ethanol is postulated to be

due to the greater amount of C_{12+} aromatics (5 wt%) produced during reaction which block the acid sites and result in slight deactivation.

Post reaction analysis on the catalyst used for the reaction of n-Butanol at 300°C showed no effect on the crystalline strucure or the TPD values.

n-Butanol decreased the activity of the catalyst for propene oligomerisation but its effect was less severe than that for acetic acid. It does, like ethanol, interact[25,31] with the zeolite hydroxyl group but the strength of interaction is stronger as evidenced by a higher heat of adsorption -18.8 J/g (-8.8 J/g for ethanol) and its easier transformation to primary products[31,32]. This difference in reaction between ethanol and n-butanol is attributed to the relative rates of reaction between the reverse proton transfer of the adsorbed alcohol and the dehydration to the corresponding olefin, a choice governed by the stability of the resulting carbenium ion. It was concluded that the C_4 ion is more stable than that of its C_2 counterpart[31,32].

Williams et al.[25] studied the mechanism of isobutyl alcohol dehydration over ZSM-5. From their experimental work they formulated the reaction mechanism represented in Figure 4.3.

They found that at the temperature (18°C) at which adsorbed butene completely oligomerised over ZSM-5, isobutyl alcohol was adsorbed as an ether and transformation to butene or its oligomers only occurred at 125°C. Results from isobutyl alcohol dehydration indicated that deactivation, via the formation of long chain hydrocarbons that remain adsorbed on the active site, was considerably faster on ZSM-5 when the alcohol feed was interupted than when the feed was not. They attributed this to the alcohol preferably reacting with the

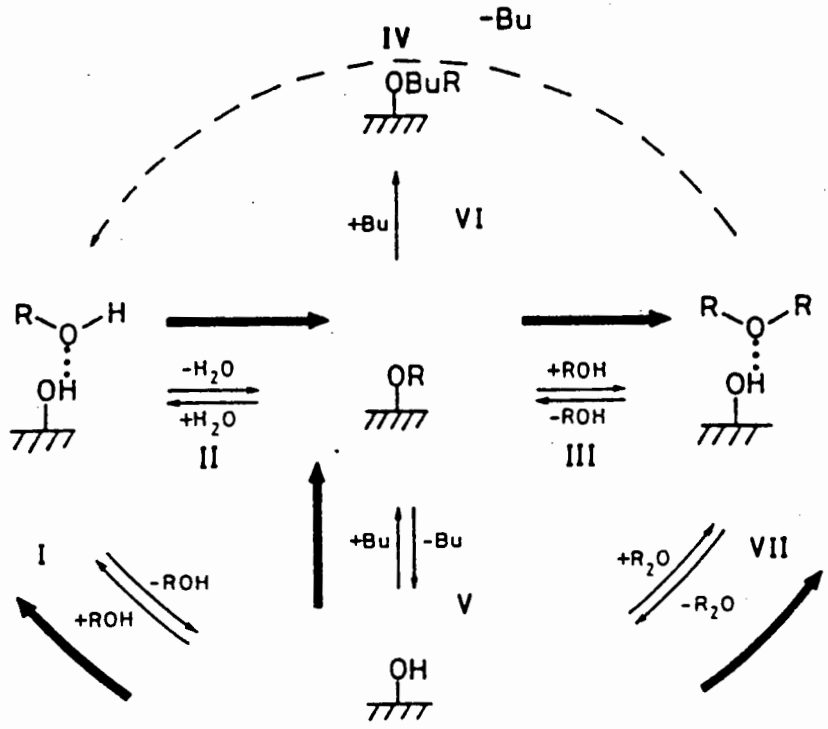

Figure 4.3 Mechanism of iso-butyl alcohol conversion over HZSM-5

active butyl alkoxy surface intermediate to produce an ether which prevents this surface species from oligomerising with free butene molecules that result in long chain hydrocarbons. This is consistent with the proposal that the alcohol may compete with, not only the active site, but with adsorped carbenium ions formed during propene oligomerisation to form a relatively stable intermediate whose reaction to oligomers is much slower than the carbenium ions.

4.4 Ketones

The reaction of both acetone and MEK over HZSM-5 resulted in a decrease in activity with time-on-stream. Since no crystalline defects (as measured by XRD) occurred and there was no loss in acidity (as indicated by NH_3-TPD) the deactivation must be due to either:

1) irreversible adsorption of reactants and/or products or

2) the blockge of pores and sites by hydrocarbon coke.

Acetone does interact with the zeolite hydroxyl groups[49,54,58] to form both protonated and hydrogen-bonded species. Theoretical calculations have shown that the molecules of the ketones acetone (DMK), methyl-ethyl-ketone (MEK) and diethyl ketone (DEK) are bonded to the zeolite H atom of the hydroxyl group through the oxygen of the ketone[58]. For acetone no additional interactions occurred between other ketone atoms and the zeolite. The zeolite affects the electron density of the ketone molecule and increases the reactivity in the order DEK > MEK > DMK. The C=O bond is considerably weakened[49] (a shift in IR frequency to lower wavenumbers) and the formation of protonated (enol form) ketones[49,54] in equilibrium with H-bonded species is similar to that in homogeneous acid media and is essential for acid-catalysed aldolisation reactions[56]. Acetone strongly interacts with ZSM-5 and the temperature-programmed-conversion of preadsorbed acetone results in the desorption of reacted products and some unreacted acetone above 150°C.

In this work the conversion of acetone over ZSM-5 at 250°C resulted in predominantly C_8 aliphatics with isobutene selectivity in the light hydrocarbons increasing from 80 wt% to almost 100 wt% with time-on-stream (Appendix K (b)).

Decreasing amounts of aromatics and acetic acid were produced with decreasing conversion (Figure 3.17). This has been shown in previous work[50]. The higher conversions in this work are due to the lower WHSV of 1 h^{-1} compared with 8-11 h^{-1} used elsewhere.

The production of acetic acid during acetone conversion is the result of the cracking of diacetone-alcohol[50,51] and the hydrolytic cleavage of mesityl oxide[53]. Acetic acid was not observed[51,60] in significant amounts (< 2 wt%) due to the high reaction temperatures (350°C), which result in complete conversion in this work. The deactivation of the catalyst during acetone conversion (Figure 3.16) has been observed previously[50] and occurs via the decomposition of higher condensation products into isobutene and an unsaturated surface cyclic ketonic species stongly bound to the surface[50,51,53] hydroxyls. This species was thermally stable up to 500°C and its precursor has been identified as mesityl oxide[50,51,53]. The nature of the coke deposit, determined by TG/DTA to be 9.3 wt% non-graphitic and 0.9 wt% graphitic coke, was not determined in this study.

The liquid product, analysed on GC/Mass Spectrometry, from MEK reaction at 250°C contained significant amounts of both acetic and propanoic acid. Previously[52] only propanoic acid was reported for MEK conversion over silica-alumina at 400°C in addition to significant quantities (12 %, see Table 1.6) of CO_2. The production of propanoic acid was explained, assuming a similar reaction mechanism to acetone, by the aldolisation reaction only occurring through the methyl, and not the methylene, hydrogen[52]. The acetic acid/propanoic acid mole ratio at 250°C is 1.01 indicating that both hydrogens react equally in the aldolisation of MEK. The selectivity to acids drops dramatically at 300°C (< 5%) but it increases with decreasing conversion. This is due to further reaction of the acids diminishing as the catalyst

activity declines. The CO_2 levels remained low (< 2%) over the entire run and could not be used to confirm this since CO_2 yields indicate the extent of acids reaction (See Section 4.2). The aromatic selectivity during MEK conversion increased from 250°C (29%) to 300°C (75%) consistent with the work of Nedomova et al.[59]. They recorded oxygen containing compounds in the product (< 10 wt%) but did not detail the composition and no CO_2 selectivity was indicated. MEK conversion over acidic zeolites (proton exchanged) is a combination of aldolisation and internal dehydration reactions[55]. The formation of acetic and propanoic acids from mesityl oxide equivalents can occur should the comparison between the aldolisation reaction of MEK and acetone be valid[52]. The decrease in activity with time for MEK conversion at both temperatures is postulated to be due to strongly adsorbed species unique for MEK conversion but similar in nature to that found during acetone reaction. This species could result from the reaction of secondary products such as acetone, acetic acid and propanoic acid.

The co-feeding of ketones with propene in high pressure oligomerisation reactions results in an activity decrease similar to that seen for alcohols. However although the recovery is greater than that from acetic acid it is not total (90% of the original activity for acetone and 50-60% for MEK) as that from the alcohols and water. This indicates that either only the ketone remains sorbed on the strong sites after the co-feeding has stopped or that partial reaction has taken place and secondary products, acids, are sorbed onto the sites.

4.5 Hexane Cracking

It is not possible to postulate which mechanism is favoured for hexane cracking in this work but it seems likely that the carbenium ion route predominates due to the low

temperatures[62] and the greater amounts of C_3-C_5 alkanes compared to the C_1-C_2 alkanes in the product (Table 3.5). The deactivation by coke formation was negligible and did not affect the conversion over the run time as the i-C_4H_{10}/n-C_4H_{10} did not change with time except during the co-feeding stage. It has been reported that the paraffin/olefin ratio decreases with decreasing conversion[61,62] and decreasing Si/Al ratio. These ratios do decrease (Table 3.7) during co-feeding stage of water and n-butanol thus indicating the drop in n-hexane activity even though, for n-butanol, reaction products may interfere with the product spectrum and give a greater conversion. Acetic acid prevented the cracking reaction of n-hexane and so these ratios were unable to be calculated. The C_4/C_4= ratio in the water run increases during co-feeding but returns to the original value on removal of the oxygenate. The reaction of butenes with water to alkanes and/or butanol may be the cause of this discrepancy. What is evident is the effect of the oxygenate on the cracking activity. Since Brönsted acid sites are crucial for hexane cracking[61-65] the only reason for the drop in activity due to co-feeding water and acetic acid is due to the blockage of those sites to access by hexane molecules. Butanol appears to cause an apparent increase in conversion but the product analysis shows a significant increase in butenes (and some aromatics) during co-feeding which can only result from the butanol reaction at this temperature. Thus it is difficult to calculate the conversion of hexane because of reaction products from both reactions. However, assuming that the C_3/C_3= ratio is indicative of conversion, all three oxygenates caused a drop in conversion. The longterm effect of co-feeding differed for the co-feeds. Product samples analysed two hours after the removal of the oxygenates showed a return to initial activity values for those runs in which water and butanol have been co-fed but the reduced activity resulting from the run where acetic acid was co-fed remained unchanged.

4.6 Water

Water is a byproduct from all the above oxygenate reactions either from the primary reaction step (Dehydration of the alcohols and MEK) or from a secondary step (Condensation reactions for acetic acid and the ketones). Although HZSM-5 is predominantly hydrophobic, water can react with the hydroxyl sites to form pockets of hydroxonium ions covering the site.

It can be seen both from the hexane cracking and the propene oligomerisation runs that water does not permanently reduce the catalyst activity at 250°C. The interaction of water with Brönsted acid sites is purely electrostatic since water desorbs intact at all temperatures. Since low temperatures and partial pressures were used no influence, due to hydrothermal effects that result in structural defects and loss in crystallinity, on the catalyst properties occurred. Thus the temporary decrease in the activity for the above reactions is probably due to the competition between water and the reacting species for the acid site. It has been shown that water affects the adsorption and oligomerisation of ethene[66] on HZSM-5 due to this phenomenon. Ison et al.[44] found that water is completely desorbed from HZSM-5 at 100°C under vacuum and TG/DTA, atmospheric conditions, showed water still interacting with the catalyst at 200°C. Thus at propene oligomerisation pressures, 50 Bar, this temperature could be a lot higher resulting in water interacting with acid sites in the presence of other reactants.

5. CONCLUSIONS

Co-feeding oxygenates such as acetic acid, acetone, MEK, n-butanol, ethanol and water have been shown to reduce the activity for reactions such as propene oligomerisation and hexane cracking. This is proposed to be due to preferential adsorption of these polar compounds onto the active (Brönsted acid) sites of the catalyst and/or, in the case of the ketones, bridging of the active site by a unsaturated cyclic ketonic species that is a by-product. Molecular acetic acid is strongly adsorped possibly due to the dual site hydrogen bonding and, during reaction, in the form of an acylium ion. Alcohols, ketones and water also interact, through their oxygen atom, with the hydroxyl group. When pure oxygenates are reacted over HZSM-5, at propene oligomerisation temperatures, acetone and MEK undergo rapid deactivation but acetic acid hardly reacts. In all cases total regeneration of the catalyst is achieved by combustion overnight in an air stream at 500°C.

6. REFERENCES

1) Smith J. V., Zeolite Chem. and Catal., *ACS Monograph 171*, J. A. Rabo (Ed.), (1979).

2) Meier W. M. and Olson D. H., "*Atlas of Zeolite Structure Types*", Structure Commission of IZA, Polycrystal Book Service, Pittsburg, (1978).

3) Vaughan D. E. W., *Chem. Eng. Progress*, (1988), 25-31.

4) Ward J. W., *J. Catal.*, **9**, (1967), 225-236.

5) Ward J. W., *J. Catal.*, **13**, (1969), 364.

6) Uytterhoeven J. B., Christner L. G. and Hall W. K., *J. Phys. Chem.*, **69**, (1965), 2117-2126.

7) Schmerling L. and Ipatieff V. N., *Adv. Catal.*, (1950), 21-71.

8) Oblad A. G., Mills G. A. and Heinemann H., *Catalysis*, P. M. Emmet (Ed.), **6**, (1950), 341-363.

9) Csicsery S. M., *Zeolites*, **4**, (1984), 202-213.

10) Kokotailo G. T., Lawton S. L. and Olson D. H., *Nature*, **272**, (1978), 437-438.

11) Haag W. O., Lago R. M. and Weisz P. B., *Nature*, **309**, (1984), 589-591.

12) Chang C. D. and Silvestri A. J., *J. Catal.*, **47**, (1977), 249-259.

13) Chang C. D., Chen N-Y., Koenig L. R. and Walsh D. E., *Amer. Chem. Soc. Div. of Fuel Chem. Preprints*, **28(2)**, (1983), 146- 152.

14) Bielanski A. and Datka J., *J. Catal.*, **32**, (1974), 183-189.

15) Kuriacose J. C. and Jewur S. S., *J. Catal.*, **50**, (1977), 330-341.

16) Kuriacose J. C. and Swaminathan R., *J. Catal.*, **14**, (1969), 348-354.

17) Swaminathan R. and Kuriacose J. C., *J. Catal.*, **16**, (1970), 357-362.

18) Gonzalez F., Munuera G. and Prieto J. A., *J. Chem. Soc. Farday Trans. 1*, **74(6)**, (1978), 1517-1529.

19) Parker L. M., *Methane Conversion*, Eds. Bibby D. M., Howe R. F. and Yurchak S., Elsevier Science Publishers, (1988), 589-595.

20) Romotowski T. and Komorek J., *Zeolites*, **11**, (1991), 35-41.

21) Servotte Y., Jacobs J. and Jacobs P. A., *Proceedings of the International Symposium on Zeolite Catalysis*, Siofok, (1985), 609-618.

22) Duncan T. M. and Vaughan R. W., *J. Catal.*, **67**, (1981), 469-471.

23) Derouane E. G., Nagy J. B., Dejaifve P., van Hooff J. H. C., Spekman B. P., Vedrine J. C. and Naccache C., *J. Catal.*, **53**, (1978), 40-55.

24) Dass D. V. and Odell A. L., *Can. J. Chem.*, **67**, (1989), 1732-1734.

25) Williams C., Makarova M. A., Malysheva L. V., Paukshtis E. A. and Zamaraev K. I., *J. Chem. Soc. Faraday Trans.*, **86(20)**, (1990), 3473-3485.

26) Nguyen T. M. and Le Van Mao R., *Appl. Catal.*, **58**, (1990), 119-129.

27) Rajadhyaksha R. A. and Anderson J. R., *J. Catal.*, **63**, (1980, 510-514.

28) Choudhary V. R. and Sansare S. D., *Appl. Catal.*, **10**, (1984), 147-153.

29) Chaudhuri S. N., Halik C. and Lercher J. A., *J. Mol. Catal.*, **62**, (1990), 289-295.

30) Costa E., Aguado J. and Hernandez P. J., *Ind. Eng. Chem. Res. Dev.*, **24**, (1984), 239-244.

31) Aronson M. T., Gorte R. J. and Farneth W. E., *J. Catal.*, **98**, (1986), 434-443.

32) Aronson M. T., Gorte R. J. and Farneth W. E., *J. Catal.*, **105**, (1987), 455-468.

33) Li-feng C., Wacker T. and Rees L. V. C., *J. Chem. Faraday Trans. 1*, **85(1)**, (1989), 33-45.

34) Groszek A. J. and Templer M. J., *Microscale Ltd.*, **79**, Southern Row, London W10 5AL, U. K. 155-162.

35) Le Van Mao R., Levesque P., Mclaughlin G. and Dao L. H., *Appl. Catal.*, **34**, (1984), 163-179.

36) Oudejans J. C., Van Den Oosterkamp P. F. and Van Bekkum H., *Appl. Catal.*, **3**, (1982), 109-115.

37) Kalvachev Y., Bezouhanova C. and Lechert H., *Zeolites*, **11**, (1991), 73-76.

38) Wolthuizen J. P., Van Den Berg J. P. and van Hooff J. H. C., *Catalysis by Zeolites*, Elsevier Publishing Company, (1980), 85-92.

39) Lago R. M., Haag W. O., Mikovsky R. J., Olson D. H., Hellring S. D., Schmitt K. D. and Kerr G. T., *Proc. 7th Int. Zeol. Conf.*, Y. Murakami, A. Iigima, J. T. Ward (Eds.), Elsevier, Amsterdam, (1986), 677-684.

40) Brunner G. O., *Zeolites*, **7**, (1987), 9-11.

41) Sano T., Suzuki K., Shoji H., Ikai S., Okabe K., Murakami T., Shin S., Hagiwara H. and Takaya H., *Chem. Lett.*, (1987), 1421-1424.

42) Sendoda Y. and Ono Y., *Zeolites*, **8**, (1988), 101-105.

43) Topsoe N., Joensen F. and Derouane E. G., *J. Catal.*, **110**, (1988), 404-406.

44) Ison A. and Gorte R. J., *J. Catal.*, **89**, (1984), 150-158.

45) Jentys A., Warecka G., Derewinski M. and Lercher J. A., *J. Phys. Chem.*, **93**, (1989), 4837-4843.

46) Vasques M. H., Ribeiro F. R., Gnep N. and Guisnet M., *React. Kinet. Catal. Lett.*, **38(2)**, (1989), 301-306.

47) Loeffler E., Lohse. U, Peuker C., Oehlmann G., Kustov L. M., Zholobenko V. L. and Kazansky V. B., *Zeolites*, **10**, (1990), 266-271.

48) Novakova J. and Kubelkova L., *J. Catal.*, **126**, (1990), 693-696.

49) Bosacek V. and Kubelkova L., *Zeolites*, **10**, (1990), 64-65.

50) Kubelkova L., Cejka J., Novakova J., Bosacek V., Jirka I. and Jiru P., "*Zeolites: Facts, Figures, Future*", Elsevier Science Publishers, Jacobs P. A. and van Santen R. A. (Eds.), (1989), 1203-1212.

51) Cejka J. and Jiru P., *Collect. Czech. Chem. Commun.*, **54**, (1989), 2998-3002.

52) Demorest M., Mooberry D. and Danforth J. D., *Ind. Eng. Chem.*, **43**, (1951), 2569-2572.

53) Kubelkova L. and Novakova J., *Zeolites*, **11**, (1991), 822-826.

54) Kubelkova L., Cejka J., Novakova J., *Zeolites*, **11**, (1991), 48-53.

55) Novakova J. and Kubelkova L., *J. Mol. Catal.*, **39**, (1987), 195-202.

56) Novakova J., Kubelkova L., Bosacek V. and Mach K., *Zeolites*, **11**, (1991), 135-141.

57) Dolejsek Z., Novakova J., Bosacek V. and Kubelkova L., *Zeolites*, **11**, (1991), 244-247.

58) Beran S. and Kubelkova L., *J. Mol. Catal.*, **39**, (1987), 13-19.

59) Nedomova K., Beran S. and Jiru P., *React. Kinet. Catal. Lett.*, **32(2)**, (1986), 353-357.

60) Cejka J., Kubelkova L. and Jiru P., *Collect. Czech. Chem. Commun.*, **54**, (1989), 2054-2063.

61) Post J. G. and van Hooff J. H. C., *Zeolites*, **4**, (1984), 9-14.

62) Borade R. B., Hegde S. G., Kulkarni S. B. and Ratnasamy P., *Appl. Catal.*, **13**, (1984), 27-38.

63) Santilli D. S., *Appl. Catal.*, **30**, (1990), 137-141.

64) Gielen B. and Palekar M. G., *Zeolites*, **9**, (1989), 208-216.

65) Abbot J., *Appl. Catal.*, **47**, (1989), 33-44.

66) Derouane E. G., Gilson J. P. and Nagy J. B., *J. Mol. Catal.*, **10**, (1981), 331-340.

67) Nayak V. S. and Choudhary V. R., *Appl. Catal.*, **10** , (1984), 137.

68) Shukla D. P. and Pandya V. P., *J. Chem. Tech.*, **44**, (1989), 147-154.

69) Jansen J. C., van der Haag F. J. and van Bekkum H., *Zeolites*, **4**, (1984), 369-372.

70) Coudurier G., Naccache C. and Vedrine J. C., *J. Chem. Soc., Chem. Comm.*, (1982), 1413-1415.

71) Freude D., Brunner E., Pfeifer H., Prager D., Jerschkewitz H. G., Lohse U. and Oehlmann G., *Chem. Phys. Lett.*, **139**, (1987), 325-330.

72) Scholle K. F. M. G. J., Veeman W. S., Frenken P. and van der Velden G. P. M., *Appl. Catal.*, **17**, (1985), 233-259.

73) Wu E. L., Lawton S. L., Olson D. H., Rohrman (Jr.) A. C. and Kokotailo G. T., *J. Phys. Chem.*, **83(21)**, (1979), 2777-2781.

74) Jablonski G. A. and Sand L. B., *Zeolites*, **6**, (1986), 396-402.

75) Argauer G. and Landolt R., *US Pat. 3702886*, (1972).

76) Bibby D. M., Milestone N. B. and Aldridge L. P., *Nature*, **285**, (1980), 30-31.

77) Choudhary V. R. and Singh A. P., *J. Catal.*, **94**, (1985), 573-575.

78) Musker W. K., *J. Amer. Chem. Soc.*, **86**, (1964), 960.

79) Derouane E. G., Detremmerie S., Gabelica Z. and Blom N., *Appl. Catal.*, **1**, (1981), 201-224.

80) Gabelica Z., Nagy J. B. and Bodart P., *Thermochimica Acta*, **93**, (1985), 749-752.

81) Nagy J. B., Gabelica Z. and Derouane E. G., *Zeolites*, **3**, (1983), 43-48.

82) Gabelica Z., Derouane E. G. and Blom N., *Appl. Catal.*, **5**, (1983), 109-117.

83) Gabelica Z., Gilson J. P. and Derouane E. G., *Second European Symposium on Thermal Analysis*, Dollimore D. (Ed.), 435-438.

84) Gabelica Z., Nagy B., Derouane E. G. and Gilson J. -P., *Clay Minerals*, **19**, (1984), 803-824.

85) Schwarz S., *PhD. Thesis*, University of Cape Town, (1990).

86) Schwarz S., Kojima M. and O'Connor C. T., *Appl. Catal.*, **56**, (1989), 263-280.

87) Tabak S. A., Krambeck F. J. and Garwood W. E., *J. AlChe.*, **32(9)**, (1986), 1529.

88) Norval G. W., Phillips M. J., Virk K. S. and Simons R. V., *Can. J. Chem. Eng.*, **67**, (1989), 521-523.

89) Gricus Kofke T. J. and Gorte R. J., *J. Catal.*, **115**, (1989), 233-243.

90) Ghosh A. K. and Kydd R. A., *J. Catal.*, **100**, (1986), 185-195.

91) Parker L. M., Bibby D. M. and Burns G. R., *Zeolites*, **11**, (1991), 293-297.

92) Hidalago C. V., Itoh H., Hatton T., Niwa M. and Murakami T., *J. Catal.*, **85**, (1985), 362-369.

93) Bolis V., Vedrine J. C., Van De Berg J. P. and Wolthuizen J. P., *J. C. S. Faraday 1*, **76**, (1980), 1606-1616.

94) Dry M. E., *Catalysis Sci. and Tech.*, Anderson J. R. and Boudart M. (Eds.), Springer Verlag, **1**, (1981), 159-256.

95) Martin A. M., Chen J. K., John V. T. and Dadyburjor D. B., *Ind. Eng. Chem. Res.*, **28**, (1989), 1613-1618.

96) McNair H. M. and Bonelli E. J., *Basic Chromatography*, Consolidated Printers Calif., (1969), 141-143.

97) Chang C. D. et al., *Chem. Eng. Commun.*, **95**, (1990), 27.

98) Kubelkova L. et al., *Z. Phys. Chem.*, NF, **168**, (1990), 231.

99) Karge H., Comparative Measurement on Acidity of Zeolites, *Studies in Surface Science and Catalysis*, Pub. Elsevier, Eds. Ohlmann G., Pfeifer H. and Fricke R., **65**, (1991), 133-156.

100) Barthomeuf D., Acidity and Basicity of Zeolites, *Studies in Surface Science and Catalysis*, Pub. Elsevier, Eds. Ohlmann G., Pfeifer H. and Fricke R., **65**, (1991), 157-170.

APPENDIX A

Calculation of Pure Oxygenate Conversion and Selectivity.

a) Conversion

1) Mass of Oxygenate fed

$$= \rho_{oxy} \times V_{oxy} = M_{oxy} \ \frac{grams}{hr}$$

2) Mass flow of Nitrogen carrier

$$= 30 \ \frac{ml}{min} \times 60 \ \frac{min}{hr} \times \frac{1}{10^6} \ \frac{m^3}{ml} \times \frac{28 \times 101325}{8.314 \times 298}$$

$$= 2.0612 \ \frac{g}{hr}$$

3) Mass Rate of CO and CO_2

$$= \frac{(W_{CO} + W_{CO2})}{W_{N2}} \times 2.0612 = S \ \frac{grams}{hr}$$

4) Carbon Balance :

Carbons in

$$= \frac{M_{oxy}}{MW_{oxy}} \times C_{oxy} = N_{oxy} \ \frac{moles}{hr}$$

Carbons in hydrocarbon product (i.e. non permanent gas product)

$$= N_{oxy} - \frac{M_{CO}}{28} - \frac{M_{CO2}}{44} = N' \ \frac{moles}{hr}$$

Mass of unreacted feed

$$= (M_{oxy} - S) \times W_{oxy} = M' \ \frac{grams}{hr}$$

APPENDIX A (cont.)

Therefore, Carbons reacted to non permanent gas product

$$= \frac{M_{oxy} - M'}{MW_{oxy}} \times C_{oxy} = N_R$$

Conversion

$$= \frac{M_{oxy} - M'}{M_{oxy}} \times 100$$

b) Selectivity of products

Assuming the following Number of carbons for the hydrocarbon groupings below:

Aliphatic C_5/C_6 = 6
Aliphatic C_{12+} = 14
Aromatic C_{12+} = 14

1) Carbons in CO and CO_2

$$= \frac{M_{CO}}{28} - \frac{M_{CO2}}{44} = N_{CO} + N_{CO2} \quad \frac{\text{moles}}{\text{hr}}$$

2) Carbons of component i in non permanent gas product

$$= (M_{oxy} - Z) \times \frac{W_i}{MW_i} \times N_i \quad \frac{\text{moles}}{\text{hr}}$$

$$= C_i$$

3) Selectivity to Component i

$$= \frac{\text{Carbons of component i}}{\text{Carbons Reacted}}$$

$$= \frac{C_i}{C_R}$$

APPENDIX B

Calculation of the Light Hydrocarbon Selectivities

Using the following hydrocarbon distribution below as an example:

Light Hydrocarbons

Propene Oligomerisation co-feeding MEK

Component	Response Factor	Area	Area*RF	Mass %
Methane	1.124	0	0	0.000
Ethane/Ethene	1.021	73584	75129.264	0.647
Propane	1.000	2208700	2208700	19.019
Propene	0.967	9033900	8735781.3	75.225
Isobutane	0.924	53706	49624.344	0.427
n-Butane	1.033	14879	15370.007	0.132
1-Butene	0.994	72930	72492.42	0.624
Isobutene	0.922	24445	22538.29	0.194
Trans-2-Butene	0.908	124940	113445.52	0.977
Cis-2-Butene	0.986	81680	80536.48	0.694
C5/C6	1.000	239236	239236	2.060

1) The relative response factors had been calculated with respect to propane whose response factor was chosen as 1.

2) The following formula for calculating the mass % of each compound was used:

e.g. for methane $$W_m\% = \frac{Area_m \times RF_m}{\sum Area_i \times RF_i}$$

where $Area_i$ is the peak area for component i.

APPENDIX C

Calculation of the Si/Al ratio using Elemental Analysis Results.

Assumptions :

a) that the density of the dissolved sample in the 50 ml polypropylene container is 1 gram/ml then:

b) the unit cell mass is calculated from the formula $Na_n(Al_nSi_{(96-n)}O_{192})$

1) Mass of Al^{3+} in sample

$$= \frac{PPM \times 50}{10^6} = M \text{ grams}$$

2) Mass % of Al^{3+}

$$= \frac{M}{\text{Initial Dry Mass of Catalyst}} = X$$

3) Therefore

$$X = \frac{26.98 \times n}{22.99 \times n + (96-n) \times 28.09 + 26.98 \times n + 3072}$$

can be solved for n

4) Thus

$$Si/Al = \frac{96 - n}{n}$$

APPENDIX D

Calculation of the Propene/Propane Oligomerisation feed Compressibility Factor (Z)

1) Equations:

Smith J. M and Van Ness H. C., Introduction to Chemical Engineering Thermodynamics, Chapters 3 and 11, Macgraw-Hill Inc., (1987).

a) $Z = 1 + (B \times P)/(R \times T)$

b) $B = \sum y_i y_j B_{ij}$

2) Data

Feed Composition (Mass %): 86% Propene (1)
14% Propane (2)

Temperature of WFGM = 26.5°C

ij	Tc_{ij} (K)	Pc_{ij} bar	Vc_{ij} cm^3/mol x 10^6	Zc_{ij}	w_{ij}
11	369.8	42.5	203	0.281	0.152
22	365	46.2	181	0.275	0.148
12	367.4	44.3	191.8	0.278	0.150

*Critical Constants and Accentric factors from above reference

APPENDIX D (cont.)

ij	Tr_{ij}	B^{o}	B^{1}	B_{ij}
11	0.810	-0.508	-0.277	-397.9
22	0.821	-0.496	-0.255	-350.3
12	0.816	-0.502	-0.266	-373.4

3) $B = (0.86)^2 \times (-350) + 2 \times 0.86 \times 0.14 \times (-373.4) + (0.14)^2 \times (-397.9)$

$= -356.8 \times 10^{-6}\ m^3/mol$

$Z = 1 + (-397.9 \times 10^{-6} \times 101325)/(8.314 \times 299.65)$

$= 0.9845$

APPENDIX E

Propene Oligomerisation Data Work-up

$WGFM_i$	= 653.56 litres
$WGFM_f$	= 654.75 litres
WGFM Temperature	= 26.5°C
Pump Setting	= 3
Catalyst Mass	= 1.0015 g
Pressure	= 50 MPa
Reactor Setpoint	= 210°C
Reactor Bed	= 257°C
Liquid Mass	= 10.2 g (after 1 hour)
Molecular mass of gas sample	= 47.075 g/gmol
Compressibility (Z)	= 0.9845
WGFM Calibration Factor	= 0.981
Flowrate of Gas	= 0.981 x (654.75 - 653.56)/1.0 = 1.171 litres/hr

APPENDIX E (cont.)

Mass Rate of Gas $= \dfrac{101325 \times 1.171 \times 47.075}{8.314 \times 299.65 \times 0.9845 \times 10^3}$

$= 2.2877$ g/hr

% dissolved gases in liquid sample $= 4.8284$ mass%

Mass Liquid Product $= 10.2 \times (1 - 0.048284)$

$= 9.693$ g

WHSV $= \dfrac{10.2 + 2.2877}{1.0015}$

$= 12.469\ h^{-1}$

Conversion based on total feed $= (9.693 \times 100)/12.469$

$= 78$ %

Conversion based on 86% propene as feed $= 78/0.86$

$= 90$ %

APPENDIX F

^{27}Al-NMR spectra of as-synthesised and regenerated catalysts

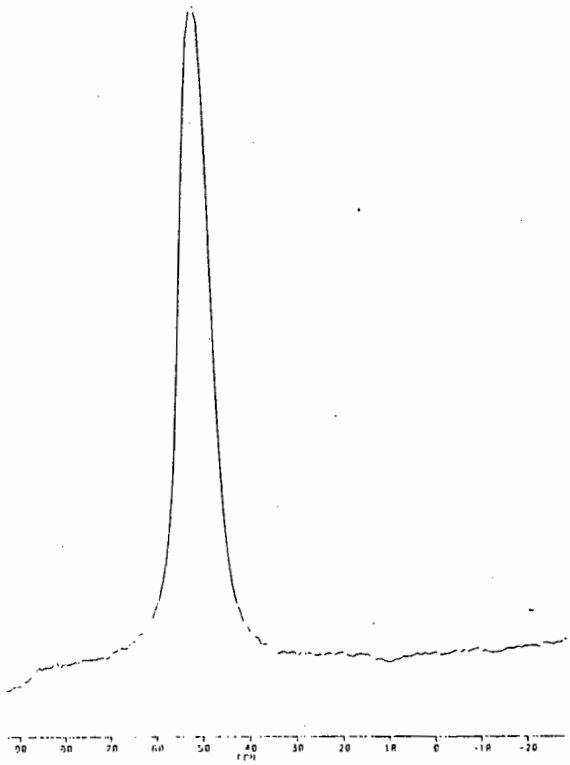

(a) ZS1

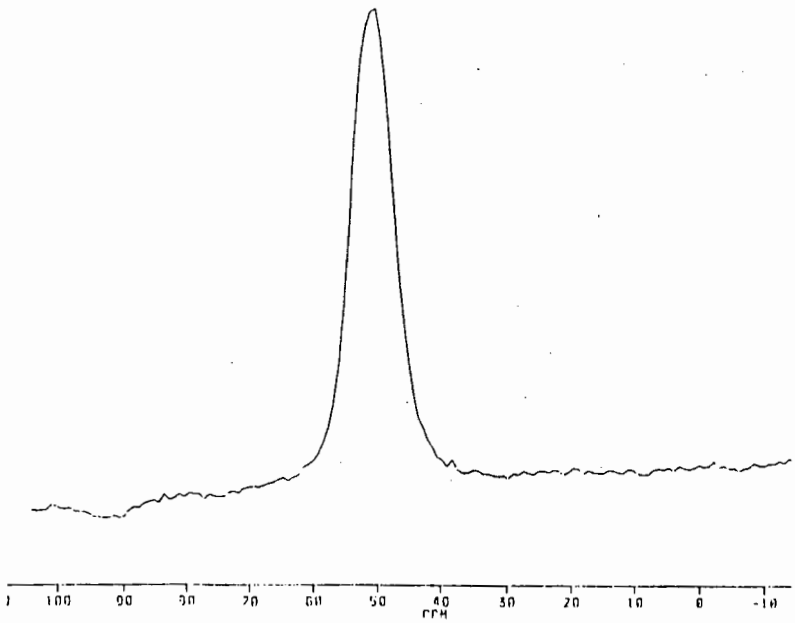

(b) Catalyst regenerated from acetic acid reaction at 350°C

APPENDIX F (cont.)

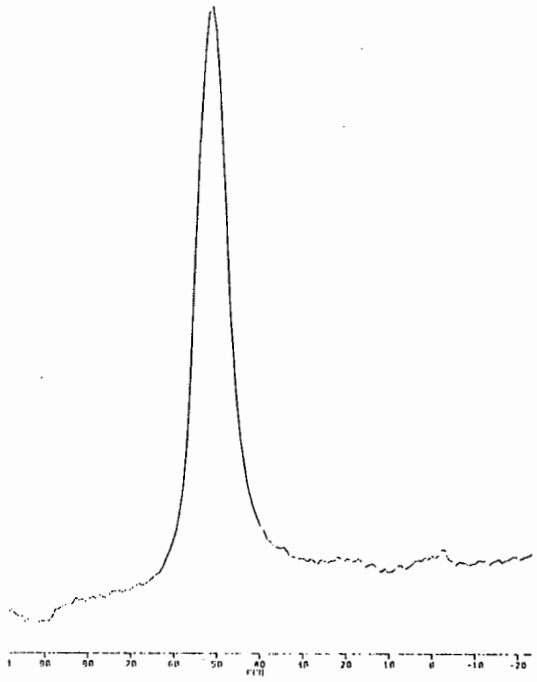

(c) Catalyst regenerated from MEK reaction at 300°C

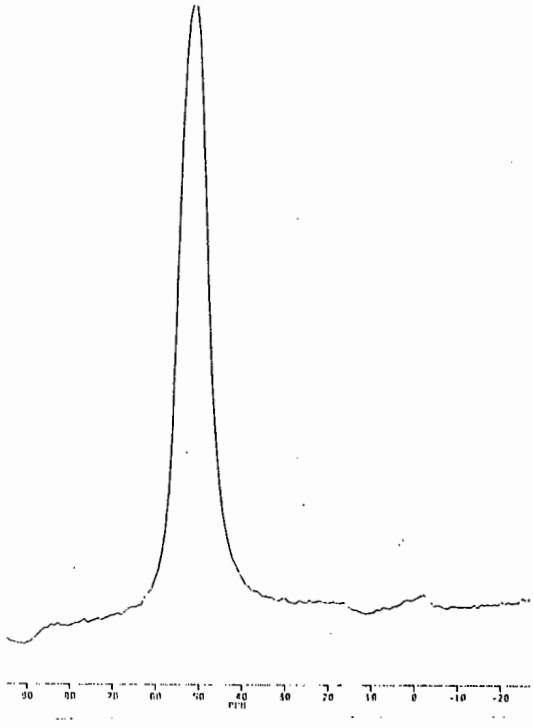

(c) Catalyst regenerated from n-butanol reaction at 300°C

APPENDIX G

X-ray diffraction patterns of as-synthesised catalysts

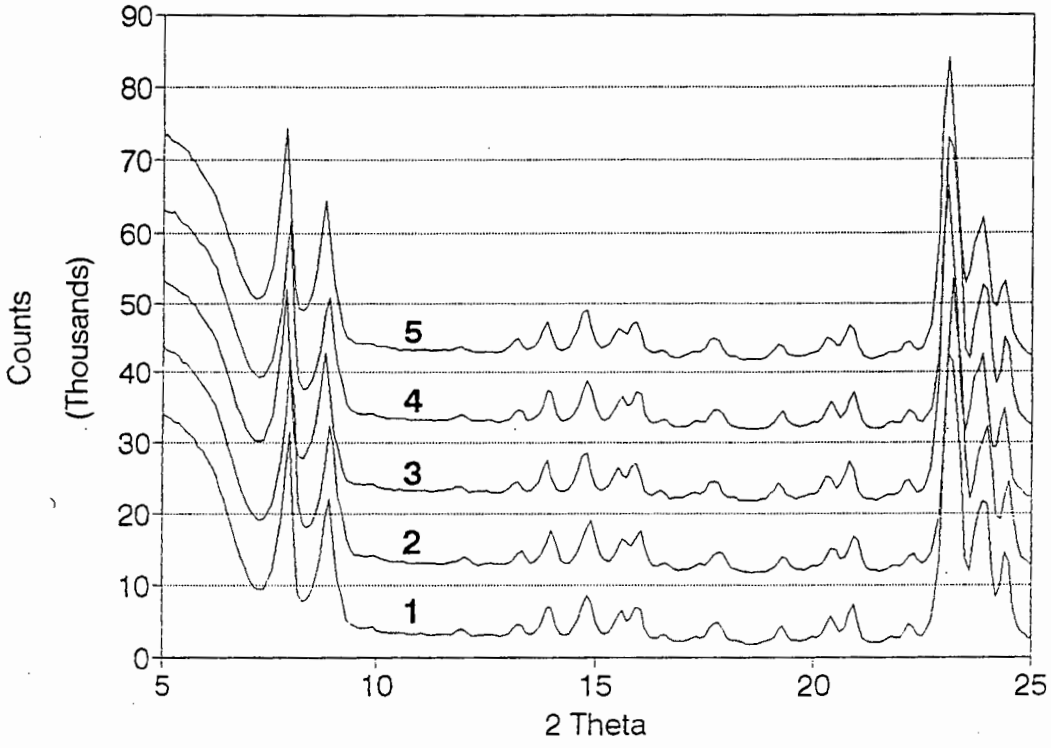

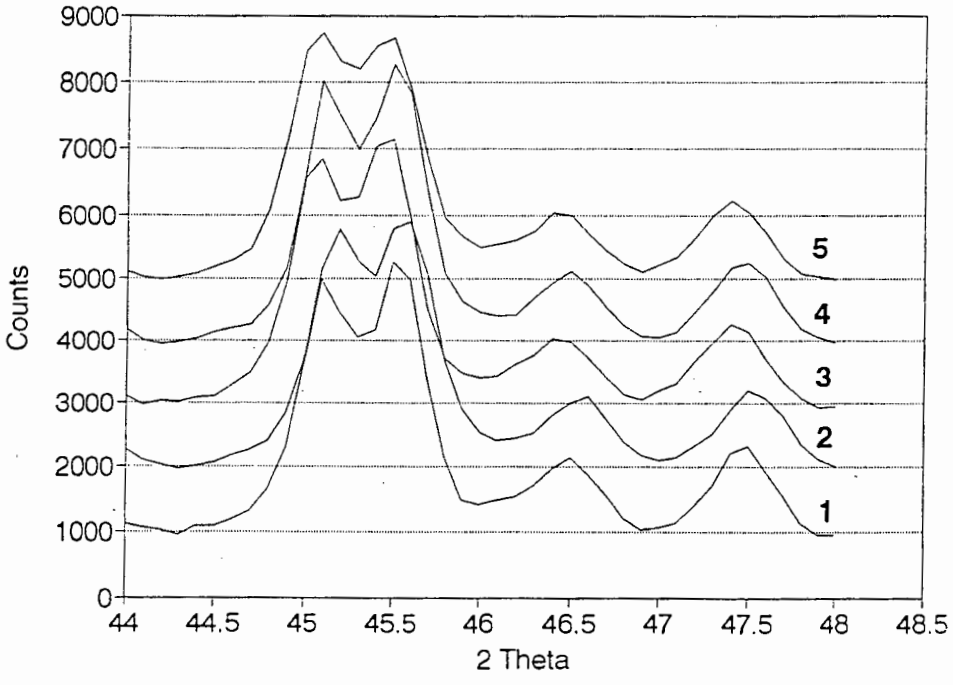

1) ZS1 2) ZS2 3) ZS3 4) ZS4 5) ZS5

APPENDIX H

X-ray diffraction patterns of regenerated ZSM-5 catalysts

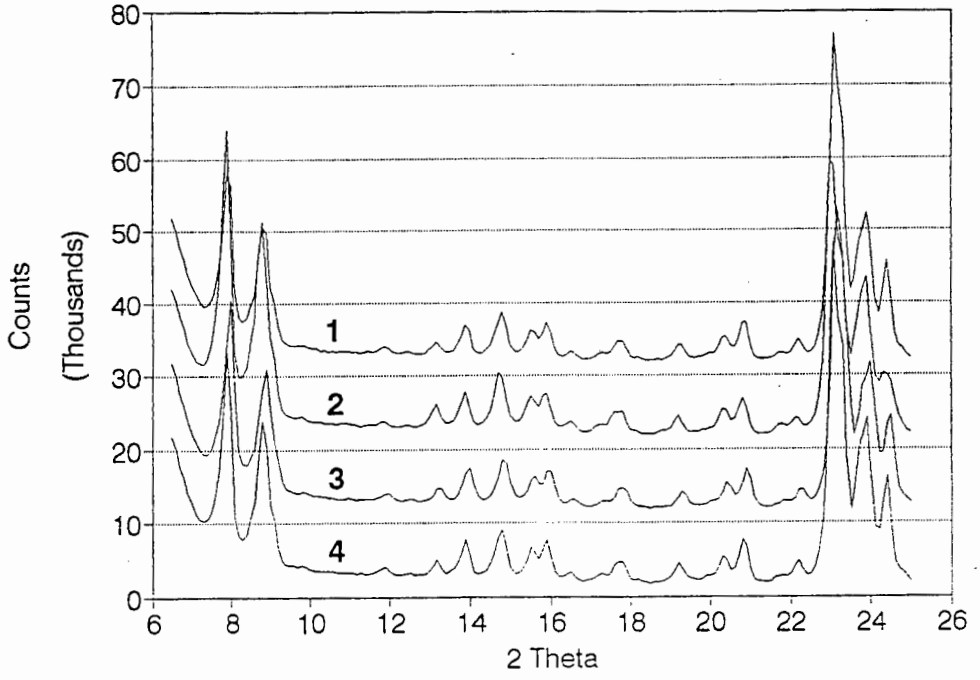

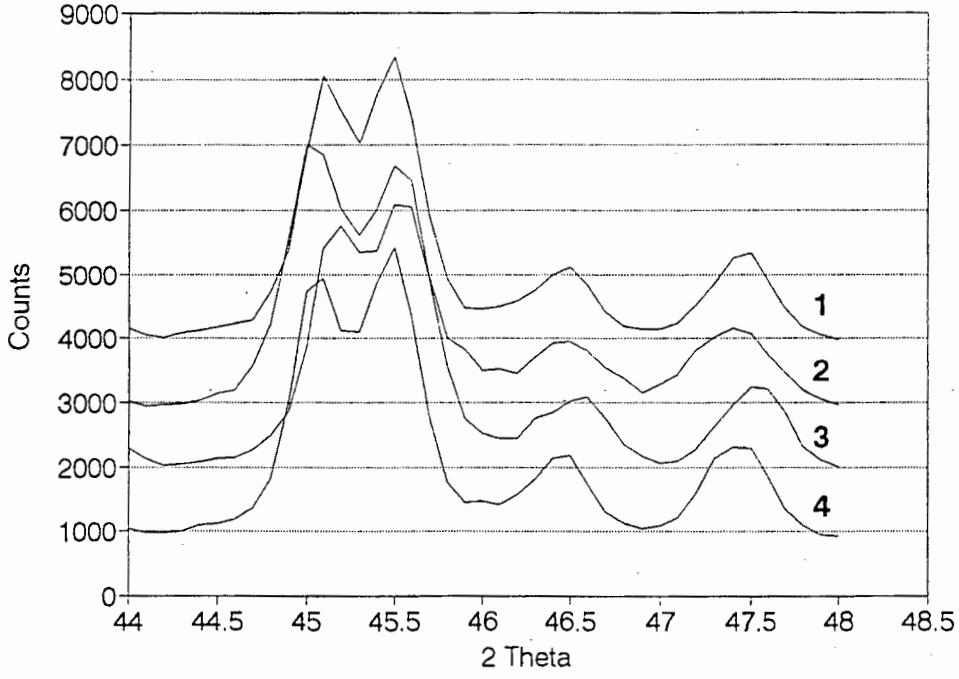

(1) After acetic acid reaction at 350°C for 10 hours

(2) After MEK reaction at 300°C for 10 hours

(3) After n-butanol reaction at 300°C for 10 hours

(4) As-synthesised ZS1

APPENDIX I

Infra-red spectra of ZS1 and regenerated catalyst

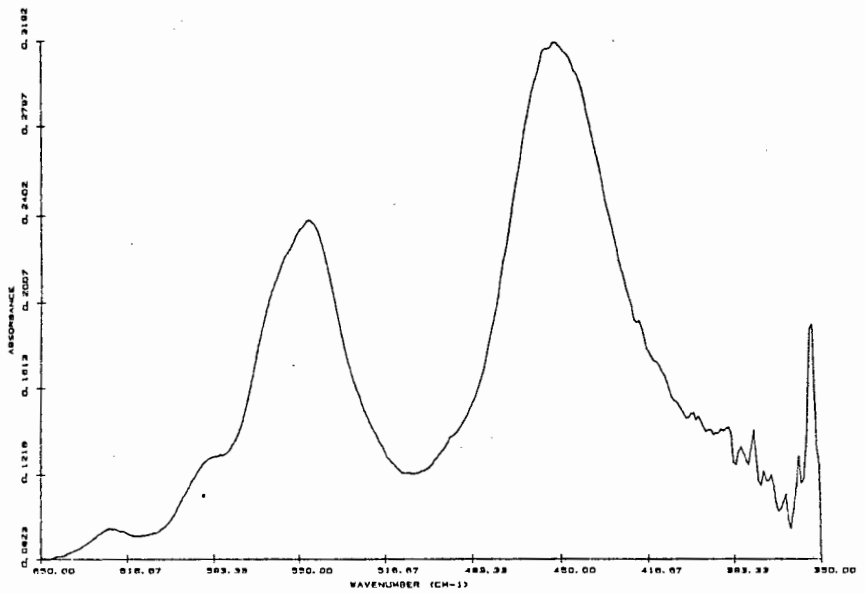

(a) As-synthesised catalyst (ZS1)

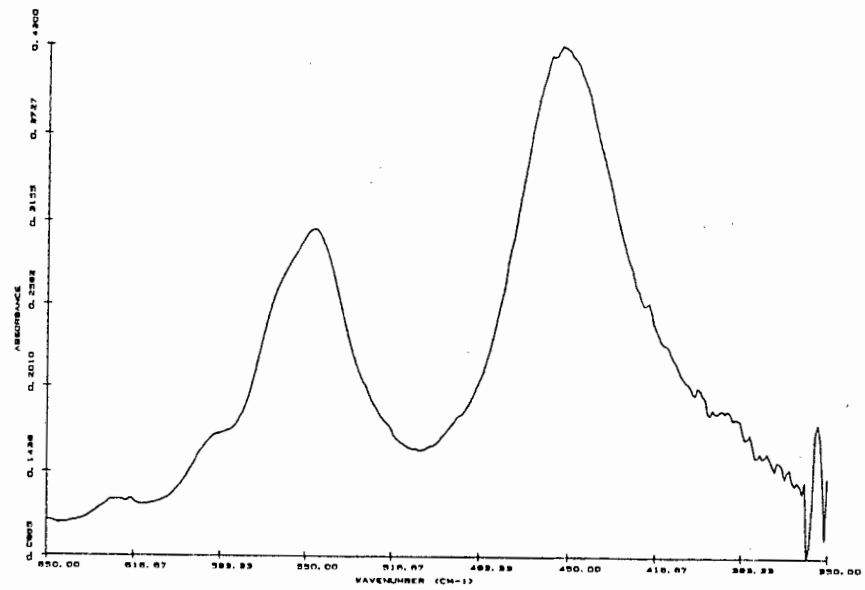

(b) Regenerated from acetic acid conversion at 350°C (10 hours)

APPENDIX J

Typical conversion vs run time and product selectivities for propene oligomerisation

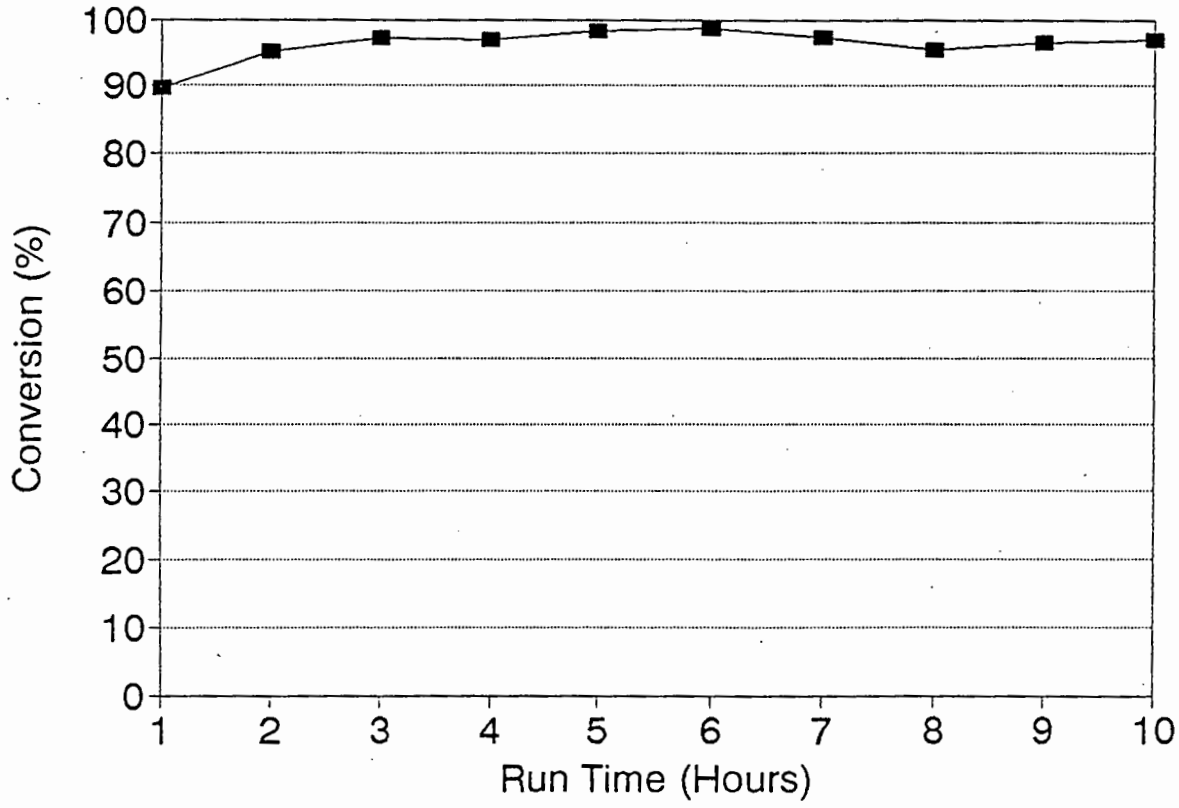

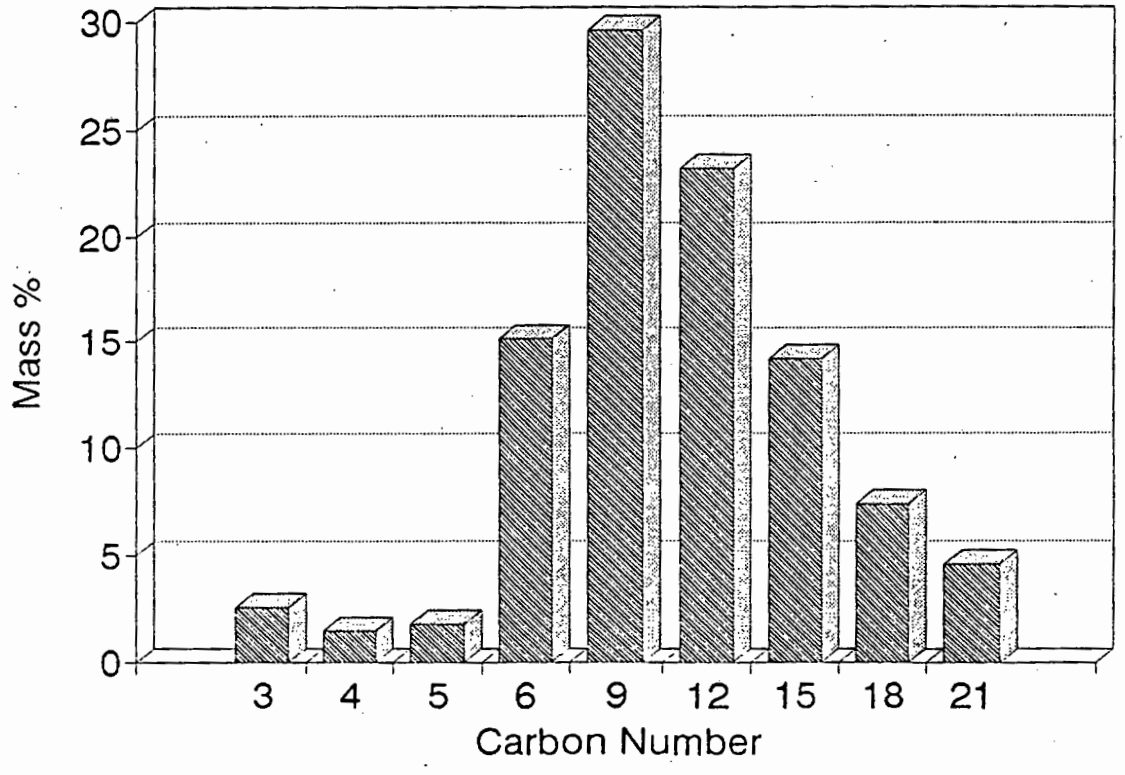

APPENDIX K

Light hydrocarbon selectivities for pure oxygenate reactions

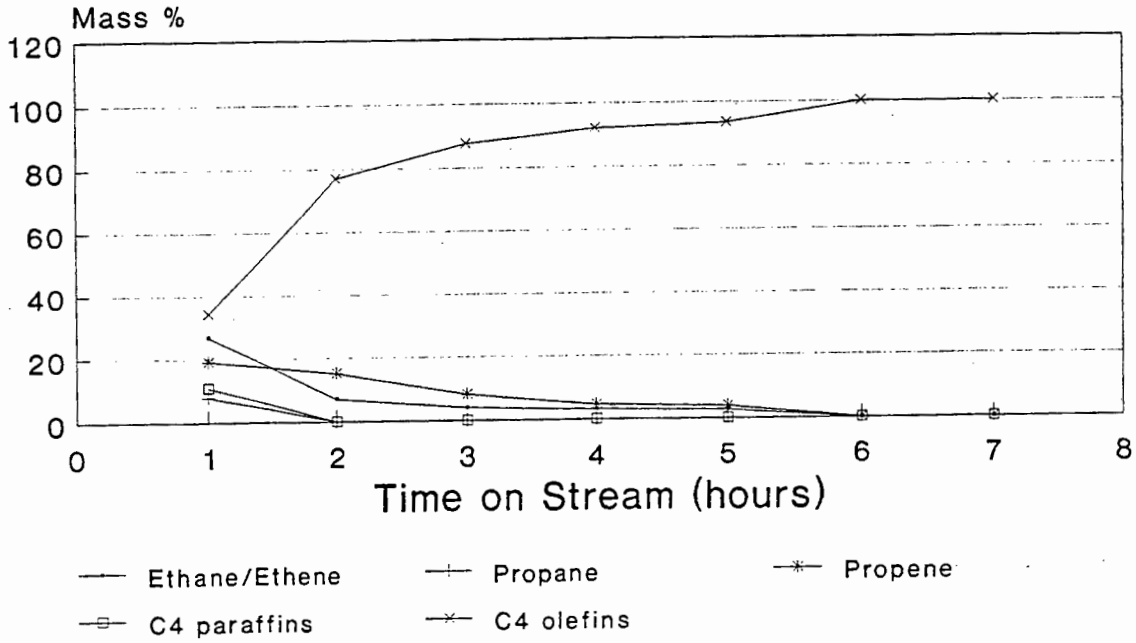

(a) Acetic acid conversion at 350°C and WHSV = 1 h^{-1}

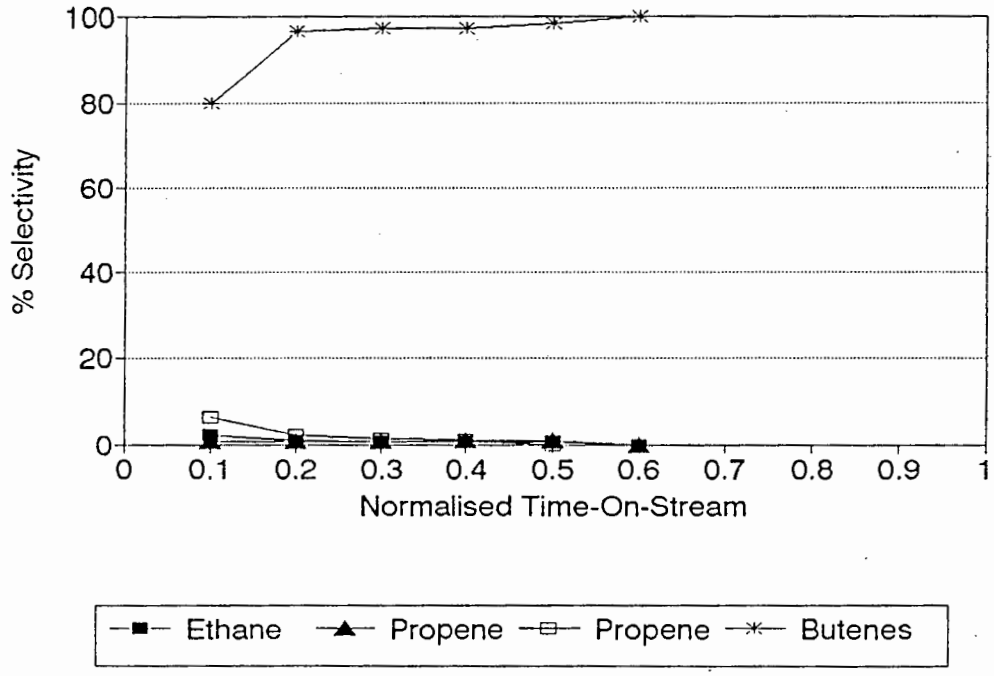

(b) Acetone conversion at 250°C and WHSV = 1 h^{-1}

APPENDIX K (cont.)

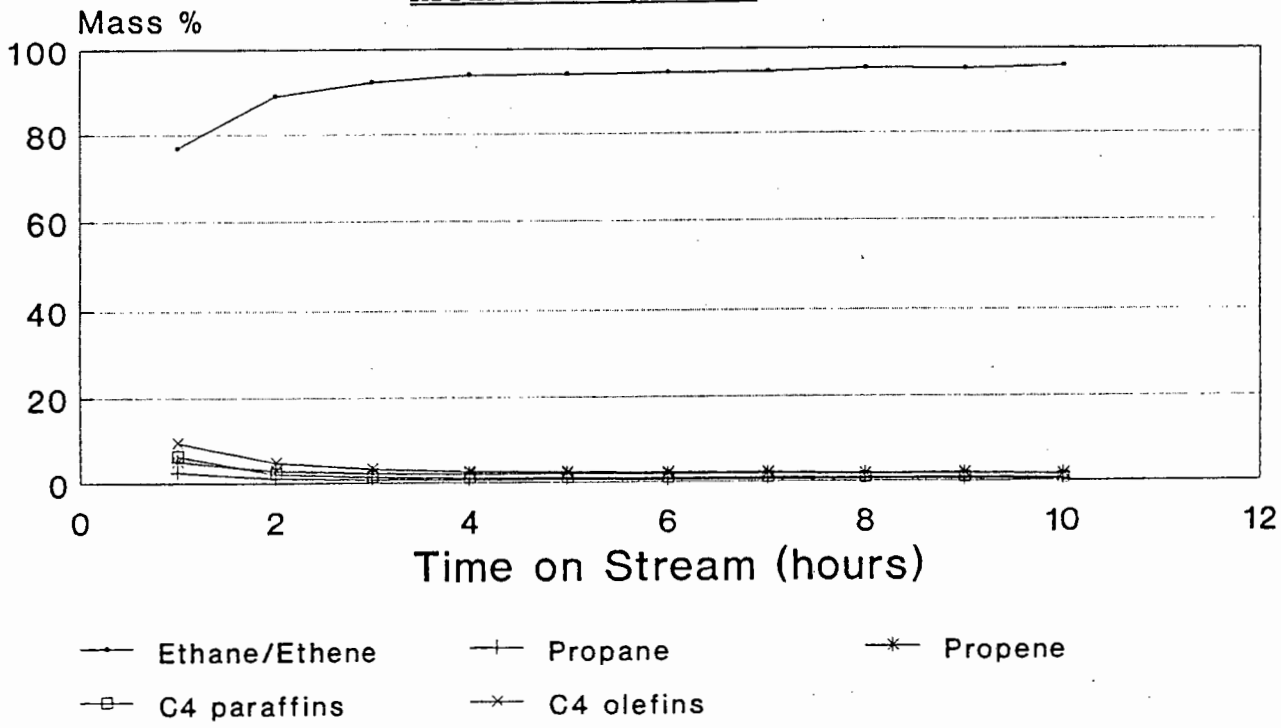

(c) Ethanol conversion at 250°C and WHSV = 1 h^{-1}

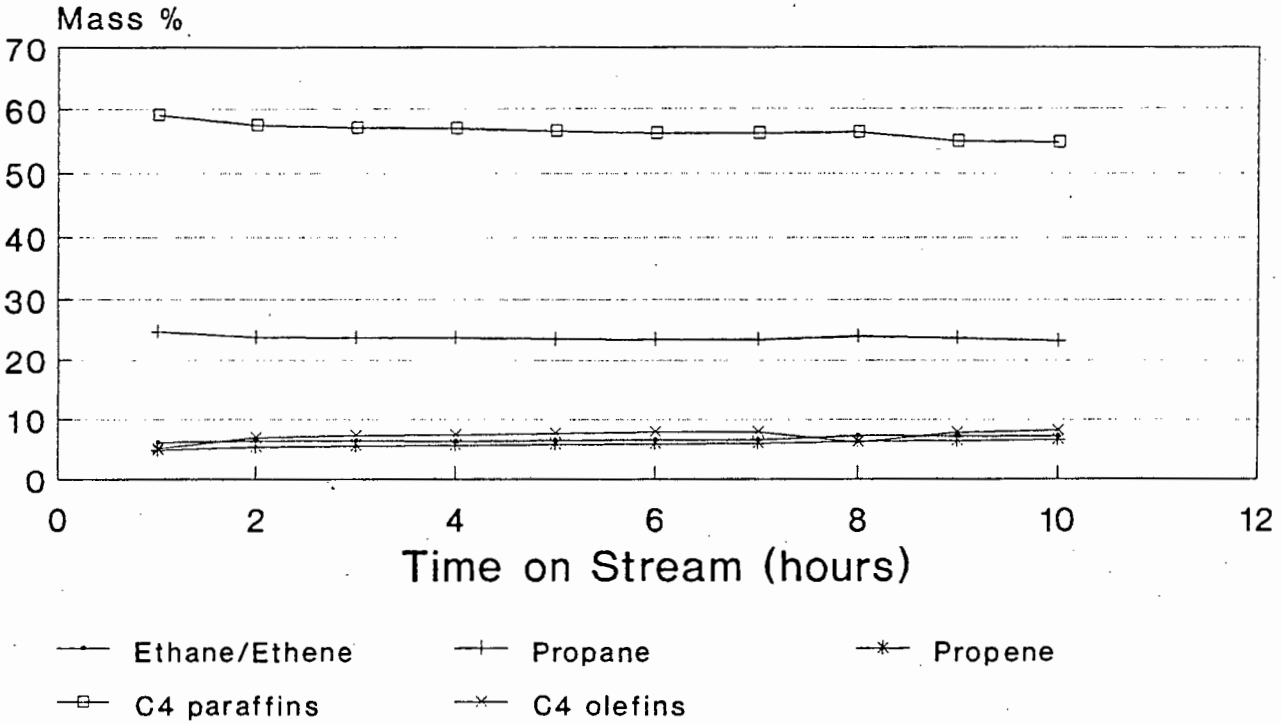

(d) Ethanol conversion at 300°C and WHSV = 1 h^{-1}

APPENDIX K (cont.)

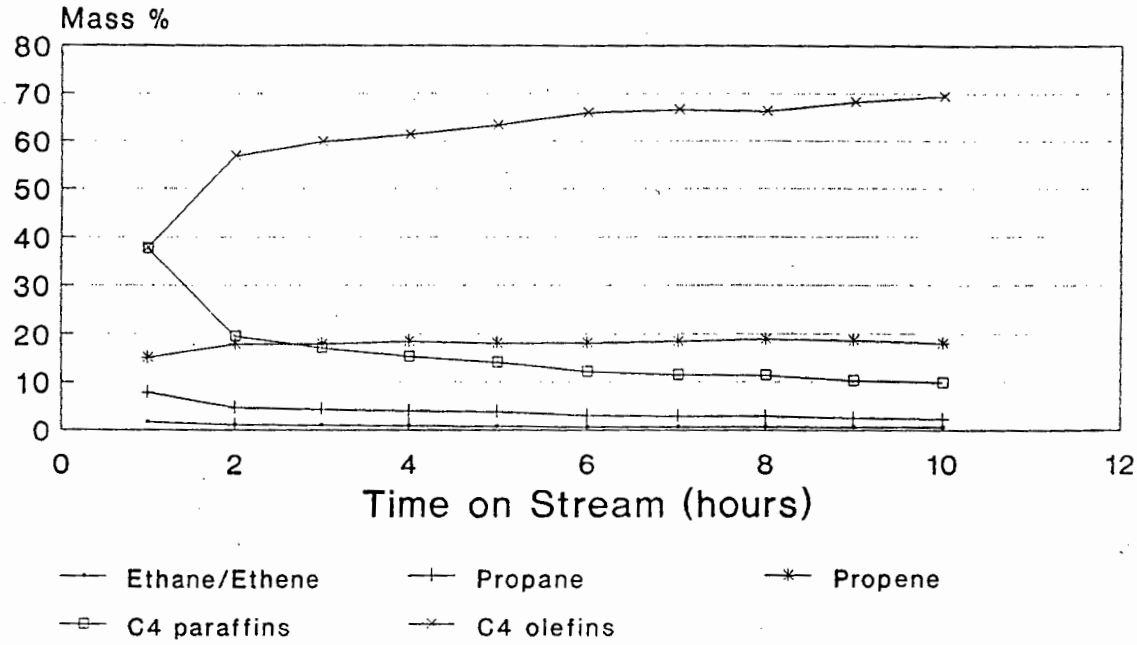

(e) n-Butanol conversion at 250°C and WHSV = 1 h^{-1}

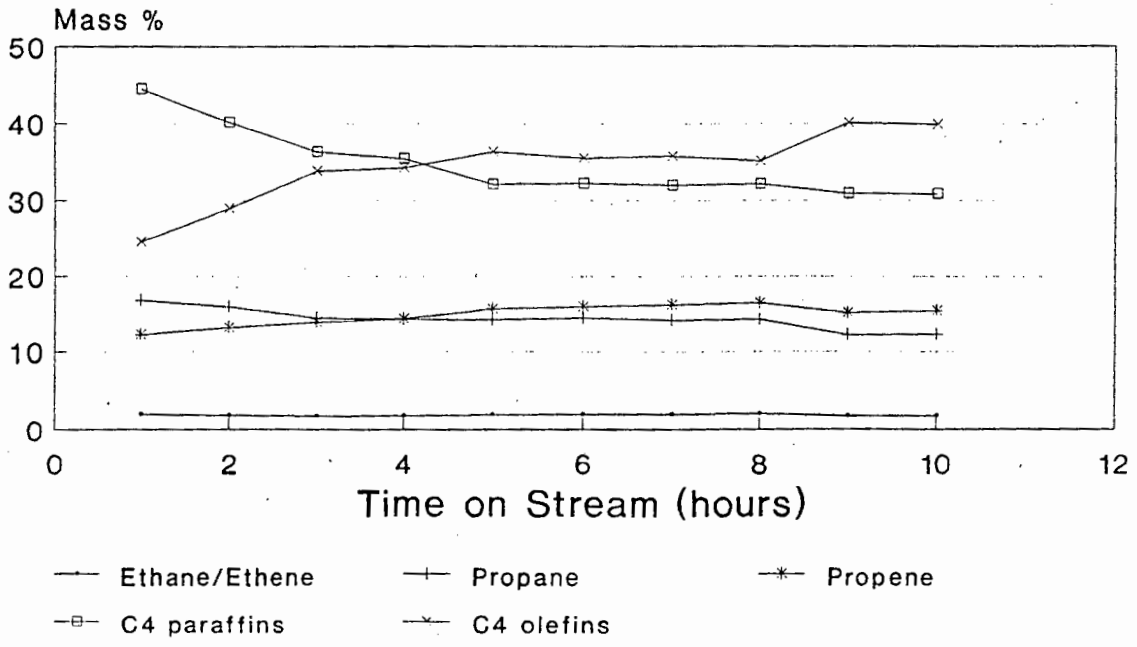

(f) n-Butanol conversion at 300°C and WHSV = 1 h^{-1}

APPENDIX K (cont.)

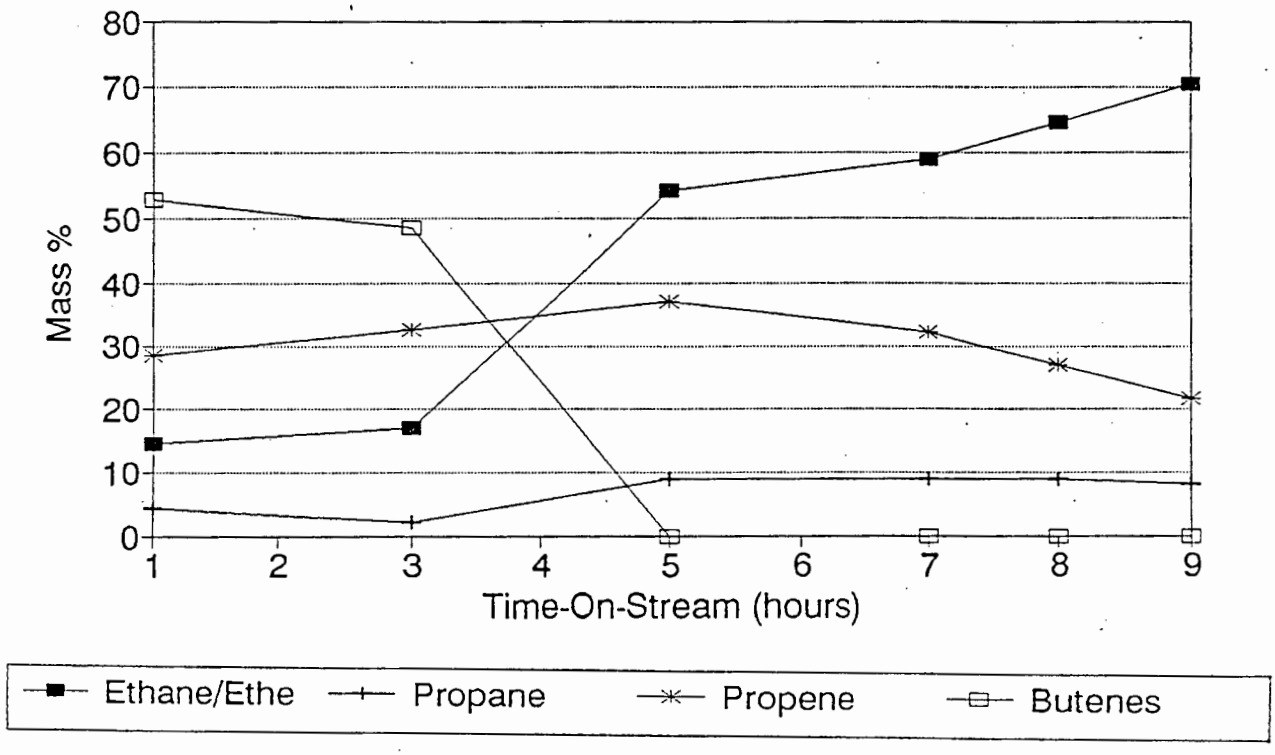

(e) MEK conversion at 250°C and WHSV = 1 h^{-1}

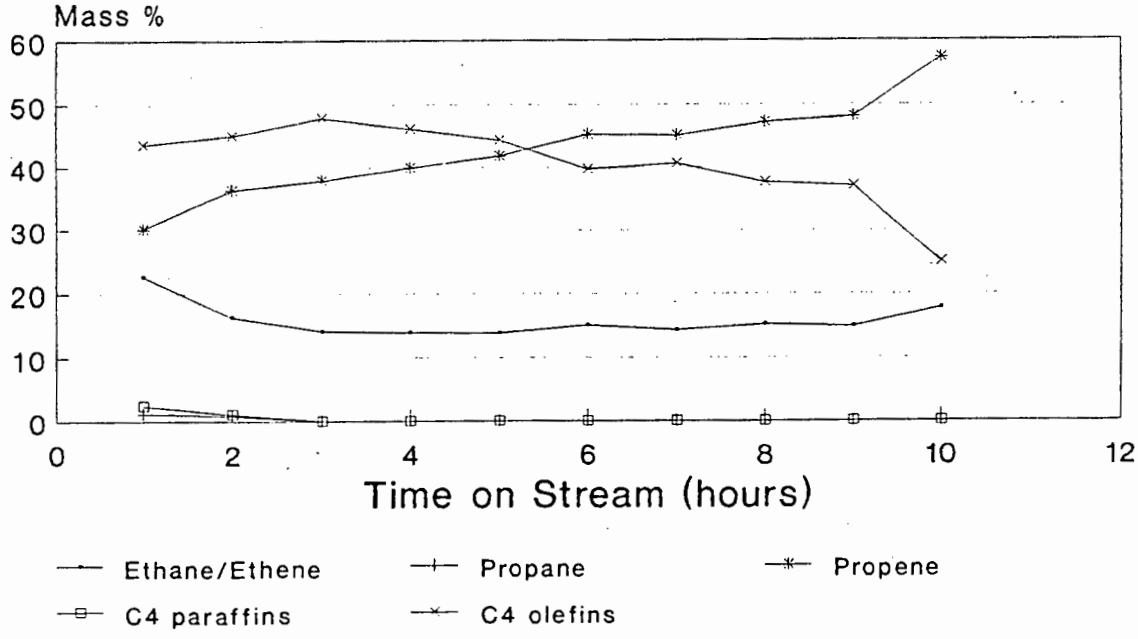

(f) MEK conversion at 300°C and WHSV = 1 h^{-1}

APPENDIX L

Co-feeding oxygenates during propene oligomerisation - Bed temperature and mass % propene in the tailgas vs normalised-time-on-stream

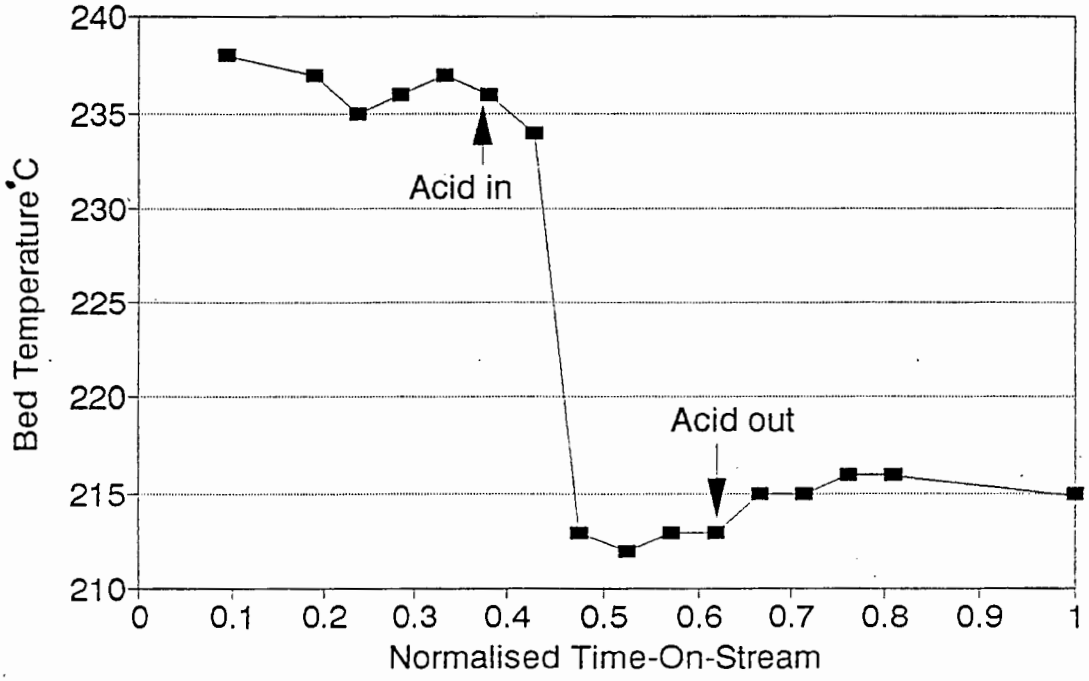

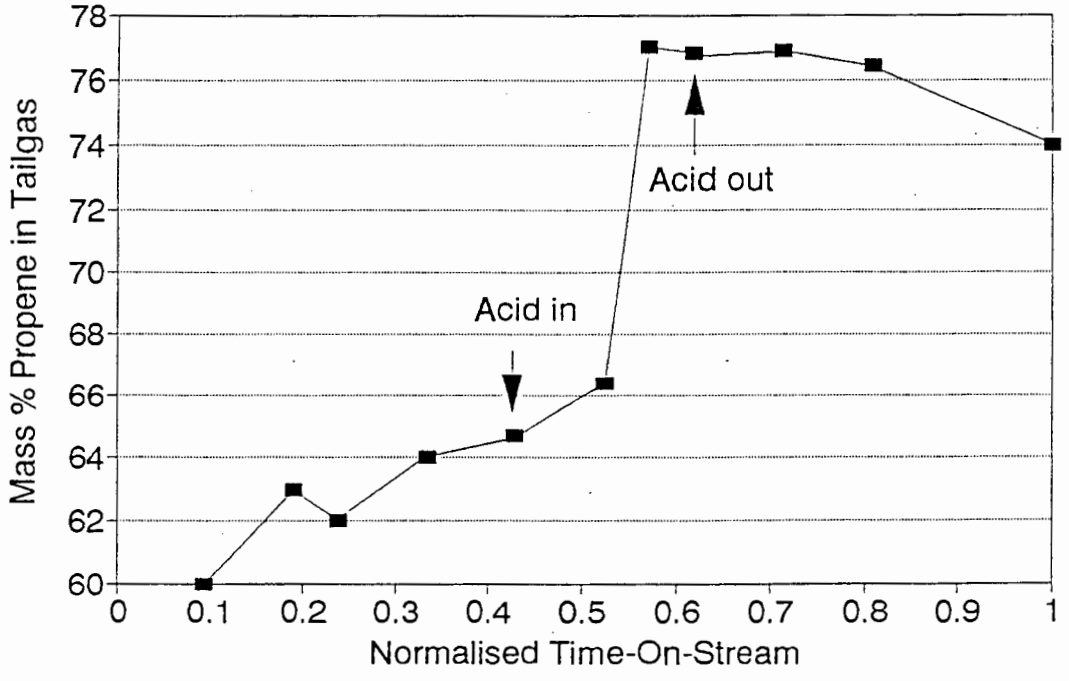

(a) Acetic acid

APPENDIX L (cont.)

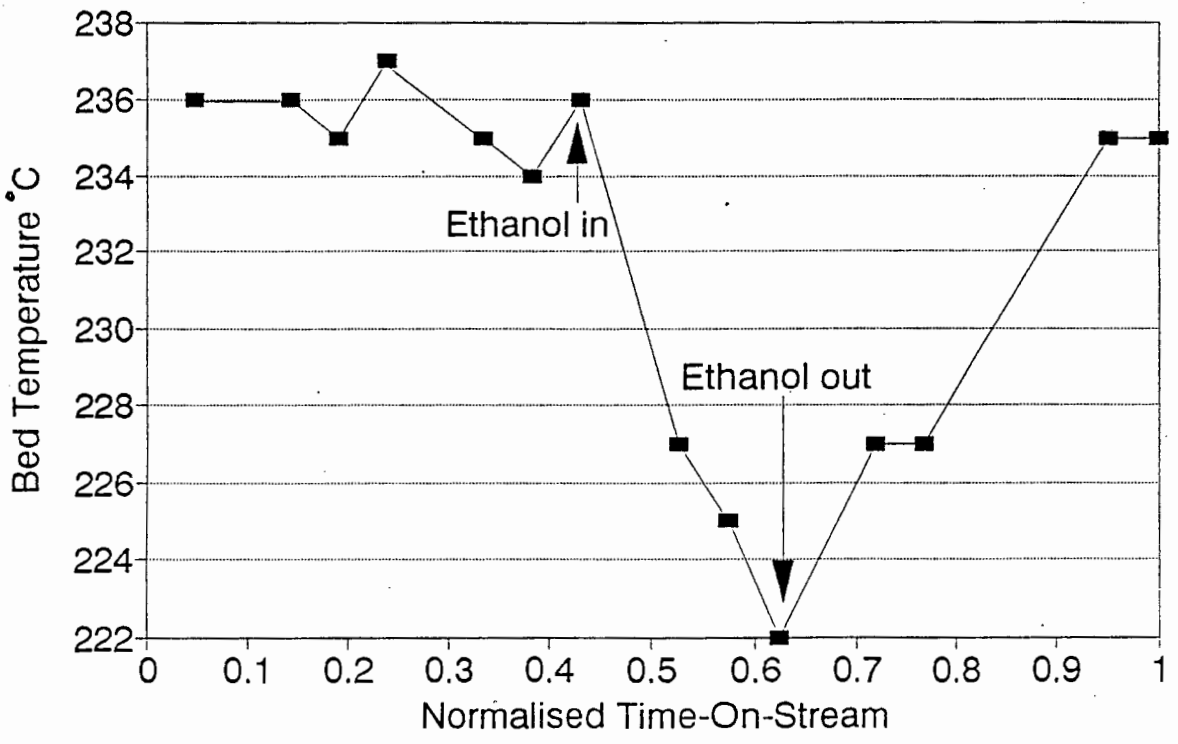

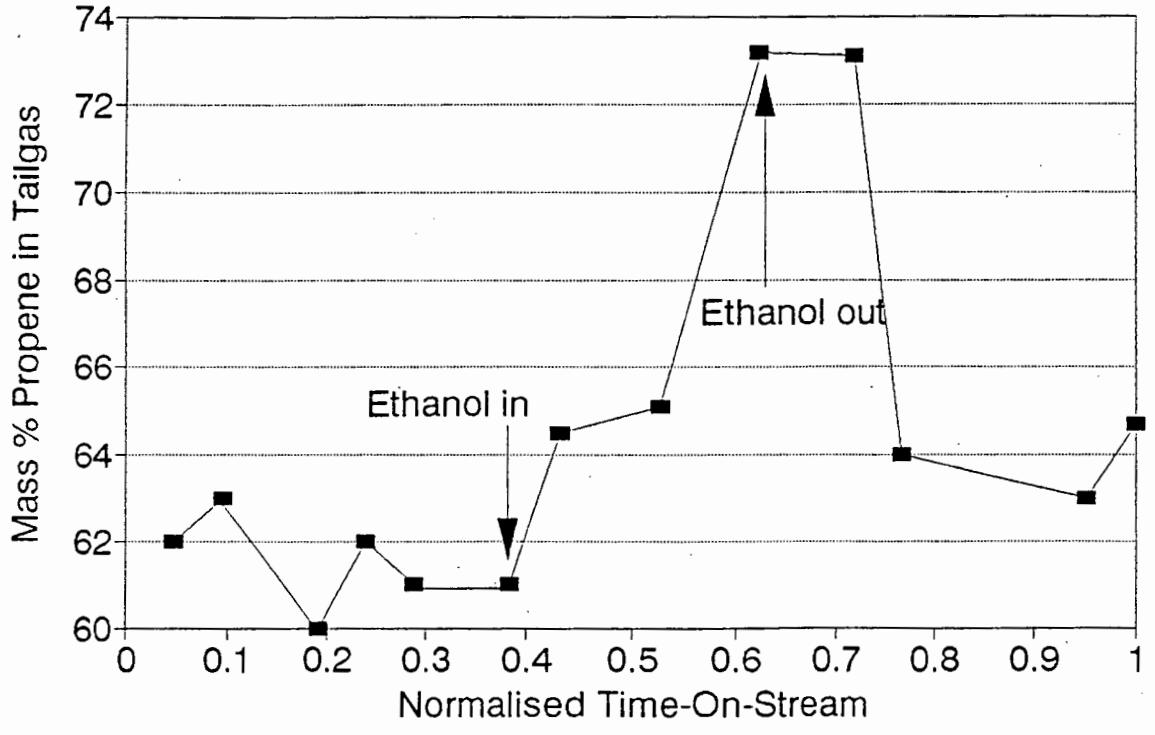

(b) Ethanol

APPENDIX L (cont.)

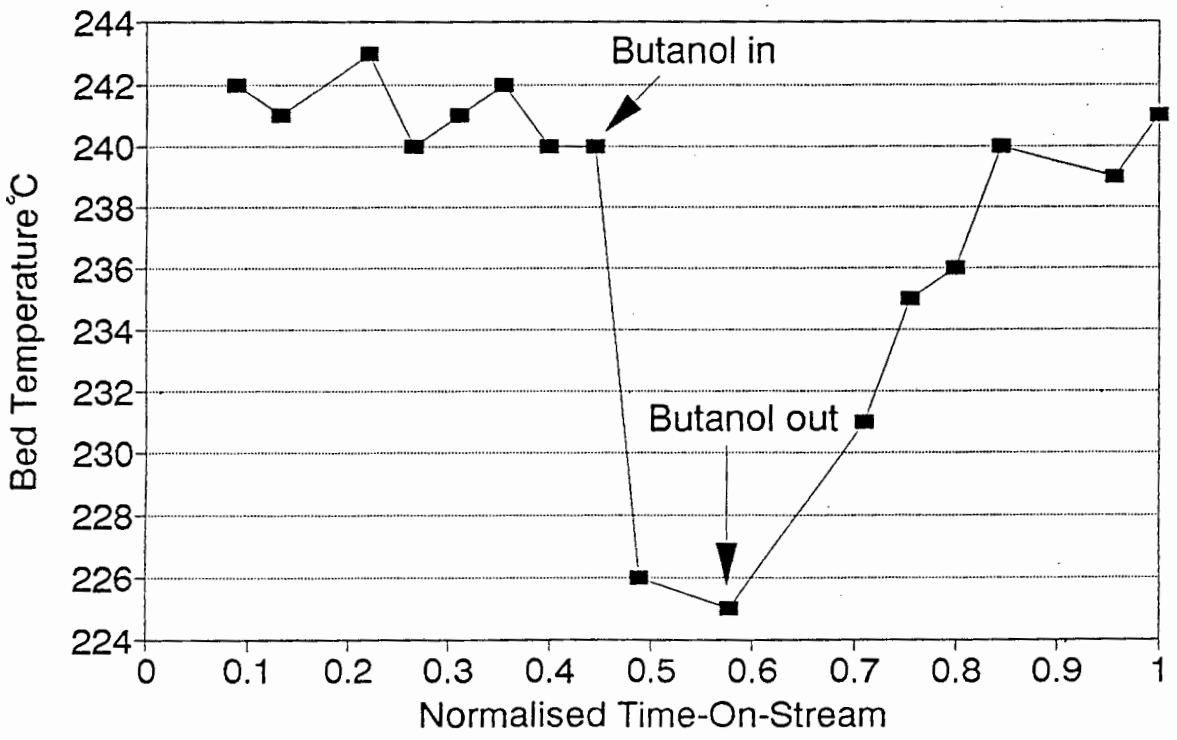

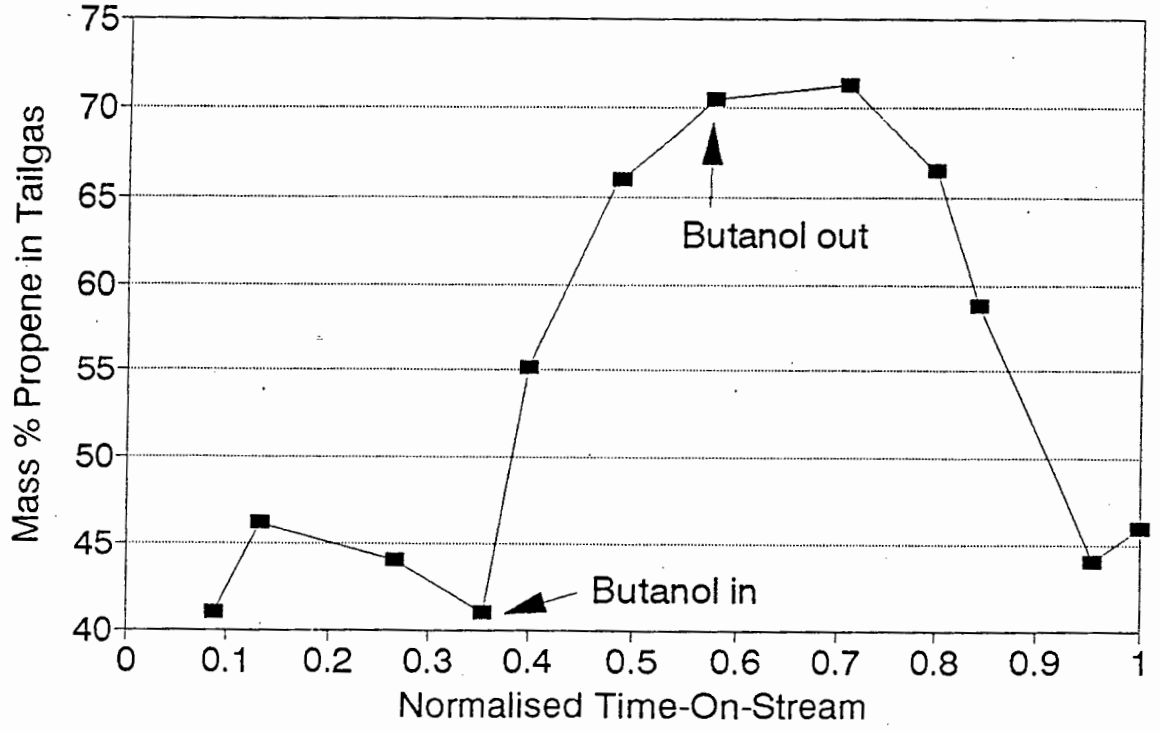

(c) n-Butanol

APPENDIX L (cont.)

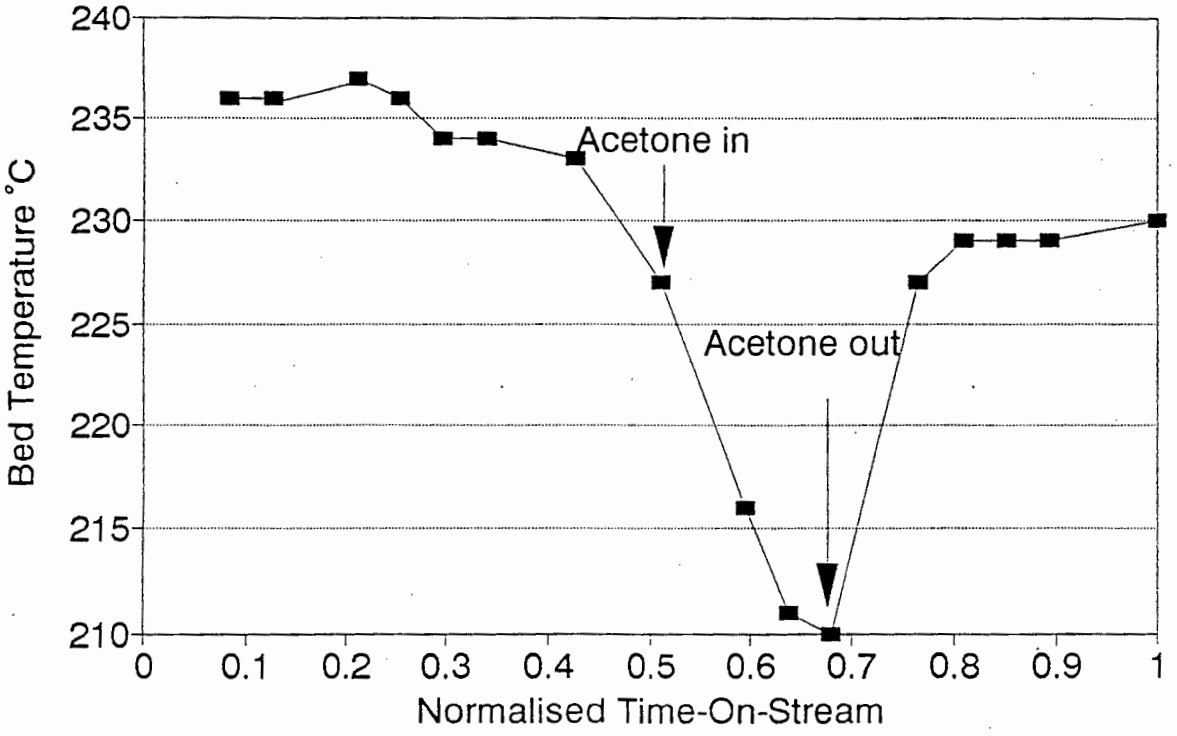

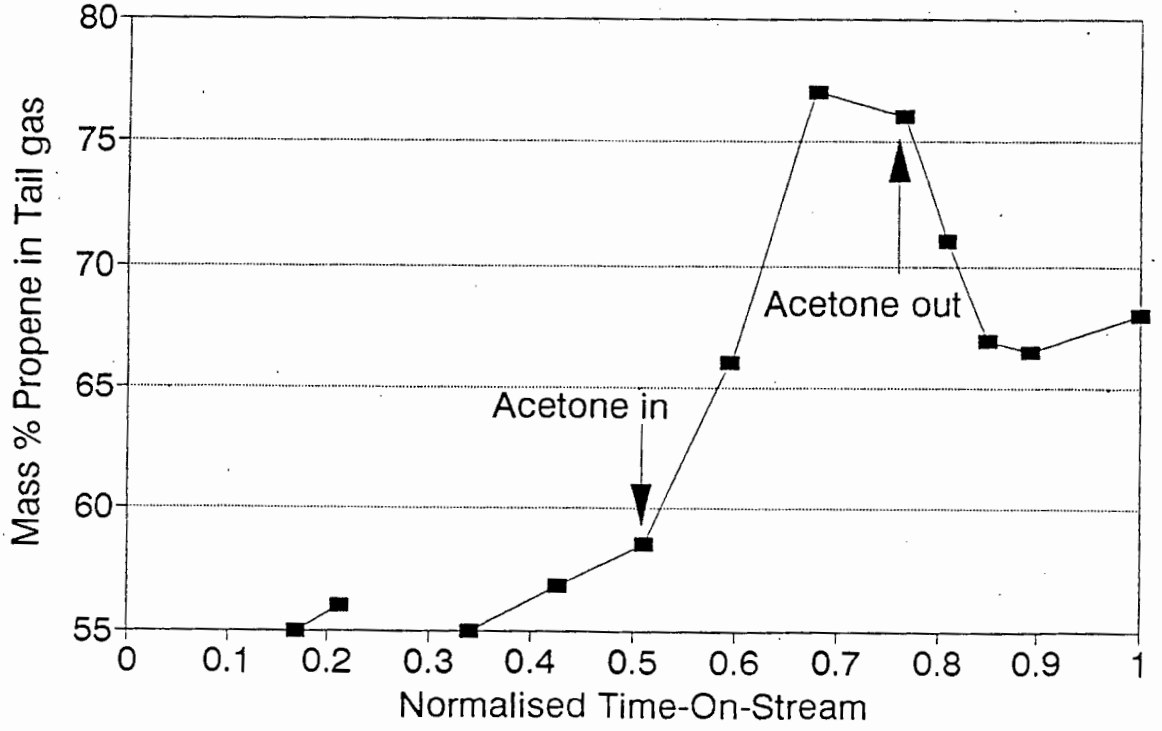

(d) Acetone

APPENDIX L (cont.)

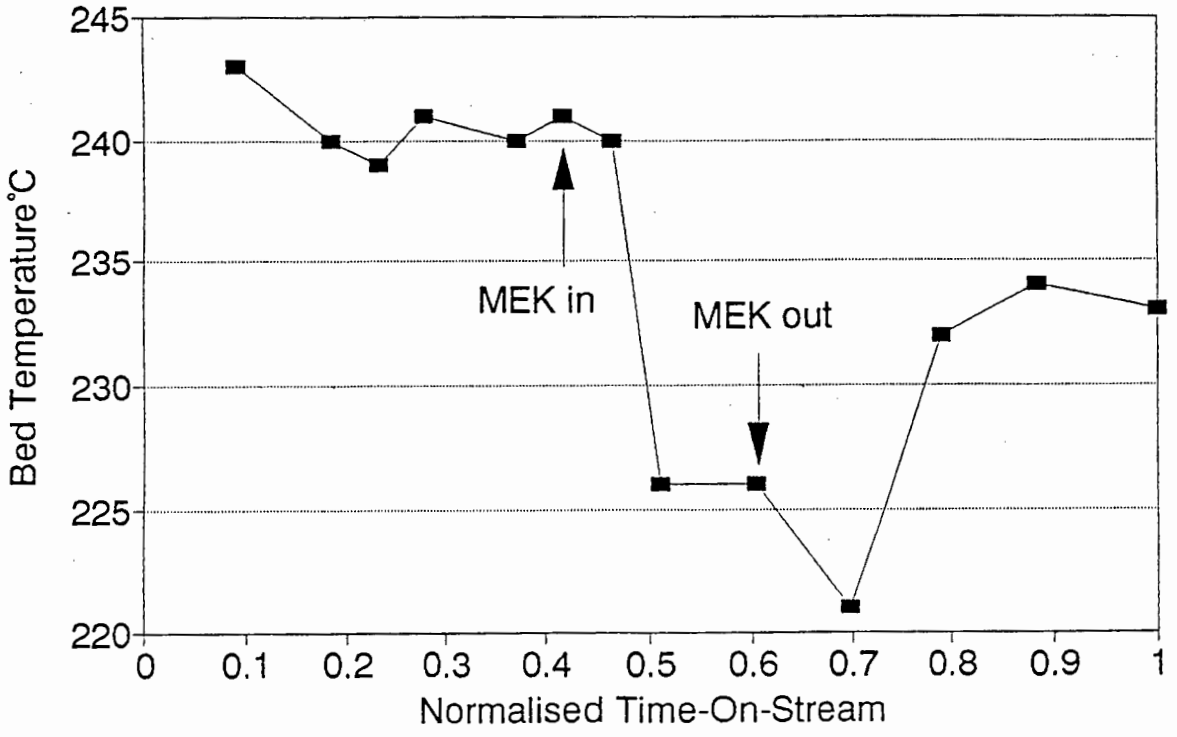

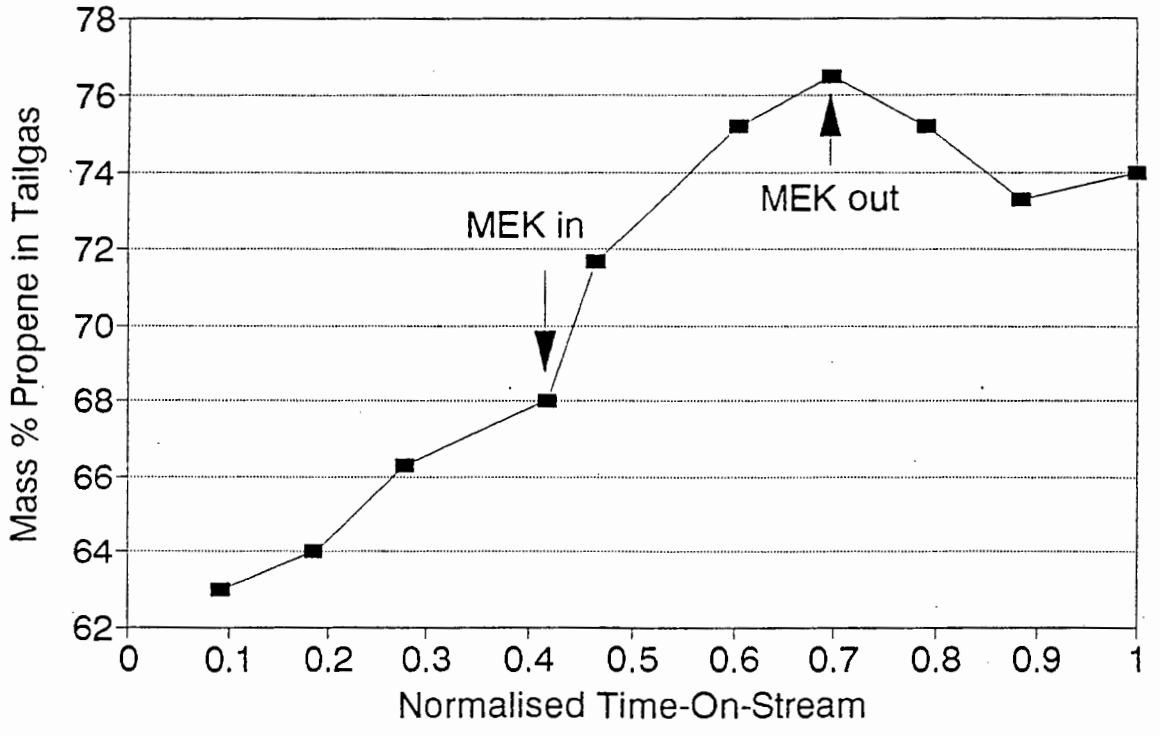

(e) Methyl-ethyl-ketone

APPENDIX L (cont.)

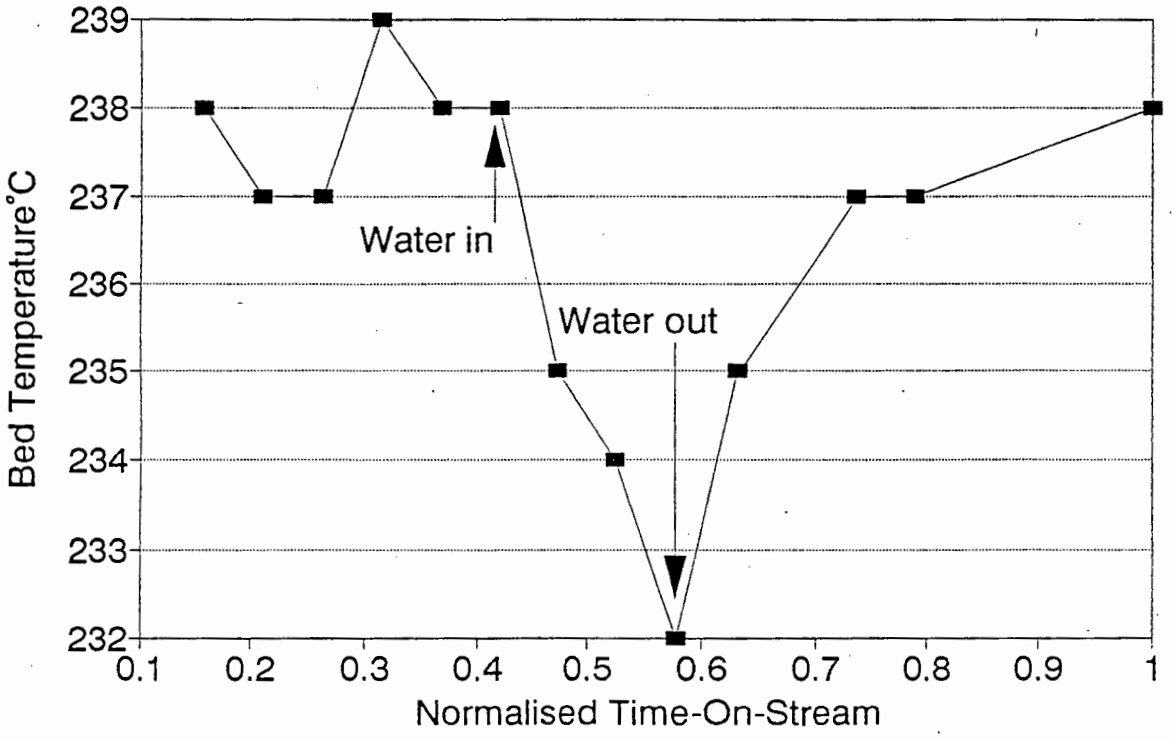

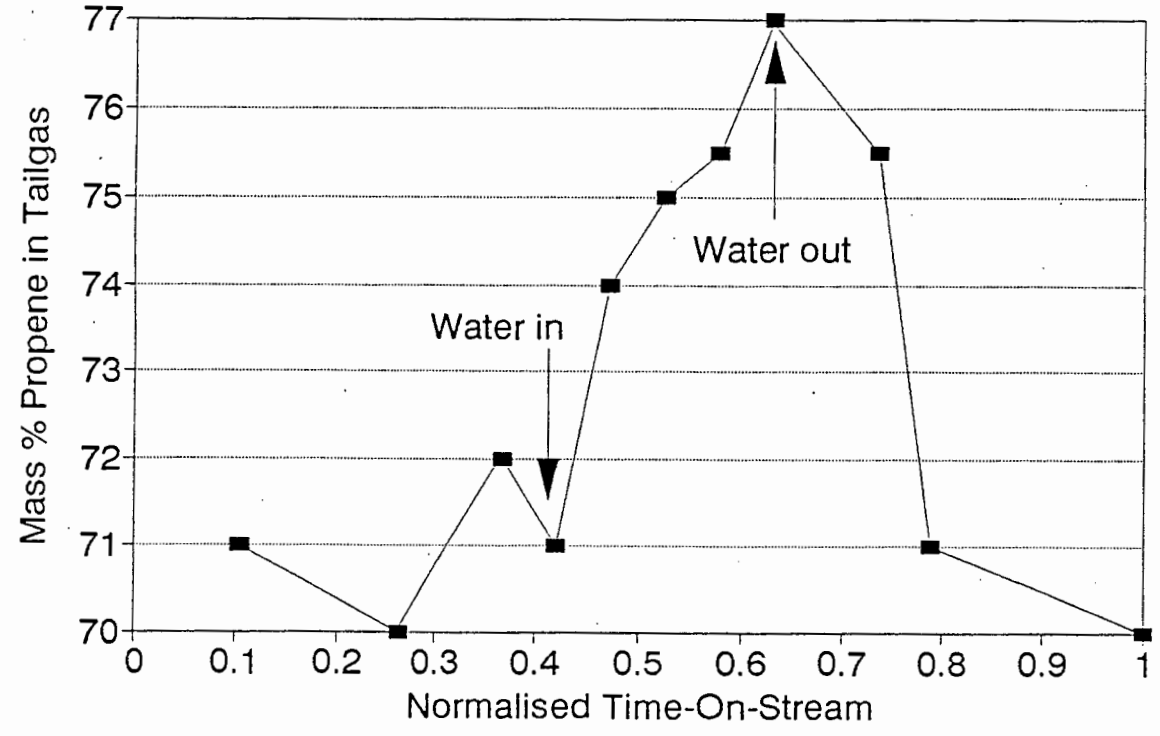

(f) Water